



HAL
open science

Natural and anthropogenic dynamics of the coastal environment in northwestern Corsica (western Mediterranean) over the past six millennia

Federico Di Rita, Matthieu Ghilardi, Nathalie Fagel, Matteo Vacchi, François Warichet, Doriane Delanghe, Jean Sicurani, Lauriane Martinet, Sébastien Robresco

► To cite this version:

Federico Di Rita, Matthieu Ghilardi, Nathalie Fagel, Matteo Vacchi, François Warichet, et al.. Natural and anthropogenic dynamics of the coastal environment in northwestern Corsica (western Mediterranean) over the past six millennia. *Quaternary Science Reviews*, 2022, 278, pp.107372. 10.1016/j.quascirev.2022.107372 . hal-03542871v1

HAL Id: hal-03542871

<https://hal.science/hal-03542871v1>

Submitted on 25 Jan 2022 (v1), last revised 26 Jan 2022 (v2)

HAL is a multi-disciplinary open access archive for the deposit and dissemination of scientific research documents, whether they are published or not. The documents may come from teaching and research institutions in France or abroad, or from public or private research centers.

L'archive ouverte pluridisciplinaire **HAL**, est destinée au dépôt et à la diffusion de documents scientifiques de niveau recherche, publiés ou non, émanant des établissements d'enseignement et de recherche français ou étrangers, des laboratoires publics ou privés.



Distributed under a Creative Commons Attribution - NonCommercial - NoDerivatives 4.0 International License

1
2 **Natural and anthropogenic dynamics of the coastal environment in**
3 **northwestern Corsica (Western Mediterranean) over the past six millennia**
4

5 **Federico Di Rita^{1*}, Matthieu Ghilardi², Nathalie Fagel³, Matteo Vacchi⁴, François Warichet³,**
6 **Doriane Delanghe², Jean Sicurani⁵, Lauriane Martinet⁶, Sébastien Robresco⁷**
7

8
9 ¹ Sapienza University of Rome, Department of Environmental Biology, Italy

10 ² CEREGE (CNRS UMR 7330-AMU-IRD-Collège de France-INRAE), Europôle de l'Arbois BP 80 13545 Aix-en-
11 Provence CEDEX 04 France

12 ³ AGES, Département de Géologie, Université de Liège, 4000 Liège, Belgium

13 ⁴ Dipartimento di Scienze della Terra, University of Pisa, Via Santa Maria 53, Pisa, Italy

14 ⁵ Association pour la Recherche Préhistorique et Protohistorique en Corse, Moncale, Corsica, France.

15 ⁶ CEPAM, CNRS UMR 7264-University of Nice Sophia Antipolis, Pôle Universitaire Saint Jean d'Angély, Nice,
16 France

17 ⁷ SIGOSPHERE, 69380 Chazay d'Azergues, France
18
19

20 * Corresponding author:

21 Federico Di Rita

22 +39 06 49912197

23 federico.dirita@uniroma1.it
24

Abstract

The present paper provides new insights into the climatic and anthropic factors that influenced a 6000-year coastal evolution in northwestern Corsica, the third largest island of the western Mediterranean. Pollen, microcharcoal, sedimentary and geochemical analyses were carried out on a core drilled in the Crovani coastal wetland to reconstruct the regional drivers of landscape change. We show that anthropogenic and climate-induced fires favoured the development of Mediterranean maquis, dominated by *Erica* and *Quercus ilex*, from ca. 6000 to 3350 cal. BP. A change in arboreal vegetation triggered a short but intense sediment input in the Crovani pond between ca. 3350 and 3200 cal. BP. This is consistent with a coeval process of runoff recorded in several coastal sites of western Corsica and related to an arid climate change occurred in many sites of the western Mediterranean around 3200 years ago. We provide evidence of agriculture during the Late Neolithic from ca. 3900 BC, which is much earlier than any archaeological evidence previously available in this area of Corsica, followed by a progressive decline of arable farming practices. Human impact has been responsible for a degradation of the maquis only from approximately 3000 cal. BP, and it intensified in Roman times, when the area experienced the first phase of galena exploitation from the Argentella mines. Over the last 500 years, the present work evidences a major development of *Castanea* related to cultivation during the Genoese administration of Corsica. Our findings suggest that solar activity and the North Atlantic Oscillation had an influence on centennial-scale forest cover variations during the last 6000 years.

Keywords: Corsica, pollen, palaeoenvironments, isotope geochemistry, geoarchaeology, western Mediterranean, Holocene

1. Introduction

The island of Corsica hosts the largest number of coastal wetlands among the Mediterranean islands (Ghilardi, 2020 and 2021). Most of them formed after the Mid-Holocene sea-level stabilization that occurred in the Mediterranean Basin between 7000 and 6000 cal. BP (Vacchi et al., 2016, 2018). Amongst the ~200 coastal wetlands of the island, brackish lagoons and coastal ponds are the most common geomorphological features (Ghilardi, 2020).

The remarkable potential of pollen analysis to trace the main changes in the coastal landscape of the island was first highlighted by the excellent palynological work of Maurice Reille (Reille, 1984, 1991, 1992a). However, these pollen data were not provided with a robust chronology and did not include the analysis of Non-Pollen Palynomorphs (NPPs) and other palaeoenvironmental proxies from the same core.

60 In the last few years, several Corsican wetlands situated at a short distance of the sea were the subject
61 of multiproxy geoarchaeological research on the environmental impact of human activities, especially
62 in Prehistoric and Protohistoric times (Early Neolithic to Final Bronze Age, ca. 7500 BP to 2800 BP)
63 (Currás et al., 2017; Ghilardi et al., 2017a; Revelles et al., 2019; Vella et al., 2019; Figure 1). The
64 study of different palaeoecological proxies, such as ostracods, molluscs, and pollen, combined with
65 the chronostratigraphy of sediments, has shown the interest of reconstructing both the paleogeography
66 and the history of the vegetation of coastal Corsica starting from the ancient Neolithic (Cardial
67 culture, starting from 7500 ± 200 cal. BP; D'Anna et al., 2001; Lugliè, 2018).

68 The information of palaeoenvironmental records from Corsica is paramount for detailed
69 reconstructions of both land-use patterns and centennial-scale climate changes in the Mediterranean
70 Basin. Indeed, the island was a crossroad for many European and North African populations in the
71 conquest of the Mediterranean and occupies a strategic geographical location, potentially sensitive to
72 both North Atlantic climate patterns and north African atmospheric drivers (Sabatier et al., 2020).

73 The aim of this paper is to outline the landscape evolution in northwestern coastal Corsica over the
74 last six millennia, taking advantage of the recent progress in palaeoenvironmental reconstructions
75 (Henry et al., 2020), chronological models (Reimer et al., 2020), and new insights into the centennial-
76 scale patterns of atmospheric circulation during the Middle and Late Holocene (Franke et al., 2017;
77 Di Rita et al., 2018a; Sabatier et al., 2020).

78 Our new palynological and stratigraphical data are addressed to contribute to prominent unsolved
79 questions about times and drivers of vegetational change in Corsica, with a special focus on the
80 replacement of *Erica* shrublands with *Quercus ilex* woody formations during the Middle Holocene.

81 A second key topic is the origin and development of land use practices in northwestern Corsica. In
82 Neolithic times, there is sparse archaeological evidence for cereal cultivation and pastoral activities
83 along the coasts of Corsica. Cereal cultivation was revealed by pollen analyses only in the eastern
84 plain of Corsica and in the Saint Florent and Bonifacio-Piantarella areas (Currás et al., 2017; Revelles
85 et al., 2019), while the osteological identification of mammals buried in sheltered caves from southern
86 and northern Corsica provided evidence about the development of stockbreeding (Vigne, 1984, 1987).

87 A third unsolved question is related to the controversial role of climate changes in modifying the
88 vegetational landscape of Corsica. While at millennial time scale the influence of climate changes on
89 the vegetation and fires of the island has been clearly recognized (Reille 1992a; Leys et al., 2013;
90 Revelles et al., 2019; Lestienne et al., 2020a, b), the role of rapid climate changes (RCC) has been
91 seldom evoked in the regional palaeobotanical narrative. The apparent lack of vegetation responses
92 to centennial climate changes was attributed to either the overshadowing effect produced by local
93 resilient shrublands (Revelles et al., 2019) or the geographical position of Corsica, located in a

94 possible climate-unsensitive transitional area between the central and western Mediterranean (Di Rita
95 and Magri, 2019), two regions where RCC often produced contrasting moisture changes (Di Rita et
96 al., 2018a).

97 New detailed palaeoenvironmental data from Corsica are thus needed to disentangle these questions,
98 which are relevant for a better understanding of the natural and anthropogenic landscape changes in
99 the Mediterranean during the Holocene.

100

101 2. Study area

102 2.1. Present day landscape and vegetation

103 The Crovani pond is located in NW Corsica, in the westernmost part of a ~1 km² coastal plain (Fig.
104 1A). The plain collects the waters from two catchment basins with intermittent flow: the Argentella-
105 Cardiccia streams (catchment basin ~6 km²), incising metamorphic rocks (shales and micaschists)
106 and syenogranite, and the Marconcellu-Fiuminale streams (total catchment area: ca. 23 km²), draining
107 granodiorites, syenogranite, and Pliocene to Pleistocene scree in the lowermost river course (Fig.
108 1B).

109 Corsica has a typical Mediterranean climate highly influenced by its relief topography. The mean
110 annual temperature on the whole Island ranges between 14.5°C and 16.5°C and the mean annual
111 precipitation is 890 mm per year. On the coastal area, mean annual temperature is higher (17°C) and
112 freezing temperatures during the year are very seldom reported (Vella et al., 2019).

113 The Crovani wetland covers an area of ~0.3 km² behind a thick coastal barrier ≤5.30 m above the
114 mean sea level (amsl), made up of large well-rounded pebbles and cobbles (Fig. 2). The pond, which
115 is at 0.75 m amsl in the winter, is seasonal dry in the summer and has no direct link to the sea.

116 The surrounding wetland is a protected area, being included in the ZNIEFF (*Zone naturelle d'intérêt*
117 *écologique, faunistique et floristique*) n. 940004139 'Etang et zones humide de Crovani' with the aim
118 of preserving the following angiosperm species: *Euphorbia peplis* L., *Polygonum scoparium* Req. ex
119 Loisel., *Ranunculus ophioglossifolius* Vill., *Staphisagria picta* (Willd.) Jabbour, *Tamarix africana*
120 Poir., and *Vitex agnus-castus* L. The pond is surrounded by a belt of *T. africana* and is characterized
121 by a wet meadow covered by palustrine species dominated by *Bolboschoenus maritimus* (L.) Palla,
122 *Juncus acutus* L. and *Juncus maritimus* Lam. The coastal bar is occupied by a population of *Pistacia*
123 *lentiscus* L. and, on the top of the beach, by one of the most important Corsican populations of *Vitex*
124 *agnus-castus* (<https://inpn.mnhn.fr/zone/znief/940004139>). In spring, the very rare *S. picta* grows
125 among the pebbles (Jeanmonod and Schlüssel, 2006). The woody vegetation of the site consists of a
126 degraded *maquis* with *Erica arborea* L., *Arbutus unedo* L., *Pistacia lentiscus* L., *Phillyrea*
127 *angustifolia* L. and sparse *Quercus ilex* L. (Reille, 1992a).

128

129 2.2. Local archaeology and history of the human occupation

130 The first evidence of human settlement in Corsica dates back to the Mesolithic (Lugliè, 2018).
131 Abundant archaeological material allows to reconstruct the Neolithic settling history of the island
132 (Lugliè, 2018; Revelles et al., 2019). In northern Corsica a rich archaeological background is found
133 in a Mesolithic to Early Neolithic occupation in the Nebbiu area, at the Saint-Florent/Patrimonio sites
134 (Revelles et al., 2019). In the Balagne area, an important human occupation in a coastal context is
135 attested by the Early Neolithic site (Cardial culture) of La Petra, situated on a peninsula north of the
136 modern town of L'Île Rousse (Weiss, 2010).

137 In the Luzzipeu sector, situated in the southern part of the Balagne micro region, where the Crovani
138 pond is located (Fig. 1A), despite the paucity of recognized prehistoric settlements and uncovered
139 archaeological material, there is evidence of occupation during the Final Neolithic (starting from ca.
140 2800 cal. BC) at Teghja di Linu (Fig. 1A). The last site consists in a small village composed of huts,
141 located at an elevation of ~40 m amsl at ~1.5 km distance from the Crovani pond, where lithics were
142 discovered together with a menhir statue (Sicurani, 2008; Sicurani and Martinet, 2019; Ghilardi,
143 2020). Possible evidence of occupation during Late Neolithic times is also possible, but the lithics
144 uncovered are still under investigation (Sicurani and Martinet, 2019). Due to the presence of acidic
145 soils, derived from the erosion of the granitic bedrock, preservation of biological remains and
146 archaeological material in this stratigraphical context is difficult, so that there is no organic material
147 left in the archaeological layers that may help to evaluate the type of activities developed at the Teghja
148 di Linu site. Excavations conducted over the last two decades have revealed the existence of a habitat
149 composed of several circular large structures, delimited by tremendous rounded granitic boulders.
150 Protohistoric settlements are hardly documented in the Luzzipeu lowlands. Bronze Age sites are
151 situated more inland, generally on top of hills (Pecche-Quilichini, 2011). Iron Age and Roman times
152 are poorly documented, but archaeological surveys have revealed the presence of *tegulae* within the
153 mining complex of the Argentella, in use in the 19th to 20th century CE, indicating a first phase of
154 galena exploitation (Leleu, 2021). This sparse human occupation from Bronze Age to Roman times
155 radically contrasts with the Medieval archaeological remains attested at San Larenzu and San Quilicu
156 (Fig. 1A). Both are Romanic churches dated from the 11th Century CE and nowadays almost
157 disappeared due to their gradual destruction. From the Genovese administration to the French
158 administration, the region was attractive for the exploitation of natural resources, especially galena
159 minerals. Evidence for mining from the 16th to the early 20th centuries has been recorded (Leleu,
160 2021) but its impact in terms of landscape changes has never been investigated.

161

3. Materials and Methods

In this paragraph we present a synthetic version of materials analysed and techniques we used. For a more exhaustive explanation of the methodology applied in this research we refer to information reported in the Supplementary data.

The analyses presented in this study were carried out on a 6.25 m long sediment sequence, which was collected with a 50-mm vibracore (COBRA TT equipment – Atlas Copco) in the central part of the Crovani pond in August 2018 (Fig. 2).

The chronostratigraphy of the core was established using a series of 14 AMS radiocarbon determinations made in the Poznan and Gliwice (Poland) Radiocarbon Dating Laboratories. The Bayesian age-depth model (Fig. 3) was constructed using the software Bacon version 2.5.5 (Blaauw and Christen, 2011) with dates calibrated using the IntCal20 curve (Reimer et al., 2020).

Loss-on-ignition (LOI) measurements were performed on sediment samples of approximately 1 g taken at 10 cm intervals throughout the sequence, following the standard procedures published in Dean (1974) and Bengtsson and Enell (1986). (Fig. 4).

Samples used for LOI measurements were also analysed for granulometry. The grain-size distribution of the fine fraction (<2 mm) was measured by laser diffraction granulometry at CEREGE.

A C/N analysis was carried out on 28 samples from the core, selected according to their organic matter content: a minimum of 5% by weight of organic matter was required to continue. The method by Stax and Stein (1993) was used as a basis for the preparation of the samples. Results were obtained using an elementary analyser (Vario Microcube, Elementar) coupled to a mass spectrometer (Isoprime 1000) (Fig. 4).

The bulk mineralogy was measured on 28 samples in the upper 261 cm of the core. Most of the samples were retrieved from clayey sediments between 116 and 261 cm (n= 20), with a sampling resolution of 4 cm. In addition, 8 samples were retrieved between 11 and 106 cm. About 1 gram of dried bulk sediment sample was hand ground for mineralogical analyses. X ray diffraction (XRD) patterns of non-oriented powders (Moore and Reynolds 1997) were acquired between 2 and 30° 2 θ angle by using a Bruker D8-Advance Eco 1 Kw diffractometer equipped with a ceramic copper (K α radiance with $\lambda = 1.5418 \text{ \AA}$). The XRD data measured under a current intensity of 25 mA and a voltage of 40 KV were recorded with a Lynxeye Xe energy dispersive detector in the laboratory AGEs at the University of Liège. The minerals were identified by their peak positions and their abundance was calculated from the intensity on selected diffraction peaks (Cook et al. 1975).

The bulk samples for Pb isotopes analyses were digested using a tri-acid attack of HF/HNO₃/HCl in a laminar flow hood. The Pb purification was made according to the procedures published in Weis et

196 al. (2006). The Pb isotopes were measured by static multicollection in dry mode on a Nu Plasma I
197 MC-ICP-MS instrument at the University of Brussels. The values were normalized using the
198 recommended NBS981 values ($^{208}\text{Pb}/^{204}\text{Pb}$ 36.7219 ± 61 , $^{207}\text{Pb}/^{204}\text{Pb}$ 15.4963 ± 17 , $^{206}\text{Pb}/^{204}\text{Pb}$
199 16.9405 ± 24) from Galer and Abouchami (1998). The Pb isotopes ratios were measured on 24 clayey
200 samples retrieved in unit VI and VIII with a ~5 cm sampling resolution between 11 and 260 cm (Table
201 S1).

202 In addition, some Pb-bearing minerals were collected in different Corsican ores or mineralised veins
203 on the Paleozoic granites from west Corsica (Fig. 5). We have sampled the main Pb mineral galena
204 (PbS) and also some Pb-bearing minerals like arsenopyrite (FeAsS). Galena was sampled in the mine
205 of Argentella, 2.5 km from the Crovani pond but also in the mine of Lozari (along the northwestern
206 coast, east of Ile Rousse) and in a mineralized vein in Prunelli (south of Porto - see locations in Fig.
207 1). In addition, an arsenopyrite mineral sample was collected in the Finosa Pb-Zn-Ag ore close to
208 Ghisoni (Fig. 1).

209 Pollen analysis was carried out on 62 samples. Pollen extraction followed the standard procedures
210 summarized by Magri and Di Rita (2015). Pollen grains and NPPs were identified by light microscope
211 at 400 and 640 magnifications, with the help of both pollen morphology atlases (e.g., Reille, 1992b;
212 Beug, 2004) and NPPs reference articles (e.g., Van Geel, 2001; Cugny et al., 2010; Gelorini et al.,
213 2011).

214 Microcharcoal analysis was carried out to reconstruct fire history, following the procedures described
215 by Clark (1982). A series of 150 microscope fields were checked for each sample. Microcharcoals
216 smaller than 5 μm were excluded from the sum. The computer program Psimpoll 4.27 (Bennett, 2009)
217 was used to plot the percentage and concentration diagrams, as well as to subdivide the pollen record
218 into 8 local assemblage zones, numbered from the base upwards and prefixed by the site abbreviation
219 CRO, by means of the CONISS method (Grimm, 1987).

220 A REDFIT spectral analysis (Schulz and Mudelsee, 2002) using the PAST 3.2 software (Hammer et
221 al., 2001) was applied to the unevenly spaced time series represented by the total Arboreal Pollen
222 (AP) percentages to detect the possible occurrence of a fundamental tempo in the forest cover
223 changes.

224

225 4. Results

226 4.1. Chronostratigraphy

227 Based on the laser grain size determination and on the organic matter/carbonate contents, eight
228 stratigraphic units were defined from the bottom to the top (Fig. 4).

229 Unit I is found between 6.25 and 5.95 m depth. It consists of a mixture of well-rounded pebbles
230 cemented within a sandy matrix and grey clays containing from 2 to 5% of organic matter. Due to the
231 paucity of organic material, radiocarbon dating of this sedimentary unit was impossible.

232 Unit II is found between 5.95 and 5.45 m depth. It comprises medium to coarse grey sands with local
233 intercalations of angular gravels (centimetric in size). Organic matter and carbonate content are very
234 low (1-2%), hindering any radiocarbon dating of Unit II. No biomarkers were identified.

235 Unit III is encountered between 5.45 and 3.73 m depth (~6300-5170 cal. BP; ~4350-3220 BC). It
236 consists of homogeneous grey clays. The organic matter content ranges between 10 and 15% while
237 carbonate content shows values comprised between 6 and 9%.

238 Unit IV occurs from 3.73 to 2.95 m depth (5170-4760 cal. BP; 3220-2810 BC). It shows features
239 similar to Unit II. It consists of coarse sands with intercalated layers of gravels with sharp edges,
240 witnessing variations in the energy of deposition, in particular at the point of changeover with Unit
241 III. In the lowermost part of Unit IV, a layer of 15 cm consists of angular gravels without sedimentary
242 matrix. Organic matter and carbonate contents (both < 2%) are low, like Unit II. Radiocarbon dating
243 of this lowermost portion is consistent with a time interval encompassing the Late to Final Neolithic.

244 Unit V, between 2.95 and 2.72 m depth (4760-4630 cal. BP; 2810-2680 BC), consists of organic
245 coarse sandy clays. Organic matter content increases upwards (1-7%). The carbonates content is
246 lower than 2%.

247 Unit VI is found from 2.72 and 1.42 m depth (4630-3320 cal. BP; 2680-1370 BC) and exhibits
248 sedimentological parameters similar to Unit V. It consists of organic clays with 10-20% of organic
249 matter and $\leq 8\%$ of carbonate. The XRD mineralogy (Fig. S1) reveals the dominance of detrital
250 minerals (~50% of quartz, K-feldspars and plagioclase with traces of amphibole and chlorite). They
251 are associated to clayey minerals (~30% of total undifferentiated clays), aragonite (3 to 8%) from
252 biogenic fragments and evaporites (8% < halite < 12% - Fig. 4). Radiocarbon dating of the unit is
253 consistent with a time interval ranging from Final Neolithic to Middle Bronze Age.

254 Unit VII is encountered from 1.42 to 1.32 m deep (3320-3190 BP; 1370-1240 BC). It consists in a
255 thin layer (10 cm) of homogeneous yellow fine sands showing a modal index of 90 μm with a mean
256 grain size of 20 μm (fine silts). The granulometric analyses exhibit a multimodal distribution of the
257 particles. Positive excursion in detrital minerals (cumulated abundance over 70 %) is observed for
258 Unit VII and corresponds to a significant increase in quartz (28%) and plagioclase (25 %) and a
259 relative drop in total clays minerals (13%) (Fig. S1).

260 Sedimentary Unit VIII is identified in the uppermost 1.32 m depth (3190-0 cal. BP; 1240 BC-1950
261 AD). Homogeneous grey clays record numerous traces of oxidation corresponding to rootlets. The
262 organic matter content is homogeneous (6 to 8%), while carbonate content is low (2-3%). The XRD

263 mineral association remains similar to unit VI, except the abundance of evaporites. A drop of halite
264 below 4% occurs between 166 and 150 cm, i.e. in the upper part of unit VII but close to the transition
265 with unit VI (Fig. 4). ~~This sedimentary unit shows conditions similar to present-day marshy~~
266 ~~environments.~~ The rate of sediment accumulation for Unit VIII is very low, with values of ~4.3 mm
267 per century.

268

269

270 4.2. C/N results

271 The uppermost 2 m sediment, spanning the last four millennia, were investigated for C/N ratio (Fig.
272 4). The averaged C/N ratio is high (> 10) and exceeds a value of 16 above 1.16 m suggesting a mainly
273 terrestrial origin of the organic matter. The values range between 11 to 14 from 1.16 to 2 m, indicating
274 a mixture of organic matter from vascular plants and algae. The highest value (~30) measured at 1.36
275 m indicates an episode of high input of sediments of continental origin, with a mix of vascular plants
276 and cellulosic plants, dated ca. 1430 to 1260 BC.

277

278 4.3. Lead isotopes analyses

279 The three Pb isotopic ratios evolve in parallel in the 260-upper cm, from Final Neolithic to present
280 (Fig. S2). The $^{208}\text{Pb}/^{204}\text{Pb}$ ranges between 38.60 and 39.01 (average 38.9353 ± 0.0019), the $^{207}\text{Pb}/^{204}\text{Pb}$
281 between 15.65 and 15.68 (average 15.6703 ± 0.0007), and the $^{206}\text{Pb}/^{204}\text{Pb}$ between 18.61 and 19.11
282 (average 19.02 ± 0.0008) (Table S1). Even if some scattering of the data is observed for the studied
283 pre-Roman period (i.e., 260-93 cm), the isotopic Pb ratios depict a marked decreasing trend upwards.
284 This major change starts at 73 cm (Fig. S2) during the Roman period and continues over the modern
285 period. The lowest isotopic ratios are measured in the shallowest samples at 11 and 17 cm.

286

287 4.4. Pollen analysis and statistical analysis on pollen time series

288 The results of pollen analysis are presented as: 1) a detailed percentage diagram, including most of
289 the pollen taxa and a summary Arboreal Pollen (AP)/Non Arboreal Pollen (NAP) percentage diagram,
290 plotted against age (Fig. 6); 2) a percentage diagram displaying the main NPPs (Fig. 7); 3) a synthetic
291 diagram including cumulative pollen percentages of ecological groups (conifers, riparian trees,
292 deciduous trees, evergreen trees and shrubs, OJCV (*Olea+Juglans+Castanea+Vitis*), anthropogenic
293 herbs, other herbs, coprophilous fungi, and saproxylic and phytopathogenic fungi), AP percentage,
294 the concentrations of AP and NAP, microcharcoals, and some climate proxies (Fig. 8).

295 The pollen preservation was good with percentages of undeterminable grains seldom exceeding 4%.

296 An average of 310 pollen grains of terrestrial taxa per sample were counted. The biodiversity was
297 represented by 92 different pollen taxa (terrestrial + aquatic plants) summed to 45 types of ferns,
298 algae, fungi, and other NPPs. The palynological richness, estimated by rarefaction analysis (Birks
299 and Line, 1992), is always over 15 terrestrial pollen types per sample. Total pollen concentrations
300 vary from 7000 to 321,000 terrestrial pollen grains/g sediment. The features of the local pollen
301 assemblage zones are summarized in the Supplementary Materials.

302 A REDFIT analysis was applied to the unevenly sampled time series represented by the total AP
303 percentages, which show a clear fluctuating trend consistent with changes in forest cover rather than
304 random fluctuations due to pollen representation and preservation (Fig. 9).

305 The results of the REDFIT exhibit a peak in power spectrum exceeding 95% of the false-alarm levels
306 of both χ^2 and Monte Carlo tests, corresponding to a statistically significant periodicity of ca. 228
307 years (time=1/frequency), and less significant frequencies centred at 996 and 430 years, which
308 however exceed 90% of the false-alarm levels of both χ^2 and Monte Carlo tests (Fig. 9).

309

310 5. Discussion

311

312 5.1. Evolution of the vegetational landscape

313 During the Middle and Late Holocene, from ca. 6100 to 1000 cal. BP (4150 BC-950 AD), the Crovani
314 pond was surrounded by a dense *Erica*-dominated tall *maquis*, accompanied by several evergreen
315 elements, such as *Q. ilex*, *Phillyrea*, *Pistacia*, and *Olea* (Figs 6, 8, and 10). This observation is
316 consistent with other palynological studies from southern Corsica (Reille, 1975, 1984; Revelles et al.,
317 2019, Vella et al., 2019) and on the Cavallo island, situated in the strait of Bonifacio (Poher et al.,
318 2017). An almost continuous record of *Arbutus* indicates that strawberry trees was a common
319 presence in the *Erica arborea* formations, as its pollen tetrads are poorly dispersed. The most
320 degraded sectors of this *maquis* vegetation were probably occupied by low shrublands of *Cistus*,
321 which played a prominent role in the dune and sandy soil vegetation together with *Olea*, *Pistacia* and
322 other thermophilous shrubs, as also reported from other coastal sites of western Corsica (Reille,
323 1992a).

324 The pollen record from Crovani provides new data to investigate the complex interplay between
325 *Erica*-dominated and *Q. ilex*-dominated vegetation and their turnover in Corsica. According to Reille
326 (1992a), *Erica* woodlands, representing the climax vegetation in lowland areas of western Corsica,
327 underwent a major degradation process since the neolithization of the island, as a result of increasing
328 human impact. It was largely replaced by *Quercus ilex* during the Mid- to Late Holocene (Reille,
329 1992a, Carcaillet et al., 1997). Recent palynological studies (Revelles et al., 2019) confirmed the
330 anthropic causation of this vegetation turnover and suggested that it started with the development of

331 agropastoral practices during the Early Neolithic, hence significantly earlier than the period
332 previously identified by Reille (1992a). Similar vegetation dynamics were reported also in Sardinia,
333 where a clear development of *Quercus ilex*, leading to a partial or complete replacement of the late
334 successional *Erica* shrublands, is recorded since the 6th millennium BP (Di Rita and Melis, 2013;
335 Beffa et al., 2016; Melis et al., 2017, 2018; Pedrotta et al., 2021). In contrast, the pollen record from
336 Crovani (Fig. 6) indicates that the frequencies of *Erica* were continuously high until ~2900 BP and
337 were not replaced by *Q. ilex*. Our pollen record even shows two temporary major increases in *Erica*
338 at the expense of holm oaks in the time-intervals 4700-4300 and 3350-2900 cal. BP. High frequencies
339 and concentrations of *Erica* and *Q. ilex* concur in depicting a *maquis* characterized by high biomass
340 and decomposed organic matter, as suggested by generally high values in the loss of ignition and a
341 significant presence of saproxylic and phytopathogenic fungi, such as *Kretzschmaria deusta*,
342 *Asterosporium* and Xylariaceae (Fig. 7)..

343 In Sardinia, Beffa et al. (2016) hypothesise that a protracted dominance of *Erica* and the absence of
344 evergreen oak forests in the first part of the Middle Holocene (until ca. 5300 cal. BP) were related to
345 warmer/drier summers and cooler/moister winters than today. They suggest that also in Corsica such
346 a climate regime, characterized by frequent and prolonged droughts during the spring and summer,
347 may have led to frequent seasonal wildfires advantaging communities dominated by *Erica scoparia*
348 and *Erica arborea*, which are two fire-adapted species able to quickly resprout and generate new
349 aboveground biomass after frequent and intense fires. In contrast, *Quercus ilex* is considered to have
350 been severely affected by natural and anthropogenic fires and favoured by a climate change leading
351 to increased summer rainfall and decreased fire occurred at the end of the Middle Holocene
352 (Colombaroli et al., 2009; Beffa et al., 2016; Pedrotta et al., 2021).

353 In contrast to this view, at Crovani, high concentrations of microcharcoal, reflecting fires, are
354 recorded in correspondence of high values of both *Erica* and *Q. ilex*. Contemporary high values of *Q.*
355 *ilex* and microcharcoal support the interpretation of Reille (1992a) and Carcaillet et al. (1997), which
356 suggest that the development of holm oak in Corsica was triggered by anthropogenic fires. At
357 Crovani, a substantial portion of the Mid-Holocene fires may be related to human activity, which is
358 witnessed by a significant presence of anthropogenic indicators (Figs 6-8). High frequencies of
359 microcharcoal in zones CRO-1 and CRO-2 are consistent with the coeval high incidence of fires
360 recorded in the region (Leys et al., 2014; Lestienne et al., 2020a, b), most of which are attributed to
361 human activity. According to Lestienne et al. (2020b), since 5000 cal. BP humans have taken control
362 of the fire regime through agro-pastoralism, favouring large and/or frequent fire events. For the same
363 reason, the marked decrease in microcharcoal recorded at Crovani during the Late Holocene after

364 ~3350 cal. BP, which matches a decrease in anthropogenic pollen indicators, may reflect decreased
365 human activity, at a time of an unsuitable climate for fires.

366 Starting from ~2900 cal. BP, there was a general decline in *Erica*, opposed to an increase in holm
367 oaks, which led to a turnover of the two woody taxa between 2300 and 1900 cal. BP. In this time-
368 interval, an increase in oaks may have been influenced by the forestry practices of Roman times. All
369 the same, in the last ~2500 years, a clear development of cork oak in Corsica (Reille, 1984, 1992a),
370 Sardinia (Di Rita and Melis, 2013), and the western Iberian Peninsula (Carrión et al., 2000) may be
371 related to silvicultural practices.

372 Between 1900 and 1000 cal. BP (pollen zone CRO-6), a new moderate increase in *Erica* at the
373 expense of *Q. ilex* suggests a new expansion of the native *Erica*-dominated shrublands.

374 Between 1000 and 500 cal. BP (pollen zone CRO-7), a major degradation of the forest cover is
375 recorded, with a massive decline of the tall *maquis* that was replaced by *Cistus*-dominated low
376 shrubland. After ~ 500 BP, *Erica* and *Q. ilex* recovered, as recorded also in other sites of Corsica (e.g.
377 Vella et al., 2019).

378 Modest oscillations of deciduous trees throughout the record (Fig. 6 and 8) suggest that they were
379 scarcely involved in the environmental processes influencing the evergreen vegetation, probably
380 because they were located at higher elevations in the island. Frequent finds of mesophilous trees such
381 as *Fagus* and *Betula*, which require temperate and humid conditions, confirm that part of the pollen
382 rain originated from the montane vegetation belt. The fingerprint of deciduous trees in the pollen
383 record of Crovani, as in other coastal pollen records of Corsica (Reille, 1992a; Currás et al., 2017;
384 Revelles et al., 2019), is clearly due the steep topography of the island, which determined a relatively
385 low distance of montane and sub-montane vegetation belts from the coast. However, it cannot be
386 excluded that sparse stands of mixed oak communities could also be preserved in humid areas at low
387 elevations, especially inside floodplain and riparian woodlands, dominated by *Alnus*, accompanied
388 by *Salix*, *Tamarix*, and possible wild *Vitis*, which are still documented in the area (Reille, 1992a).

389 Conifers are mostly represented by *Pinus*, substantially reflecting the persistence of *Pinus nigra*
390 subsp. *laricio* at montane and sub-montane elevations since the late glacial period (Leys et al. 2014).
391 The occurrence of *Pinus pinaster* since the Bronze Age is probably related to human activity (Reille,
392 1992a). In addition to pine, conifers include taxa distributed in both lowland/coastal areas, such as
393 *Juniperus*, and in montane sectors, such as *Abies* and *Taxus* (Fig. 7). Rare occurrences of *Picea*,
394 whose current natural range does not include Corsica, are of distant origin.

395

396

397

398 5.2. *Environmental responses to hydrological and morphosedimentary processes*

399 The local aquatic environment outlined by the pollen record ranged from brackish (6100-3400 cal.
400 BP) to freshwater conditions (~3400 cal. BP-present day) (Fig. 10). This range is documented by the
401 presence of freshwater taxa, such as *Spirogyra*, *Zygnema* and *Myriophyllum*, salt-tolerant species,
402 such as *Ruppia maritima*, and marine organisms, represented by foraminiferal linings, pointing to
403 inputs of salt-water into the pond (Bellotti et al., 2016). This was likely related to the morphological
404 response of the pond to the Mediterranean sea-level rise whose average rates decreased from ~2 mm
405 a⁻¹ at ~6100 BP to less than ~0.5 mm a⁻¹ in the last 3500 years (Vacchi et al., 2021). These major
406 changes in the rising rates probably have an influence on the connection of the pond with the open
407 sea as already observed in lagoonal setting both in Corsica (e.g. Vacchi et al., 2017; Revelles et al.,
408 2019) and in Sardinia (Melis et al., 2017, 2018). However, the absence of fossil faunal associations
409 hampered a detailed reconstruction of the nature of this backshore environment and its millennial
410 evolution.

411 The lower part of the record (~6100 to ~4800 cal. BP) is characterized by high frequencies of
412 *Spiniferites* sp. (Fig. 7), dinoflagellate cysts often difficult to identify at the species level by routine
413 observation in light microscopy (de Vernal et al 2018). The genus *Spiniferites* is characterized by
414 marine species, but it cannot be excluded that some Mediterranean species live in freshwater
415 environments (Kouli et al., 2001; Zonneveld et al., 2013). Based on pollen records obtained from
416 central Mediterranean regions, the presence of *Spiniferites* is often associated to brackish water (Di
417 Rita et al., 2018b). Irrespective of water salinity, high frequencies of *Spiniferites* in the lower part of
418 the Crovani sequence may reflect the pioneer stages of a hydrosere succession connected to the early
419 phases of development of the coastal pond.

420 From ~4800 to ~3350 cal. BP (zone CRO-2), a significant increase in *Ruppia maritima*, a submerged
421 angiosperm with large salinity tolerance (Kantrud, 1991), coupled with occurrences of foraminiferal
422 linings, highlights a brackish environment. It is consistent with the observed presence of halite in unit
423 VI (Fig. 4). Beds of submerged usually occur on muddy sand and mud in brackish pools. They
424 accumulate sediment and may be associated with terrestrial saltmarsh plants, forming a hydrosere
425 succession in coastal wetlands (Rodwell, 2000).

426 Starting from ~3350 cal. BP, the abrupt decrease in *Ruppia* and the disappearance of most spores of
427 fungi, coupled with a major increase in *Pseudoschizaea* (2%) and fern spores, are the results of
428 complex sedimentological and ecological changes leading to a lowering of the water level and to the
429 establishment of the present-day marshy environments. *Pseudoschizaea* suggests both desiccation
430 (Scott, 1992) and freshwater flows accompanied by erosive processes, sometimes associated with
431 runoff events (Pantaléon-Cano et al., 2003), while the disappearance of most fungal spores, the

432 decrease in pollen concentrations, and the high percentages of Cichorioideae (Figs 6-8) can be
433 interpreted as selective preservation of palynomorphs (Bottema, 1975; Havinga, 1984).

434 It is noteworthy that Reille (1992a) recorded a sharp drop in *Ruppia* at 150 cm depth and correlated
435 it with a local change in sediment accumulation. This was caused by an event of forest clearance,
436 followed by an increase in runoff, leading to the accumulation of a sandy layer and a significant
437 development of ferns. In our record, a phase of increased terrestrial runoff is revealed by an input of
438 organic matter of continental origin recorded by a positive excursion of C/N ratio at 1.36 m (ca. 3250
439 cal. BP - Fig. 4) and by a significant increase in detrital minerals (Fig. S1), but is not preceded by
440 clear changes in AP percentages that may testify to a deforestation process, although there is a drop
441 in AP concentrations around 3350 cal. BP. A clearance of local shrubs, represented by a sharp decline
442 in *Erica* frequencies, was recorded only after ~3100 cal. BP (Figs 6 and 8).

443 Summarizing, initially the opening of the vegetation did not change the composition of the shrubland,
444 which was later affected by the drop of *Erica*. Sedimentological analyses indicate an increase of the
445 granulometry within a broader context of swamp environment of deposition characterized by
446 homogeneous clays. At ~136 cm depth (ca. 3250 cal. BP), there is an event of higher energy of
447 deposition characterized by the punctual presence of coarse silts to fine sands. In the Canniccia pond,
448 located in SW Corsica, Ghilardi et al. (2017b) and Vella et al. (2019) identified a high detrital input
449 dated ca. 3350 cal. BP. At a regional scale, the southern France recorded an intense phase of
450 alluviation within the Rhone drainage basin (Berger et al., 2007) and the Pyrenean mountains (Galop
451 et al., 2007).

452 This is possibly explained by the occurrence of a cooler and more arid period that resulted in
453 deforestation on a regional scale (Ghilardi et al., 2017a), recognized in western Mediterranean pollen
454 records (Carrión, 2002; Fletcher et al., 2013) and in speleothems from Tuscany located only ca. 200
455 km from Crovani (Regattieri et al., 2014). However, the eastern coast of Corsica did not record such
456 event (Currás et al., 2017), which seems to have especially affected western Corsica.

457 Since ~2900 cal. BP, an expansion of ferns and other hydrophytes (Fig. 7) suggests stagnant water,
458 which may have been produced by a lowering of the lake enhanced by runoff and a salinity change
459 towards more freshwater conditions. This change is confirmed by the observed decrease in the halite
460 since the final part of units VI (Fig. 4). Such pattern is consistent with a substantial sea-level stability,
461 which occurred in the NW Mediterranean Sea in the last ~2000 years (Vacchi et al., 2021). This
462 stabilization process significantly decreased the salinity input within the pond triggering the
463 progressive transition in pure freshwater environment.

464 Overall, the sequence dinoflagellates (*Spiniferites*) → aquatic plants (*Ruppia maritima*) → ferns
465 profiled throughout the pollen record corresponds to a hydrosere succession, whose evolution is

466 strictly related to the sediment infilling of lakes (Fig. 6). This ecological succession typically involves
467 reed swamp vegetation at an intermediate stage, here represented by pollen of Cyperaceae and partly
468 of Poaceae, and *Alnus* at a mature stage. In several coastal sedimentary archives of the central
469 Mediterranean, temporary expansions of Cyperaceae and Poaceae are followed by an increase in
470 *Alnus* (Magri et al., 2019 and references therein). At Crovani this pattern is especially clear in the
471 interval between ~2600 and ~1700 cal. BP, when complete hydrosere succession with a climax
472 woodland stage occurred in marginal sectors of the basin, in relation to a lagoon reduction (Fig. 6).

473

474 5.3. Human impact on the landscape

475 Human activity is evident throughout the pollen record with different intensity and type of land use
476 (Fig. 10). During the Late Neolithic, from ~3900 to ~3250 BC, the continuous curve of cereal-type
477 pollen testifies to early cultivations (Fig. 6). Evidence for agriculture is also observed at the Saint
478 Florent site starting from ~4000 cal. BC (Revelles et al., 2019), but only the extreme south of the
479 island (Bonifacio-Piantarella area) exhibits continuous agricultural practices all along the Neolithic
480 period. At Crovani, the pollen record reveals human activity older than the archaeological finds,
481 indicating that farming was practiced ~1000 years before the earliest trace of human occupation at
482 the Teghja di Linu site (Sicurani and Martinet, 2019).

483 Cereal cultivation appears associated to livestock rearing activities, which contributed to the
484 development of disturbed meadows, as highlighted by a significant record of *Sporormiella*, *Sordaria*,
485 and *Podospora*, and by pollen indicators for Mediterranean pasturelands, such as *Carduus*-type,
486 *Plantago*, *Polygonum aviculare*-type, as well as some species of the subfamilies Asteroideae and
487 Cichorioideae (Desprat et al., 2013; Florenzano et al., 2015) (Figs 6 and 8). The high values of
488 microcharcoal may partly reflect the use of fire for farming purposes, such as slash-and-burn
489 practices, which however did not affect the fire-adapted local shrubland. In general, human activity
490 during the Late Neolithic certainly influenced the vegetation evolution of the area, but its impact did
491 not produce a marked local deforestation. While we cannot advance any precise explanation for this
492 pattern, we can speculate that local settlements were not populated enough to produce forest declines
493 detectable in the pollen diagram.

494 During the Final Neolithic and Bronze Age (from ~3000 to ~800 BC), both cereal cultivation and
495 livestock rearing appear less intense and discontinuous. The archaeological history of Corsica
496 indicates that Early to Middle Bronze Age are periods of human implantation in the upper part of the
497 hills (Casteddi) when lowlands and coastal areas were less occupied (Cesari and Pêche Quilichini,
498 2015). The pollen record from Crovani confirms this pattern, even if in some coastal areas the Mid-
499 to Late Bronze Age corresponds to a phase of renewed agriculture (Ghilardi et al., 2017a).

500 In the Iron Age, cereals disappeared and scattered occurrences of pasture weeds (e.g., *Carduus*,
501 *Plantago*, and *Rumex*) testify to poor farming practices addressed to livestock rearing, suggesting a
502 scarce human frequentation in the area (Fig. 6).

503 Human activity at Crovani is also revealed by the record of cultivated trees (OJCV curve, Fig. 8),
504 which also include pollen of wild individuals of *Olea* and *Vitis* that is difficult to differentiate from
505 pollen of cultivated plants (Reille, 1992a).

506 In the period encompassing the Neolithic to the Bronze Age the pollen record of Crovani shows some
507 early occurrences of *Juglans* (ca. 3700 BC) and *Castanea* (ca. 1200 BC) (Fig. 6). Similar early finds
508 are also recorded in pollen diagrams from recently published coastal sites (Poher et al., 2017; Currás
509 et al., 2017; Revelles et al., 2019). Although these occurrences are generally found during phases of
510 intense human activity, as confirmed by the presence of other anthropogenic pollen indicators, it is
511 difficult to hypothesize that cultivation of these trees was such early, without a clear archaeobotanical
512 evidence. Unfortunately, the palynological studies of Reille (1992a; 1999) and Lestienne (2020a) do
513 not contribute to solve this question, since their records do not show any *Castanea* and *Juglans* before
514 2500 cal. BP. They interpret these finds as a result of cultivation in the island in historical times. In
515 addition, the absence of palynological investigations from Pleistocene sediments prevents us to
516 speculate on a possible redeposition of pollen from older deposits. We would exclude a long-distance
517 origin, especially for *Juglans*, whose pollen dispersal occurs over short distance despite its renowned
518 anemophily (Carrión and Sánchez-Gómez, 1992).

519 Phylogeographical studies demonstrate that the post-glacial distribution of chestnut and walnut in
520 Europe and in the Mediterranean regions started from multiple glacial refugia (Mattioni et al., 2013;
521 Pollegioni et al., 2017). However, due to both the scarcity of palaeobotanical knowledge and
522 incomplete genetic sampling, as in the case of Corsica and Sardinia, there is still much uncertainty in
523 detecting glacial refugia and drawing up robust biogeographical histories of cultivated trees (Médail
524 et al., 2019).

525 In historical time, the OJCV record shows two major phases of tree cultivation. The first one, between
526 ~250 BC and ~150 AD, reflects a widespread exploitation of olive resources during the Roman
527 Period, also documented by archaeological evidence (Terral et al., 2004). The second increase, after
528 ~1450 AD, testifies to an intensification of *Olea* cultivation and a regional plantation of *Castanea* in
529 the uplands. From 1548 until the 17th century, the Genoese Authority introduced the compulsory
530 cultivation of chestnut, whose fingerprint in the Crovani record is represented by a peak of *Castanea*
531 (Fig. 6) (Michon, 2011). The consequence of this decree was a large reorganization of the food,
532 economy, and socio-cultural systems, as shepherds slowly became chestnut growers and settled more
533 permanently in mid-mountain villages. The chestnut culture fully developed during the 18th and 19th

534 centuries, providing flour for daily meals, fodder for animals, and fruits for trade. By the end of the
535 19th century, the development of local industries and the related outflow of rural population toward
536 urban centres determined the collapse of the chestnut culture (Michon, 2011).

537 Human impact on the forest cover is recorded since ~1000 BC (Final Bronze Age), mostly by
538 decreases in evergreen trees and shrubs staggered over time (Fig. 8), coupled with increases in both
539 herbaceous vegetation and *Cistus* dominated low shrublands (Figs 6 and 8). Considering the local
540 modest farming practices of the last three millennia, this pattern may mostly reflect clearance
541 practices of the *Erica* shrubland at a regional scale. This is consistent with the human-induced
542 opening of the forests recorded in several other pollen sites of Corsica (Reille, 1992a; Revelles et al.,
543 2019; Lestienne et al., 2020a), and in coastal sites of the central Mediterranean since ~1000 cal. BC
544 (Di Rita and Magri, 2012). According to Roberts et al. (2019), after ~1000 BC human activity became
545 the dominant causation in determining landscape openings in the Mediterranean regions

546 Despite clear land use changes are recorded, human activities at Crovani did not completely transform
547 the structure of the vegetation in terms of forest canopy, except for a temporary dramatic drop of the
548 *maquis* vegetation between 950 and 1450 AD (1000-500 cal. BP), for which a prominent
549 anthropogenic causation cannot be ruled out. Pollen indicators of human activity are scarce in this
550 period, but the reappearance of coprophilous fungi (*Sporormiella*) and the increase in *Castanea* and
551 *Olea*, together with a slight increase in fire frequency, may reflect silvicultural practices addressed to
552 the felling of shrublands to gain land available for both stock rearing and olive cultivation in the
553 lowlands, as well as for chestnut cultivation in the uplands. A similar observation was advanced in
554 the Saint-Florent area, where an important deforestation phase was coeval to the development of
555 pastoral activities (Revelles et al., 2019). Between ~1000 and ~500 cal. BP, also frequencies >2% of
556 *Pseudoschizaea* and *Glomus* support soil erosion and local deforestation (Figs 7 and 10). This was
557 also the time when several churches were locally built (Fig. 1A).

558 The human activities may also be tracked from the Pb isotope signature of the Crovani sediments.
559 The sedimentary Pb data are aligned along a linear trend in a binary $^{208}\text{Pb}/^{206}\text{Pb}$ - $^{206}\text{Pb}/^{207}\text{Pb}$ diagram
560 (Fig. 5A and B). Such distribution indicates a mixing between two end-members, a natural end-
561 member with higher isotope Pb ratios and a probable anthropogenic-derived end-member
562 characterised by lower isotope ratios.

563 (a) The first end-member has been defined by the average signature of 3 samples dated from the
564 Final Neolithic period (196 to 260 cm). They are used to define the local detrital source with low
565 isotopes ratios (i.e., $^{208}\text{Pb}/^{204}\text{Pb} = 38.9584 \pm 0.0020$, $^{207}\text{Pb}/^{204}\text{Pb} = 206\text{Pb}/^{204}\text{Pb} 15,6719 \pm 0.0008$ and
566 $^{206}\text{Pb}/^{204}\text{Pb} = 19,0775 \pm 0.0008$) (Table S1). This end-member represents the natural background end-
567 member. **There is no significant difference between the Final Bronze age and Final Neolithic and the**

568 ~~Bronze Age signatures.~~ The composition of the samples corresponding to the Iron age, only defined
569 by 2 measurements, is slightly different from the previous Bronze and Final Neolithic periods, with
570 a position closer to the sample from the Roman representative average. The Pb isotope ratios of the
571 sediments roughly decrease upwards from the natural background end-member. The oldest pre-
572 Roman samples (n= 19, 93-260 cm) are clustered with an average signature of 38.9667 ± 0.0235 ,
573 15.6716 ± 0.0007 and 19.0702 ± 0.0008 for $^{208}\text{Pb}/^{204}\text{Pb}$, $^{207}\text{Pb}/^{204}\text{Pb}$ and $^{206}\text{Pb}/^{204}\text{Pb}$, respectively.
574 ~~Note there is no significant difference in the Pb signature between the Bronze Age samples (106-186~~
575 ~~cm) and the Iron age samples (measured at 93 and 99 cm) (Fig. 5 and Table S1).~~

576 (b) A shift towards lower Pb isotope ratios is marked for the Roman samples (53 and 73 cm) and
577 for the modern samples (11-23 cm). The first Roman shift may be related to some exploitation of Pb
578 ores. The isotope composition of both regional Pb-bearing ores and modern urban airborne particles
579 (Bollhöfer and Rosman, 2001) are reported in order to confirm any anthropogenic contribution in the
580 sediment Pb isotope composition. The isotope Pb ratios of the Roman and modern samples become
581 closer and closer to the Corsican Pb minerals (Fig. 5). The analysed Pb-bearing minerals display close
582 Pb isotope signatures, with an average composition of 1.1779 for $^{206}\text{Pb}/^{207}\text{Pb}$ and 2.0894 for
583 $^{208}\text{Pb}/^{206}\text{Pb}$. The first decrease of the Pb isotopic ratio observed in the Roman Crovani sediments is
584 in agreement with the historical exploitation of the Pb-Ag ores from the Argentella during the Roman
585 period (Gauthier, 2006). The linear trend defined by the modern samples does not point towards the
586 modern urban airborne particles but rather towards the Pb signature of the Sardinian ores (Stos-Gale
587 et al., 1995). In the Crovani sediments, Sardinia seems to be the most probable anthropogenic source
588 of Pb among the main Pb mines exploited in the Mediterranean area, i.e. in Greece, Turkey, Italy and
589 Spain since the Antiquity (see more details in Fagel et al., 2017). In the binary $^{206}\text{Pb}/^{207}\text{Pb}$ - $^{208}\text{Pb}/^{206}\text{Pb}$
590 diagram, the Crovani samples define a linear trend that, if extrapolated, points to the representative
591 average signature of Sardinian ores (Fig. 5 B).

592 593 5.4. Effects of Rapid Climate Changes on the coastal tree-cover

594 In the palaeobotanical narrative of Corsica, no clear tree-cover change has ever been attributed to a
595 “Bond event” (Bond et al., 2001) (Fig. 8) or other RCC of global interest, such as the 4.2 ka event
596 (Bini et al., 2019), the Homeric minimum (2.8 ka BP) (Martin-Puertas et al., 2012) and the Little Ice
597 Age (Trouet et al., 2009). These events have produced major changes in forest cover in many sites of
598 central and western Mediterranean regions, although with contrasting trends (Fletcher et al., 2013,
599 Magny et al., 2013; Di Rita et al., 2018a).

600 The 4.2 cal. BP event, perceived in south-central Italy as an aridity crisis producing a forest decline,
601 did not trigger a rapid response in the regional forest vegetation in Corsica and in the northern

602 Apennines (Di Rita and Magri, 2019; Revelles et al., 2019; Di Rita et al., 2022). However, previous
603 studies in Corsica have shown that the 4.2 event played an influence on geomorphological and
604 sedimentological processes, due to increased storm and fluvial activities as recorded in several lagoon
605 archives (Revelles et al., 2019 and references therein). In our record from Crovani, rapid fluctuations
606 of the forest cover are found, marked by maximum values of AP (92%) at ca. 4450 cal. BP (Figs 6
607 and 8). Between 4700 and 3500 cal. BP, a long-lasting increase in *Fagus* suggests permanent humid
608 conditions during the Mid- to Late Holocene transition (Fig. 6), which are recorded also in other
609 montane (Reille, 1975; Reille et al., 1999) and pollen sequences from coastal Corsica (Poher et al.,
610 2017; Revelles et al., 2019). The development of beech corresponds to relatively wet climatic
611 conditions in central Italy, as revealed by lake level highstands at Lake Accessa ca. 160 km far from
612 Crovani (Magny et al., 2013). Lake level highstands reflecting humid conditions are also recorded in
613 northern Italy (cf. Lake Ledro: Magny et al., 2012), and in west-central Europe (Magny et al., 2013
614 and references therein).

615 The development of beech corresponds also to periods of increased storm activity in southern France
616 (Sabatier et al., 2012) (Fig. 8). Although these periods were previously interpreted as the result of
617 southward westerly winds bringing moisture to mid-latitudes in Europe (Sabatier et al., 2012; Magny
618 et al., 2013), they may also reflect an increase in the frequency of marine storms that are not directly
619 interpretable as periods of regional increased precipitation (Azuara et al., 2020). An alkenone record
620 from the Gulf of Lion suggests moisture increase in southern France since ca. 4200 cal. BP (Jalali et
621 al., 2017; Azuara et al., 2020).

622 The general pattern of increased humidity in western Corsica contrasts with the drier conditions
623 indicated by precipitation proxies from the speleothems of the Corchia and Renella caves in Tuscany
624 (Zanchetta et al., 2016; Isola et al., 2019), and depicts a complex geographic expression of the 4.2 ka
625 event (Bini et al., 2019; Di Rita and Magri, 2019; Di Rita et al., 2022).

626 The Homeric Minimum (2750-2550 cal. BP, Martin-Puertas et al., 2012) was associated to forest
627 declines influenced by human impact and dryer climate conditions in many records of the south-
628 central Mediterranean (Di Rita et al., 2018c). At Crovani, it corresponds to a modest peak in AP,
629 possibly related to slightly wetter conditions. Relatively higher precipitations were recorded from
630 lake-level highstands since 2800 cal. BP at Lake Accessa (Fig 8), and from lake-level highstands and
631 pollen evidence at Lake Ledro (Magny et al., 2012; Peyron et al., 2017). More humid climate
632 conditions were also found in the western Mediterranean, possibly associated to the negative NAO
633 index that characterizes this interval (Fletcher et al., 2013). This phase corresponds also to increased
634 storm activity in the Gulf of Lion (Sabatier et al., 2012).

635 During the Little Ice Age, the record of Crovani shows a marked increase in *Erica* and *Q. ilex maquis*,
636 accompanied by significant frequencies of cultivated trees related to orchards and conifer plantations
637 (Figs 6 and 8). The development of natural and cultivated woody taxa was probably favoured by
638 relatively wet climate conditions, which were also recorded in both central and northern Italy from
639 lake-level highstands (Magny et al., 2013), as well as in southern France from records of major
640 flooding (Benito et al., 2015, Pichard et al., 2017), coinciding with a mostly negative NAO index
641 (Franke et al., 2017) (Figs 8 and 10). Climate reconstructions in Corsica are still fragmentary,
642 however the few published studies indicate the occurrence of periods characterized by wet and cool
643 conditions (Szyczak et al., 2012; Vella et al., 2014).

644 The archaeological and paleoenvironmental literature does not provide noticeable examples of rapid
645 and dry climate events in Corsica. As previously discussed, the complex sedimentological pattern at
646 ~3250. cal. BP (Fig. 4) might be related to an arid climate event observed around the same age in
647 other palaeoenvironmental records. Relatively dry and warm climate conditions may have also
648 contributed to produce the major forest decline recorded between 1000 and 500 cal. BP, limiting the
649 resprout of the natural forest vegetation affected by felling activities. In the western Mediterranean,
650 the dry and warm climate of the Medieval Climate Anomaly is usually associated to an overall
651 positive NAO index (Trouet et al., 2009; Franke et al., 2017) (Fig. 8).

652 Sabatier et al. (2020) have found a strong relationship between the transport of Saharan dust conveyed
653 to Corsica during the last ~3000 years and both total solar irradiance (TSI) and NAO activity. They
654 have shown that the NAO was the main climatic forcing for centennial to decadal variations since
655 ~1070 AD, with an increase in Saharan dust input during positive NAO phases. Before ~1070 AD,
656 TSI was the main forcing factor, with increases in African dust input during low TSI phases.

657 We applied a REDFIT analysis to the total AP percentages to investigate the effects of the
658 atmospheric circulation on the tree cover record from Crovani (Fig. 9). The prominent 230-year cycle
659 found in our statistical elaboration by and large corresponds to the Suess-de Vries cycle of solar
660 activity, which has been held responsible for environmental and atmospheric changes in several
661 records around the world, including the Mediterranean (Castagnoli et al., 1992; Galloway et al., 2013;
662 Di Rita, 2013; Degeai et al., 2014; Sabatier et al., 2020). The Suess-de Vries cycle is commonly
663 identified as a conventional 210-year periodicity; however, an increasing number of studies
664 demonstrates its non-stationary variability, which may have a range of ~200-300 years (Vecchio et
665 al., 2017). Similarly, its expression in palaeoenvironment proxies shows a non-stationary periodicity
666 (Galloway et al., 2013). A 230-year cycle was detected in direct proxies of solar magnetic activity,
667 such as ¹⁴C time series and naked-eye observations of sunspots (Ma and Vaquero, 2020).

668 The REDFIT analysis from Crovani shows also two periodicities of ca. 430 and 1000 years,
669 respectively (Fig. 9). The first one corresponds to the ca. 430-years and 450-year cycles detected by
670 Sabatier et al. (2020) in the records of Saharan dust in Corsica, as shown by both TSI and ITCZ,
671 although the authors attribute a low significance to this cycle. A 440-year cycle (together with a 230-
672 year cycle) was found in $\delta^{13}\text{C}$ records of speleothems from northern Iberia and was interpreted as the
673 result of climate forcing mechanisms related to changes in solar irradiance and North Atlantic
674 circulation patterns (Márton-Chivelet et al., 2011). Periodicities of ~400-years were recognized in
675 various palaeoclimate proxies from both marine (e.g., Bond et al., 2001) and lake records (e.g., Yu
676 and Ito, 2002; Wu et al., 2009) of the Middle-Late Holocene.

677 The last periodicity we found at Crovani matches a prominent ~1000-year cycle of moisture supply
678 reported in proxy records from the western Mediterranean, especially during the Early Holocene,
679 which have been associated to solar activity (Debret et al., 2009; Fletcher et al., 2013; Jiménez
680 Moreno et al., 2020 and references therein).

681 Overall, our results show that the forest oscillations at Crovani present a fundamental tempo of
682 variability consistent with the atmospheric forcing held responsible for the transport of Saharan dust
683 to Corsica. Although the relationship between solar activity and forest dynamics in Corsica is only
684 sketched, our findings encourage future research in the central Mediterranean, interpreted in the light
685 of the regional patterns of vegetation change.

686

687 *5.5. Coastal landscape evolution of the Crovani area*

688 Based on the cross combination of sedimentological, palynological and geochemical proxies, we
689 propose a synthetic palaeogeographical reconstruction of the investigated area, even if additional
690 cores would be necessary to evaluate in a comprehensive way both the morphological changes and
691 the spatial evolution of the Crovani wetland since the Mid-Holocene. The bottom of the core records
692 a detrital environment with a mixture of well-rounded pebbles and coarse material, ranging from
693 sands to gravels. Unfortunately, this section of the core did not contain enough organic material for
694 obtaining a radiocarbon age. Furthermore, facies identification was difficult due to the lack of fossil
695 fauna. However, on the basis of the sedimentological information, two types of energy of deposition
696 can be identified. The first is controlled by terrestrial dynamics being characterized by the finest
697 particles (grey clays). The second is conversely controlled by coastal dynamics as indicated by the
698 presence of well-rounded pebbles that are analogue in shape and petrography to the sediments which
699 compose the modern coastal barrier. These data suggest that the continental dynamics likely prevailed
700 during the first half of the Holocene. This was followed by a mid-Holocene marine transgression that
701 reached its maximum ~6500 cal. BP, when the sea-level in Corsica was ca. 3.5 to 4 m below the

702 present-day position (Vacchi et al., 2018). At that time, which broadly correspond to Middle to Late
703 Neolithic, a marine incursion occurred in the Crovani coastal pond following a pattern that was also
704 observed in other coastal lagoons in Corsica, such as Saint Florent (Revelles et al., 2019) and Del
705 Sale (Curras et al., 2017). As a result, the pond turned into brackish conditions after ~6100 cal. BP,
706 as confirmed by the presence of *Spiniferites*, which substantially indicates a connection with the sea
707 (Fig. 6 and 10). However, probably due to the presence of Late Pleistocene alluvial formations and
708 relict coastal deposits (former coastal barriers), the marine incursion inland was spatially limited. This
709 could explain the lack of faunal assemblages typical of coastal lagoon made by ostracods,
710 foraminifera and molluscs faunas. After ~5100 cal. BP, during the Late to Final Neolithic
711 characterized by the first occupation of the nearby site of Teghja di Linu, data show detrital input that
712 suddenly modified the brackish conditions on the pond. However, our data indicates that nor a climate
713 event neither human impact provoked deforestation associated to intense erosion on the foothills and
714 sedimentary accumulation of coarse material, even if there is a clear land-use at that time (Fig. 10).
715 A second phase of wetland development is well attested from the Final Neolithic to Middle/Recent
716 Bronze Age. Presence of salt intrusion is confirmed by both the vegetation composition and the
717 geochemical analyses (presence of halite) but there is no clear evidence for a direct of the coastal
718 pond connection to the sea (e.g., presence of faunal assemblages typical of coastal lagoons). A second
719 detrital input is observed during the Late Bronze Age (Unit VII). The C/N Ratio exhibits the highest
720 values for the entire sequence studied, thus indicating a terrestrial deposition of organic matter (see
721 section 4.2.) (Fig. 4). This is likely a rapid event (not more than a century in duration) that could have
722 caused the silting up of the wetland. Finally, the present-day landscape configuration is established
723 since Final Bronze Age (unit VIII) with very little morphological changes afterwards. Since ~3200
724 cal. BP, Crovani coastal pond has been a backshore freshwater body with probable aeolian input of
725 salt, no permanent connection to the sea, and low sediment accumulation rate (Fig. 10).

726

727

728 6. Conclusions

729 The new multidisciplinary dataset obtained from northwest Corsica helps to reconstruct the past
730 environmental dynamics (Fig. 10) within an archaeological context, and to frame it into the wider
731 scenario of the central Mediterranean landscape evolution. Our results contribute to the lively
732 discussion on the vegetation response to rapid climate changes, raising also new questions about
733 planetary drivers of past atmospheric circulation and their possible influence on the forested
734 ecosystems of this strategic region of the Mediterranean. In particular, the following conclusions can
735 be traced:

736 1) A dense *Erica*-dominated shrubland rich in many evergreen elements characterized the
737 landscape from ~6100 to ~1000 cal. BP, being temporarily replaced by mixed woodlands
738 dominated by *Q. ilex* between 2300 and 1900 cal. BP. A major opening of the landscape occurred
739 only between ~1000 and ~500 cal. BP, featured by a temporary decline in *Erica*-dominated tall
740 shrublands, paralleled by an expansion of *Cistus*-dominated low shrublands and followed by the
741 recovery of the tall *maquis* formations.

742 2) Fires played a prominent role in the development and maintenance of the *Erica*-dominated
743 shrublands, especially during the Middle Holocene (from ~5900 to ~5200 cal. BP), when frequent
744 and intense wild and anthropogenic fires boosted the sprout of *Erica* species. Differently from
745 other sites in Corsica and Sardinia, at Crovani fires did not affect *Q. ilex*, whose development
746 cannot be univocally explained in the region and may be influenced by a long-lasting ecological
747 legacy. The general decrease of fires after ~3300 cal. BP may reflect a combination of decreased
748 human activity and climate unsuitable for fires.

749 3) The Crovani wetland has been little influenced by marine incursions over the last six
750 millennia, as indicated by sedimentological data, pollen and NPPs. Moderate brackish conditions
751 occurred only from the Late Neolithic to part of the Bronze Age, while during the last three
752 millennia general freshwater conditions prevailed. The sequential development of dinoflagellates,
753 *Ruppia*, and ferns appears to reflect a hydrosere succession, whose evolution is strictly related to
754 the infilling of the lake. After ~3300 cal. BP, this ecological process was influenced by a sudden
755 deposition of continental organic-rich sediments, following rapid deforestation and runoff of
756 regional extension, coeval to an arid climate event occurred around ~3200 cal. BP.

757 4) Evidence for human activity is present throughout the pollen record, with important
758 differences through time. Between ~6000 and ~5200 cal. BP, a continuous curve of cereal-type
759 pollen testifies to the earliest cultivations in this area. Farming activities are also confirmed by the
760 presence of disturbed meadows for livestock rearing, indicated by coprophilous fungi and pollen
761 indicators of plants frequently living in Mediterranean pasturelands. Starting around 3300 cal. BP,
762 indicators of cereal cultivation and stock rearing practices became sparse, and evidence for human
763 activity comes from cultivated trees, especially after ca. 2000 cal. BP and even more after ~500
764 cal. BP. The former increase reflects olive exploitation during the Roman Period, the latter points
765 to both olive cultivation in lowland areas and chestnut culture in the uplands. A clear forest
766 degradation dates back to the last three millennia, with a dramatic opening of the landscape only
767 from ~1000 to ~500 cal. BP, related to human activity in the medieval times and Genovese
768 domination.

769 5) The spectral analysis applied to total AP revealed a ~230-year cycle, in the bandwidth of the
770 Suess-de Vries cycle, and other cyclicities attributed to the magnetic activity of the Sun,
771 recognized also in other climate proxies from the Mediterranean. This suggests that the
772 atmospheric modifications of solar activity and North Atlantic Oscillation had some influence on
773 the tree cover fluctuations in Corsica. However, known rapid climate changes, such as the 4.2 ka
774 BP event, the Homeric minimum, and the Little Ice Age, did not determine at Crovani extensive
775 forest declines as they did in sites of the south-central Mediterranean. In contrast, in northwestern
776 Corsica these phases correspond to a forest development consistent with the humid phases detected
777 in southern France and northern Italy. The high-resolution record from Crovani is an important
778 piece of information to define the spatial pattern of vegetation response to the atmospheric
779 arrangements produced by rapid climate changes over the Mediterranean Basin during the
780 Holocene.

781

782 Acknowledgements

783 This article is a contribution of the PCR “Approche géoarchéologique des paysages de Corse à
784 l’Holocène, entre mer et intérieur des terres « Tra Mare è Monti » programme, funded by the DRAC
785 Corsica and directed by Matthieu Ghilardi. It is also part of the MISTRALS-PALEOMEX
786 programme of CNRS (INEE-INSU scientific departments) and was funded by the ARCHEOMED
787 workshop (Dir. Laurent Lespez). The authors are grateful to the Conservatoire du Littoral (branch of
788 Corsica) and its Director, Michel Muracciole, for delivering the work permits. We thank Donatella
789 Magri for her precious suggestions.

790

791

792

793 **Reference list**

794

- 795 Azuara, J., Sabatier, P., Lebreton, V., Jalali, B., Sicre, M.-A., Dezileau, L., Bassetti, M.-A., Frigola,
796 J., Combourieu-Nebout, N., 2020. Mid- to Late-Holocene Mediterranean climate variability:
797 contribution of multi-proxy and multi-sequence comparison using wavelet spectral analysis
798 in the northwestern Mediterranean basin. *Earth Sci. Rev.* 208, 103232.
799 <https://doi.org/10.1016/j.earscirev.2020.103232>.
- 800 Beffa, G., Pedrotta, T., Colombaroli, D., Henne, P.D., van Leeuwen, J.F.N., Süssstrunk, P.,
801 Kaltenrieder, P., Adolf, C., Vogel, H., Pasta, S., Anselmetti, F.S., Gobet, E., Tinner, W., 2016.
802 Vegetation and fire history of coastal north-eastern Sardinia (Italy) underchanging Holocene
803 climates and land use. *Veg. Hist. Archaeobotany* 25, 271-289
- 804 Bellotti, P., Calderoni, G., Di Rita, F., D'Orefice, M., D'Amico, C., Esu, D., Magri, D., Preite
805 Martinez, M., Tortora, P., Valeri, P., 2011. The Tiber river delta plain (central Italy): coastal
806 evolution and implications for the ancient Roman Ostia settlement. *Holocene* 21, 1105-1116.
- 807 Benito, G., Macklin, M. G., Zielhofer, C., Jones, A. F., Machado, M. J., 2015. Holocene flooding and
808 climate change in the Mediterranean. *Catena* 130, 13-33.
- 809 Bengtsson, L., Enell, M., 1986. Chemical analysis, in: Berglund, B. E. (ed.), *Handbook of Holocene*
810 *Palaeoecology and Palaeohydrology*. John Wiley & Sons Ltd., Chichester, 423–451.
- 811 Bennett, K., 2009. “psimpoll” and “pscomb”: CPrograms for Analysing Pollen Data and Plotting
812 Pollen Diagrams (Version 4.27). Available online from Queen's University Quaternary
813 Geology program at URL. <http://www.chrono.qub.ac.uk/psimpoll/psimpoll.html>.
- 814 Berger, J.F., Brochier, J.L., Vital, J., Delhon, C., Thiebault, S., 2007. Nouveau regard sur la
815 dynamique des paysages et l'occupation humaine à l'Âge du bronze en moyenne vallée du
816 Rhône, in: Mordant C., Richard H., Magny M. (Eds.), *Environnements et cultures à l'âge du*
817 *Bronze en Europe occidentale*. Actes du 129e colloque du CTHS, Besançon, avril 2004,
818 Editions du CTHS, Documents Préhistoriques 21, 260-283.
- 819 Beug, H., 2004. *Leitfaden der Pollenbestimmung für Mitteleuropa und angrenzende Gebiete*. Verlag
820 Dr. Friederich Pfeil, München.
- 821 Bini, M., Zanchetta, G., Perşoiu, A., Cartier, R., Català, A., Cacho, I., Dean, J.R., Di Rita, F.,
822 Drysdale, R.N., Finnè, M., Isola, I., Jalali, B., Lirer, F., Magri, D., Masi, A., Marks, L.,
823 Mercuri, A.M., Peyron, O., Sadori, L., Sicre, M.-A., Welc, F., Zielhofer, C., Brisset, E., 2019.
824 The 4.2 ka BP Event in the Mediterranean region: an overview. *Clim. Past* 15, 555-577.
- 825 Birks, H.J.B., Line, J.M., 1992. The use of rarefaction analysis for estimating palynological richness
826 from Quaternary pollen-analytical data. *The Holocene* 2, 1-10.
- 827 Blaauw, M., Christen, J. A., 2011. Flexible paleoclimate age-depth models using an autoregressive
828 gamma process. *Bayesian analysis* 6, 457-474.
- 829 Bollhöfer, A., Rosman, K.J.R., 2001. Isotopic source signature for atmospheric lead: the Northern
830 Hemisphere. *Geochim. Cosmochim. Acta* 65, 1727-1740.
- 831 Bond, G., Kromer, B., Beer, J., Muscheler, R., Evans, M.N., Showers, W., Hoffmann, S., Lotti-Bond,
832 R., Hajdas, I., Bonani, G., 2001. Persistent solar influence on North Atlantic climate during
833 the Holocene. *Science* 294, 2130-2136.
- 834 Bottema, S., 1975. The interpretation of pollen spectra from prehistoric settlements (with special
835 attention to Liguliflorae). *Palaeohistoria* 17, 17-35.
- 836 Carcaillet, C., Barakat, H. N., Panaiotis, C., Loisel, R., 1997. Fire and late-Holocene expansion of
837 *Quercus ilex* and *Pinus pinaster* on Corsica. *J. Veg. Sci.* 8, 85-94.
- 838 Carrión, J.S., 2002. Patterns and processes of Late Quaternary environmental change in a montane
839 region of southwestern Europe. *Quaternary Sci. Rev.* 21, 2047-2066.
- 840 Carrión, J.S., Sánchez-Gómez, P., 1992. Palynological data in support of the survival of walnut
841 (*Juglans regia* L.) in the western Mediterranean area during last glacial times. *J. Biogeogr.*
842 19, 623-630.

- 843 Carrión, J.S., Parra, I., Navarro, C., Munuera, M., 2000. Past distribution and ecology of the cork oak
844 (*Quercus suber*) in the Iberian Peninsula: a pollen-analytical approach. *Divers. Distrib.* 6, 29-
845 44.
- 846 Castagnoli, G.C., Bonino, G., Serio, M., Sonnett, C.P., 1992. Common spectral features in the 5500-
847 year record of total carbonate in sea sediments and radiocarbon in tree rings. *Radiocarbon* 34,
848 798–805.
- 849 Caudullo, G., Tinner, W., de Rigo, D., 2016. *Picea abies* in Europe: distribution, habitat, usage and
850 threats. In: San-Miguel-Ayán, J., de Rigo, D., Caudullo, G., Houston Durrant, T., Mauri, A.
851 (Eds.), *European Atlas of Forest Tree Species*. Publications Office of the European Union,
852 Luxembourg e012300b
- 853 Cesari, J., Pêche-Quilichini, K., 2015. L'âge du Bronze corse. L'émergence d'une élite guerrière, in
854 Leandri F., Istria D. (coord.), *Corse, richesses archéologiques de la Préhistoire à l'époque*
855 *moderne. Dossiers d'archéologie*, 370, 24-29
- 856 Clark, R.L., 1982. Point count estimation of charcoal in pollen preparations and thin sections of
857 sediments. *Pollen Spores* 24, 523–535.
- 858 Colombaroli, D., Tinner, W., Leeuwen, J. van, Noti, R., Vescovi, E., Vanniere, B., Magny, M.,
859 Schmidt, R., Bugmann, H., 2009. Response of broadleaved evergreen Mediterranean forest
860 vegetation to fire disturbance during the Holocene: in-sights from the peri-Adriatic region. *J.*
861 *Biogeogr.* 36, 314-326.
- 862 Cook, H.E., Johnson, P.D., Matti, J.C., Zemmels, I., 1975. Methods of sample preparation and X-ray
863 diffraction analysis in X-ray mineralogy laboratory, in: Kaneps, A.G., et al. (Eds.), *Init. Repts*
864 *DSDP XXVIII*. Print. Office, Washington DC, pp. 997-1007.
- 865 Cugny, C., Mazier, F., Galop, D., 2010. Modern and fossil non-pollen palynomorphs from the Basque
866 mountains (western Pyrenees, France): the use of coprophilous fungi to reconstruct pastoral
867 activity. *Veg. Hist. Archaeobot.* 19, 391–408.
- 868 Currás, A., Ghilardi, M., Pêche-Quilichini, K., Fagel, N., Vacchi, M., Delanghe, D., Contreras, D.,
869 Vella, C., Ottaviani, J.C., 2017. Reconstructing past landscapes of the eastern plain of Corsica
870 (NW Mediterranean) during the last 6000 years based on molluscan, sedimentological and
871 palynological analyses. *J. Archaeol. Sci.: Report* 12, 755-769.
- 872 D'Anna, A., Marchesi, H., Tramoni, P., Gilabert, C., Demouche, F., 2001. Renaghju (Sartène, Corse-
873 du-Sud), un habitat de plein-air néolithique ancien en Corse. *Bulletin de la Société*
874 *préhistorique française* 98, 431-444.
- 875 Dean, W.E. Jr., 1974. Determination of carbonate and organic matter in calcareous sediments and
876 sedimentary rocks by loss on ignition: Comparison with other methods. *J. Sed. Petrol.* 44:
877 242–248
- 878 Debret, M., Sebag, D., Crosta, X., Massei, N., Petit, J.R., Chapron, E., Bout-Roumazielles, V., 2009.
879 Evidence from wavelet analysis for a mid-Holocene transition in global climate forcing. *Quat.*
880 *Sci. Rev.* 28, 2675-2688.
- 881 Degeai, J.P., Devillers, B., Dezileau, L., Oueslati, H., Bony, G., 2015. Major storm periods and
882 climate forcing in the Western Mediterranean during the Late Holocene. *Quaternary Sci. Rev.*
883 129, 37-56.
- 884 Desprat, S., Combourieu-Nebout, N., Essallami, L., Sicre, M.A., Dormoy, I., Peyron, O., Siani, G.,
885 Bout Roumazielles, V., Turon, J.L., 2013. Deglacial and Holocene vegetation and climatic
886 changes in the southern Central Mediterranean from a direct land-sea correlation. *Clim. Past*
887 9, 767-787.
- 888 de Vernal, A., Eynaud, F., Henry, M., Limoges, A., Londeix, L., Matthiessen, J., Marret, F.,
889 Pospelova, V., Radi, T., Rochon, A., Van Nieuwenhove, N., Zaragosi, S., 2018. Distribution
890 and (palaeo)ecological affinities of the main *Spiniferites* taxa in the mid-high latitudes of the
891 Northern Hemisphere. *Palynology* 42, 182–202.
- 892 Di Rita, F., 2013. A possible solar pacemaker for Holocene fluctuations of a saltmarsh in southern
893 Italy. *Quatern. Int.* 288, 239-248.

- 894 Di Rita, F., Magri, D., 2012. An overview of the Holocene vegetation history from the central
895 Mediterranean coasts. *J. Mediterr. Earth Sci.* 4, 35-52.
- 896 Di Rita, F., Magri, D., 2019. The 4.2 ka event in the vegetation record of the central Mediterranean.
897 *Clim. Past* 15, 237-251.
- 898 Di Rita, F., Melis, R.T., 2013. The cultural landscape near the ancient city of Tharros (central West
899 Sardinia): vegetation changes and human impact. *J. Archaeol. Sci.* 40, 4271-4282.
- 900 Di Rita, F., Fletcher, W. J., Aranbarri, J., Margaritelli, G., Lirer, F., Magri, D., 2018a. Holocene forest
901 dynamics in central and western Mediterranean: periodicity, spatio-temporal patterns and
902 climate influence. *Scientific Reports* 8, 8929.
- 903 Di Rita, F., Molisso, F., Sacchi, M., 2018b. Late Holocene environmental dynamics, vegetation
904 history, human impact, and climate change in the ancient *Literna Palus* (Lago Patria;
905 Campania, Italy). *Rev. Palaeobot. Palyno.* 258, 48-61.
- 906 Di Rita, F., Lirer, F., Bonomo, S., Cascella, A., Ferraro, L., Florindo, F., Insinga, D.D., Lurcock, P.C.,
907 Margaritelli, G., Petrosino, P., Rettori, R., Vallefucio, M., Magri, D., 2018c. Late Holocene
908 forest dynamics in the Gulf of Gaeta (central Mediterranean) in relation to NAO variability
909 and human impact. *Quaternary Sci. Rev.* 179, 137–152.
- 910 Di Rita, F., Michelangeli, F., Celant, A., Magri, D., 2022. Sign-switching ecological changes in the
911 Mediterranean Basin at 4.2 ka BP. *Global Planet. Change* 208, 103713.
- 912 Fagel, N., Lechenault, M., Fontaine, N., Pleuger, E., Otten, J., Allan, M., Ghilardi, M., Mattielli, N.,
913 Goiran, J-P., 2017. Record of human activities in the Pb isotopes signatures of coastal
914 sediments from the Roman archaeological site of Cala Francese, Cape Corsica (France). *J.*
915 *Archaeol. Sci.: Reports* 12, 770-781.
- 916 Fletcher, W.J., Debret, M., Goñi, M.F.S., 2013. Mid-Holocene emergence of a low-frequency
917 millennial oscillation in western Mediterranean climate: Implications for past dynamics of the
918 North Atlantic atmospheric westerlies. *The Holocene*, 23, 153-166.
- 919 Florenzano, A., Marignani, M., Rosati, L., Fascetti, S., Mercuri, A.M., 2015. Are Cichorieae an
920 indicator of open habitats and pastoralism in current and past vegetation studies? *Plant*
921 *Biosyst.* 149, 154-165.
- 922 Franke, J.G., Werner, J.P., Donner, R.V., 2017. Reconstructing Late Holocene North Atlantic
923 atmospheric circulation changes using functional paleoclimate networks. *Clim. Past* 13, 1593-
924 1608.
- 925 Galloway, J.M., Wigston, A., Patterson, R.T., Swindles, G.T., Reinhardt, E., Roe, H.M., 2013.
926 Climate change and decadal to centennial-scale periodicities recorded in a late Holocene NE
927 Pacific marine record: Examining the role of solar forcing. *Palaeogeography,*
928 *Palaeoclimatology, Palaeoecology* 386, 669-689.
- 929 Galop, D., Carozza, L., Marembert, F., Bal, M.C., 2007. Activités agropastorales et climat durant
930 l'Âge du Bronze dans les Pyrénées : l'état de la question à la lumière des données
931 environnementales et archéologiques, in: Mordant C., Richard H., Magny M. (Eds.),
932 Environnements et cultures à l'âge du Bronze en Europe occidentale. Actes du 129e colloque
933 du CTHS, Besançon, avril 2004, Editions du CTHS, Documents Préhistoriques, 21, 107-119.
- 934 Gauthier, A., 2006. Des roches, des paysages et des hommes. *Géologie de la Corse*, Ajaccio, Edition
935 Albiana, France, 276 p.
- 936 Gelorini, V., Verbeken, A., van Geel, B., Cocquyt, C., Verschuren, D., 2011. Modern non-pollen
937 palynomorphs from East African lake sediments. *Rev. Palaeobot. Palyno.* 164, 143-173.
- 938 Ghilardi, M., 2020. Lagunes et marais littoraux de Corse. De la Préhistoire à nos jours. *Collec. Orma:*
939 *la Corse archéologie*, Editions ARAC, 5, 105 p.
- 940 Ghilardi, M., 2021. Geoarchaeology: Where Geosciences Meet the Humanities to Reconstruct Past
941 Human–Environment Interactions. An Application to the Coastal Areas of the Largest
942 Mediterranean Islands. *Appl. Sci.* 11, 4480. <https://doi.org/10.3390/app11104480>
- 943 Ghilardi, M., Istria, D., Currás, A., Vacchi, M., Contreras, D., Vella, C., Dussouillez, P., Crest, Y.,
944 Colleu, M., Guiter, F., Delanghe, D., 2017a. Reconstructing the landscape evolution and the

945 human occupation of the Lower Sagone River (Western Corsica, France) from the Bronze
946 Age to the Medieval period, in: Ghilardi M. and Lespez L. (Eds.), *Geoarchaeology of the*
947 *Mediterranean islands*. *J. Archaeol. Sci.: Reports*, 12, 741-754.

948 Ghilardi, M., Delanghe, D., Demory, F., Leandri, F., Pêche-Quilichini, K., Vacchi, M., Vella, M.A.,
949 Rossi, V., Robresco, S., 2017b. Enregistrements d'événements extrêmes et évolution des
950 paysages dans les basses vallées fluviales du Taravo et du Sagone (Corse occidentale, France)
951 au cours de l'âge du Bronze moyen à final: une perspective géoarchéologique.
952 *Géomorphologie, Relief, Processus et Environnement* 23, 15-35.

953 Grimm, E.C., 1987. CONISS: a FORTRAN 77 program for stratigraphically constrained cluster
954 analysis by the method of incremental sum of squares. *Computers & Geosciences* 13, 13-35.

955 Hammer, Ø., Harper, D.A.T., Ryan, P.D., 2001. PAST: paleontological Statistics software package
956 for education and data analysis. *Palaeontol. Electron.* 4, 9.

957 Havinga, A.J., 1984. A 20-year experimental investigation into the differential corrosion
958 susceptibility of pollen and spores in various soil types. *Pollen Spores* 26, 541–58.

959 Henry, A.G. (Ed.), 2020. *Handbook for the Analysis of Micro-particles in Archaeological Samples*.
960 Springer International Publishing.

961 Isola, I., Zanchetta, G., Drysdale, R.N., Regattieri, E., Bini, M., Bajo, P., Hellstrom, J.C., Baneschi,
962 I., Lionello, P., Woodhead, J., 2019. The 4.2 ka event in the Central Mediterranean: new data
963 from a Corchia speleothem (Apuan Alps, Central Italy). *Clim. Past* 15, 135–151.

964 Jalali, B., Sicre, M.-A., Kallel, N., Azuara, J., Combourieu-Nebout, N., Bassetti, M.-A., Klein, V.,
965 2017. High-resolution Holocene climate and hydrological variability from two major
966 Mediterranean deltas (Nile and Rhone). *The Holocene* 27 (8), 1158–1168.

967 Jeanmonod, D., Schlüssel, A., 2006. Notes and contributions on Corsican flora, XXI. *Candollea*, 61,
968 93-134.

969 Jiménez-Moreno, G., Anderson, R.S., Ramos-Román, M.J., Camuera, J., Mesa-Fernández, J.M.,
970 García-Alix, A., Jiménez-Espejo, F.J., Carrión, J.S., López-Avilés, A., 2020. The Holocene
971 *Cedrus* pollen record from Sierra Nevada (S Spain), a proxy for climate change in N Africa.
972 *Quaternary Sci. Rev.* 242, 106468.

973 Kantrud, H.A., 1991. Wigeongrass (*Ruppia maritima* L.): A Literature Review, vol. 10. U.S. Fish and
974 Wildlife Service, Fish and Wildlife Research, 58 pp.

975 Kouli, K., Brinkhuis, H., Dale, B., 2001. *Spiniferites cruciformis*: a fresh water dinoflagellate cyst?.
976 *Rev. Palaeobot. Palynolo* 113, 273-286.

977 Lestienne, M., Jouffroy-Bapicot, I., Leyssenne, D., Sabatier, P., Debret, M., Albertini, P. J.,
978 Colombaroli, D., Didier, J., Hély, C., Vannièrè, B., 2020a. Fires and human activities as key
979 factors in the high diversity of Corsican vegetation. *The Holocene* 30, 244-257.

980 Lestienne, M., Hely, C., Curt, T., Jouffroy-Bapicot, I., Vannièrè, B., 2020b. Combining the Monthly
981 Drought Code and Paleoecological Data to Assess Holocene Climate Impact on
982 Mediterranean Fire Regime. *Fire* 3(2), 8.

983 Leleu, F., 2021. Calenzana–Les mines de l'Argentella. Prospection thématique (2018). ADLFI.
984 *Archéologie de la France - Informations* [Online], Corse, Online since 08 January 2021,
985 connection on 14 December 2021. URL: <http://journals.openedition.org/adlfi/50226>

986 Leys, B., Carcaillet, C., Dezileau, L., Ali, A.A., Bradshaw, R.H., 2013. A comparison of charcoal
987 measurements for reconstruction of Mediterranean paleo-fire frequency in the mountains of
988 Corsica. *Quaternary Res.* 79, 337-349.

989 Leys, B., Finsinger, W., Carcaillet, C., 2014. Historical range of fire frequency is not the Achilles'
990 heel of the Corsican black pine ecosystem. *J. Ecol.* 102, 381-395.

991 Lugliè, C., 2018. *Your path led trough the sea...* the emergence of Neolithic in Sardinia and Corsica.
992 *Quatern. Int.* 470, 285-300.

993 Ma, L., Vaquero, J.M., 2020. New evidence of the Suess/de Vries cycle existing in historical naked-
994 eye observations of sunspots. *Open Astronomy* 29, 28-31.

- 995 Magny, M., Joannin, S., Galop, D., Vanni re, B., Haas, J. N., Bassetti, M., Bellintani, P., Scandolari,
996 R., Desmet, M., 2012. Holocene palaeohydrological changes in the northern Mediterranean
997 borderlands as reflected by the lake-level record of Lake Ledro, northeastern Italy. *Quaternary*
998 *Res.*, 77, 382–396.
- 999 Magny, M., Combourieu-Nebout, N., de Beaulieu, J.L., Bout-Roumazeilles, V., Colombaroli, D.,
1000 Desprat, S., Francke, A., Joannin, S., Ortu, E., Peyron, O., Revel, M., Sadori, L., Siani, G.,
1001 Sicre, M.A., Samartin, S., Simonneau, A., Tinner, W., Vanni re, B., Wagner, B., Zanchetta,
1002 G., Anselmetti, F., Brugiapaglia, E., Chapron, E., Debret, M., Desmet, M., Didier, J.,
1003 Essallami, L., Galop, D., Gilli, A., Haas, J.N., Kallel, N., Millet, L., Stock, A., Turon, J.L.,
1004 Wirth, S., 2013. North-south palaeohydrological contrasts in the central Mediterranean during
1005 the Holocene: tentative synthesis and working hypotheses. *Clim. Past* 9, 2043-2071.
- 1006 Magri, D., Di Rita, F., 2015. Archaeopalynological preparation techniques, in: Yeung, E.C.T.,
1007 Stasolla, C., Sumner, M.J., Huang, B.Q. (Eds.), *Plant Microtechniques and Protocols*. Springer
1008 International Publishing, Cham, pp. 495–506.
- 1009 Magri, D., Celant, A., Di Rita, F., 2019. The vanished *Alnus*-dominated forests along the Tyrrhenian
1010 coast. *Catena* 182, 104136.
- 1011 Mart n-Chivelet, J., Mu oz-Garc a, M.B., Edwards, R.L., Turrero, M.J., Ortega, A.I., 2011. Land
1012 surface temperature changes in Northern Iberia since 4000 yr BP, based on $\delta^{13}\text{C}$ of
1013 speleothems. *Global Planet. Change* 77, 1-12.
- 1014 Mart n-Puertas, C., Matthes, K., Brauer, A., Muscheler, R., Hansen, F., Petrick, C., Aldahan, A.,
1015 Possnert, G., van Geel, B., 2012. Regional atmospheric circulation shifts induced by a grand
1016 solar minimum. *Nat. Geosci.* 5, 397-401.
- 1017 Mattioni, C., Martin, M. A., Pollegioni, P., Cherubini, M., Villani, F., 2013. Microsatellite markers
1018 reveal a strong geographical structure in European populations of *Castanea sativa* (Fagaceae):
1019 evidence for multiple glacial refugia. *Am. J. Bot.* 100, 951-961.
- 1020 M dail, F., Monnet, A.-C., Pavon, D., Nikoli c, T., Dimopoulos, P., Bacchetta, G., Arroyo, J., Barina,
1021 Z., Albassatneh, M.C., Domina, G., Fady, B., Matevski, V., Mifsud, S., Leriche, A., 2019.
1022 What is a tree in the Mediterranean Basin hotspot? A critical analysis. *Forest Ecosyst.* 6, 17.
- 1023 Melis, R.T., Depalmas, A., Di Rita, F., Montis, F., Vacchi, M., 2017. Mid to late Holocene
1024 environmental changes along the coast of western Sardinia (Mediterranean Sea *Global Planet.*
1025 *Change* 155, 29-41.
- 1026 Melis, R.T., Di Rita, F., French, C., Marriner, N., Montis, F., Serreli, G., Sulas, F., Vacchi, M., 2018.
1027 8000 years of coastal changes on a western Mediterranean island: a multiproxy approach from
1028 the Posada plain of Sardinia. *Mar. Geol.* 403, 93-108.
- 1029 Michon, G., 2011. Revisiting the resilience of chestnut forests in Corsica: from social-ecological
1030 systems theory to political ecolog. *Ecol. Soc.* 16, 5.
- 1031 Moore, D.M., Reynolds, R.C. Jr., 1997. X-Ray diffraction and the identification and analysis of clay
1032 minerals. Oxford New York, Oxford Univ. Press, 378 pp.
- 1033 Pantale n-Cano, J., Yll, E.I., P rez-Obiol, R. Roure, J.M., 2003. Palynological evidence for
1034 vegetational history in semi-arid areas of the western Mediterranean (Almer a, Spain). *The*
1035 *Holocene* 13, 109–19.
- 1036 Peche-Quilichini, K., 2011. Les monuments turriformes de l'Age du bronze en Corse: tentative de
1037 caract risation spatiale et chronologique sur fond d'historiographie. In: Dominique Garcia
1038 (ed.) *L'Age du bronze en M diterran e. Recherches r centes*, Errance, Paris, 155-170.
- 1039 Pedrotta, T., Gobet, E., Schw rer, C., Beffa, G., Butz, C., Henne, P.D., Morales-Molino, C., Pasta,
1040 S., van Leeuwen, J.F.N., Vogel, H., Zwimpfer, E., Anselmetti, F.S., Grosjean, M., Tinner, W.,
1041 2021. 8,000 years of climate, vegetation, fire and land-use dynamics in the thermo-
1042 mediterranean vegetation belt of northern Sardinia (Italy). *Veget Hist Archaeobot.* 30, 789-
1043 813.
- 1044 Peyron, O., Combourieu-Nebout, N., Brayshaw, D., Goring, S., Andrieu-Ponel, V., Desprat, S.,
1045 Fletcher, W., Gambin, B., Ioakim, C., Joannin, S., Kotthoff, U., Kouli, K., Montade, V., Pross,

- 1046 J., Sadori, L., Magny, M., 2017. Precipitation changes in the Mediterranean basin during the
1047 Holocene from terrestrial and marine pollen records: a model-data comparison. *Clim. Past* 13,
1048 249-265.
- 1049 Pichard, G., Arnaud-Fassetta, G., Moron, V., Roucaute, E., 2017. Hydro-climatology of the Lower
1050 Rhône Valley: historical flood reconstruction (AD 1300–2000) based on documentary and
1051 instrumental sources. *Hydrolog. Sci. J.* 62, 1772-1795.
- 1052 Poher, Y., Ponel, P., Médail, F., Andrieu-Ponel, V., Guiter, F., 2017. Holocene environmental history
1053 of a small Mediterranean island in response to sea-level changes, climate and human impact.
1054 *Palaeogeogr. Palaeoecol.* 465, 247-263.
- 1055 Pollegioni, P., Woeste, K., Chiocchini, F., Del Lungo, S., Ciolfi, M., Olimpieri, I., Tortolano, V.,
1056 Clark, J., Hemery, G.E., Mapelli, S., Malvolti, M.E., 2017. Rethinking the history of common
1057 walnut (*Juglans regia* L.) in Europe: its origins and human interactions. *PLoS One* 12,
1058 e0172541.
- 1059 Regattieri, E., Zanchetta, G., Drysdale, R.N., Isola, I., Hellstrom, J.C., Dallai, L., 2014. Lateglacial
1060 to holocene trace element record (Ba, Mg, Sr) from corchia cave (Apuan Alps, central Italy):
1061 paleoenvironmental implications. *J. Quaternary Sci.* 29, 381-392.
- 1062 Reille, M., 1975. Contribution pollen analytique à l'histoire tardiglaciaire et holocène de la végétation
1063 de la montagne corse. Thèse des sciences Aix-Marseille III.
- 1064 Reille, M., 1984. Origine de la végétation actuelle de la Corse sud-orientale; analyse pollinique de
1065 cinq marais côtiers. *Pollen Spores* 1 XXVI, 43-60.
- 1066 Reille, M., 1991. Les données de l'analyse pollinique. Rapport fouille programme Grotte du Norte di
1067 Tuda. *Olmata di Tuda*, pp. 149-160.
- 1068 Reille, M., 1992a. New pollen-analytical researches in Corsica: the problem of *Quercus ilex* L. and
1069 *Erica arborea* L., the origin of *Pinus halepensis* Miller forests. *New Phytol.* 122, 359-378.
- 1070 Reille, M., 1992b. Pollen et spores d'Afrique du nord. *Laboratoire de Bot. Hist. et Palynologie*,
1071 Marseille
- 1072 Reille, M.J., Gamisans, V., Andrieu-Ponel, V., De Balieu, J.-L., 1999. The Holocene at Lac de Creno,
1073 Corsica, France: a key site for the whole island. *New Phytol.* 141, 291-307.
- 1074 Reimer, P.J., Austin, W.E., Bard, E., Bayliss, A., Blackwell, P.G., Ramsey, C.B., Butzin, M., Cheng,
1075 H., Edwards, R.L., Friedrich, M., Grootes, P.M., et al., 2020. The IntCal20 Northern
1076 Hemisphere Radiocarbon Age Calibration Curve (0-55 cal kBP). *Radiocarbon* 62, 725-757.
- 1077 Revelles J., Ghilardi, M., Vacchi, M., Rossi, V., Currás, A., López-Bultò, O., Brkojewitsch, G., 2019.
1078 Coastal landscape evolution of Corsica: palaeoenvironments, vegetation history and human
1079 impacts since the Early Neolithic period. *Quaternary Sci. Rev.* 225, 105993.
- 1080 Revelles, J., Ghilardi, M., 2021. 49. Saint Florent (north Corsica, France). *Grana* 60, 158-160.
- 1081 Roberts, C. N., Woodbridge, J., Palmisano, A., Bevan, A., Fyfe, R., Shennan, S., 2019. Mediterranean
1082 landscape change during the Holocene: Synthesis, comparison and regional trends in
1083 population, land cover and climate. *The Holocene*, 29(5), 923-937.
- 1084 Rodwell, J.S. (ed.), 2000. *British plant communities*, vol. 5, Maritime communities and vegetation of
1085 open habitats. Cambridge: Cambridge University Press.
- 1086 Sabatier, P., Dezileau, L., Colin, C., Briquieu, L., Bouchette, F., Martinez, P., Siani, G., Raynal, O.,
1087 Von Grafenstein, U., 2012. 7000 years of paleostorm activity in the NW Mediterranean Sea
1088 in response to Holocene climate events. *Quat. Res.* 77, 1–11.
- 1089 Sabatier, P., Nicolle, M., Piot, C., Colin, C., Debret, M., Swingedouw, D., Perrette, Y., Bellingery,
1090 M.-C., Chazeau, B., Develle, A.-L., Leblanc, M., Skonieczny, C., Copard, Y., Reyss, J.-L.,
1091 Malet, E., Jouffroy-Bapicot, I., Kelner, M., Poulénard, J., Didier, J., Arnaud, F., Vannièrè, B.,
1092 2020. Past African dust inputs in the western Mediterranean area controlled by the complex
1093 interaction between the Intertropical Convergence Zone, the North Atlantic Oscillation, and
1094 total solar irradiance. *Clim. Past* 16, 283–298
- 1095 Schulz, M., Mudelsee, M., 2002. REDFIT: estimating red-noise spectra directly from unevenly
1096 spaced paleoclimatic time series. *Computers & Geosciences* 28, 421-426.

- 1097 Scott, L., 1992. Environmental implications and origin of microscopic *Pseudoschizaea* Thiergart and
1098 Frantz ex R Potonié emend. in sediments. *J. Biogeogr.* 19, 349-354.
- 1099 Szymczak, S., Joachimski, M. M., Bräuning, A., Hetzer, T., Kuhlemann, J., 2012. A 560 yr summer
1100 temperature reconstruction for the Western Mediterranean basin based on stable carbon
1101 isotopes from *Pinus nigra* ssp. *laricio* (Corsica/France). *Clim. Past* 8, 1737-1749.
- 1102 Sicurani, J., 2008. Étude technologique et typologique du matériel lithique taillé néolithique trouvé
1103 en place sur quelques sites majeurs du Nord-Ouest (Balagne) de la Corse. Thèse de Doctorat,
1104 Université de Corse, 714 p.
- 1105 Sicurani, J., Martinet, L., 2019. Teghja di Linu: un site de plein air du début du iiiie millénaire av. J.-
1106 C. (Luzipeu, Haute-Corse). In Sicurani J. (dir.), *L’habitat pré- et protohistorique/L’alloghju*
1107 *prestoricu è protostoricu*, acte du Ier colloque de Calvi (Calvi, 28-30 avril 2017), ARPPC, 45-
1108 70.
- 1109 Stax, R., Stein, R., 1993. Long-term changes in the accumulation of organic carbon in Neogene
1110 sediments, Ontong Java Plateau, Proc. Ocean Drill. Program Sci. Results 130, 573-584.
- 1111 Stos-Gale, Z., Gale, N.H., Houghton, J., Speakman, R., 1995. Lead isotope data from the Isotracer
1112 Laboratory, Oxford: Archaeometry data base 1, ores from the Western Mediterranean.
1113 *Archaeometry* 37, 407-415.
- 1114 Terral, J.-F., Alonso, N., Buxó i Capdevila, R., Chatti, N., Fabre, L., Fiorentino, G., Marinval, P.,
1115 Pérez Jordá, G., Pradat, B., Rovira, N., Alibert, P., 2004: Historical biogeography of olive
1116 domestication (*Olea europaea* L.) as revealed by geometrical morphometry applied to
1117 biological and archaeological material. *J. Biogeogr.* 31, 63-77.
- 1118 Trouet, V., Esper, J., Graham, N.E., Baker, A., Scourse, J. D., Frank, D.C., 2009. Persistent positive
1119 North Atlantic Oscillation mode dominated the medieval climate anomaly. *Science*
1120 324(5923), 78-80.
- 1121 Vacchi, M., Ghilardi, M., Spada, G., Currás, A., Robresco, S., 2017. New insights into the sea-level
1122 evolution in Corsica (NW Mediterranean) since the late Neolithic. *J. Archaeol. Sci.: Reports*,
1123 12, 782-793.
- 1124 Vacchi, M., Joyse, K. M., Kopp, R. E., Marriner, N., Kaniewski, D., Rovere, A., 2021. Climate pacing
1125 of millennial sea-level change variability in the central and western Mediterranean. *Nature*
1126 *communications* 12(1), 1-9.
- 1127 Vacchi, M., Marriner, N., Morhange, C., Spada, G., Fontana, A., Rovere, A., 2016. Multiproxy
1128 assessment of Holocene relative sea-level changes in the western Mediterranean: sea-level
1129 variability and improvements in the definition of the isostatic signal. *Earth Sci. Rev.* 155, 172-
1130 197.
- 1131 Vacchi, M., Ghilardi, M., Melis, R.T., Spada, G., Giaime, M., Marriner, N., Lorscheid, T., Morhange,
1132 C., Burjachs, F., Rovere, A., 2018. New relative sea-level insights into the isostatic history of
1133 the Western Mediterranean. *Quat. Sci. Rev.* 201, 396-408.
- 1134 van Geel, B., 2001. Non-pollen palynomorphs. In: Smol, J.P., Birks, H.J.B., Last, W.M. (Eds.),
1135 *Tracking Environmental Change Using Lake Sediments. Terrestrial, Algal and Silicaceous*
1136 *Indicators, Volume 3.* Kluwer, Dordrecht, pp. 99-119.
- 1137 Vecchio, A., Lepreti, F., Laurenza, M., Alberti, T., Carbone, V., 2017. Connection between solar
1138 activity cycles and grand minima generation. *Astronomy & Astrophysics* 599, A58.
- 1139 Vella, M. A., Tomas, É., Thury-Bouvet, G., Muller, S., 2014. Nouvelles données sur le petit âge de
1140 glace en Corse: apports de l’analyse croisée des informations géomorphologique,
1141 palynologique et archéologique de la piève de Santo Pietro (désert de l’Agriate, Corse).
1142 Méditerranée. *Revue géographique des pays méditerranéens/Journal of Mediterranean*
1143 *geography*, (122), 99-111.
- 1144 Vella, M.A., Andrieu-Ponel, V., Cesari, J., Leandri, F., Pêche-Quilichini, K., Reille, M., Poher, Y.,
1145 Demory, F., Delanghe, D., Ghilardi, M., Ottaviani-Spella, M.D., 2019. Early impact of
1146 agropastoral activities and climate on the littoral landscape of Corsica since mid-Holocene.
1147 *PloS One*, 14(12), e0226358.

- 1148 Vigne, J.D., 1984. Premières données sur les débuts de l'élevage du Mouton, de la Chèvre et du Porc
1149 dans le sud de la Corse (France), in: Clutton-Brock J. et Grigson C. (Eds.), *Animals and*
1150 *Archaeology*, 3 - Early Herders and their Flocks. Proceedings 4th Int. Council for
1151 *Archaeozoology*, Londres, 1982, Oxford, Archaeopress, BAR International Series, 202, 47-
1152 65.
- 1153 Vigne, J.D., 1987. L'exploitation des ressources alimentaires en Corse du VIIe au IVe millénaire. In
1154 : Guilaine, J., Courtin, J., Roudil, J.L. et al. (Eds.), *Premières communautés paysannes en*
1155 *Méditerranée occidentale*. CNRS éditions, 193-199.
- 1156 Weis, D., Kieffer, B., Maerschalk, C., Barling, J., de Jong, J., Williams, G.A., Hanano, D., Pretorius,
1157 W., Mattielli, N., Scoates, J.S., Goolaerts, A., Friedman, R.M., Mahoney, J.B., 2006. High-
1158 precision isotopic characterization of USGS reference materials by TIMS and MC-ICP-MS.
1159 *Geochem. Geophys. Geosyst.* 7, Q08006.
- 1160 Weiss, M.-C., 2010. Au VIe millénaire avant notre ère. A Petra à L'île Rousse : campagnes de fouilles
1161 (2003-2006), Ajaccio, Albiana, 247 p.
- 1162 Wu, J., Yu, Z., Zeng, Z., Wang, N., 2009. Possible solar forcing of 400-year wet-dry climate cycles
1163 in northwestern China. *Climatic Change* 96, 473-482.
- 1164 Yu, Z.C., Ito, E., 2002. The 400-year wet-dry climate cycle in Interior North America and its solar
1165 connection. In: West, G.J., Blomquist, N.L. (Eds.), *Proceedings of the nineteenth annual*
1166 *pacific climate workshop*. Technical Report 71, 159-163.
- 1167 Zanchetta, G., Regattieri, E., Isola, I., Drysdale, R., Bini, M., Baneschi, I., Hellstrom, J., 2016. The
1168 so-called "4.2 event" in the central Mediterranean and its climatic teleconnections. *Alp.*
1169 *Mediterr. Quat.* 29, 5-17.
- 1170 Zonneveld, K.A.F., Marret, F., Versteegh, G.J.M., Bonnet, S., Bouimetarhan, I., Crouch, E., de
1171 Vernal, A., Elshanawany, R., Edwards, L., Esper, O., Forke, S., Grøsfjeld, K., Henry, M.,
1172 Holzwarth, U., Kieft, J.-F., Kim, S.-Y., Ladouceur, S., Ledu, D., Chen, L., Limoges, A.,
1173 Londeix, L., Lu, S.-H., Mahmoud, M.S., Marino, G., Matsouka, K., Matthiessen, J.,
1174 Mildenhall, D.C., Mudie, P., Neil, H.L., Pospelova, V., Qi, Y., Radi, T., Richerol, T., Rochon,
1175 A., Sangiorgi, F., Solignac, S., Turon, J.-L., Verleye, T., Wang, Y., Wang, Z., Young, M.,
1176 2013. Atlas of modern dinoflagellate cyst distribution based on 2405 datapoints. *Rev.*
1177 *Palaeobot. Palynol.* 191, 1-197.
- 1178
1179

LabID	Material	Depth (cm)	¹⁴ C Age±error BP	Cal. yr BP (2σ)	Cal. yr AD/BC (2σ)
GdA-5806	Organic sediment	49	1585±25	1527-1404	423-546 AD
Poz-115796	Organic sediment	50	3090±40	3389-3179	1440-1230 BC
GdA-5807	Organic sediment	77	2215±30	2330-2146	381-197 BC
GdA-5808	Organic sediment	93	2280±25	2349-2177	400-209 BC
Poz-110261	Charcoal	125	3260±90	3699-3252	1750-1301 BC
GdA-5809	Organic sediment	138	3090±35	3382-3210	1433-1261 BC
GdA-5810	Organic sediment	154	3215±30	3480-3373	1531-1424 BC
Poz-110260	Plant + Peat	185	3420±35	3823-3569	1874-1620 BC
GdA-5811	Organic sediment	229	4170±40	4834-4577	2885-2628 BC
Poz-110258	Peat	270	4175±35	4835-4580	2886-2631 BC
Poz-109794	Charcoal	340	4470±40	5297-4967	3348-3018 BC
Poz-110198	Peat	397	4530±30	5312-5051	3363-3102 BC
Poz-109887	Charcoal	450	4730±40	5581-5325	3632-3376 BC
Poz-105992	Bulk Sediment	487	5080±40	5917-5730	3968-3781 BC

1180

1181 Table 1. AMS Radiocarbon ages obtained from the materials of Crovani core. The calibrated ages
1182 are based on Intcal20 dataset ([Reimer et al., 2020](#)).

1183

1184 Figure Captions

1185 Figure 1. Location map of the study area and **coastal** sites of previous palynological research (white
1186 circle) conducted over the last decade for Corsica island (Del Sale: [Currás et al., 2017](#); Sagone:
1187 [Ghilardi et al., 2017a](#); Palo, Piantarella and Saint-Florent: [Revelles et al., 2019](#), [Revelles and](#)
1188 [Ghilardi, 2021](#); Canniccia: [Vella et al., 2019](#)). The purple squares indicate the position of known
1189 mining sites of galena/lead in Corsica. A: Hydrography and archaeology of the catchment basins
1190 ending in the Crovani Bay, green circle: Final Neolithic to Bronze Age site; Red circle: possible
1191 roman site of occupation; Orange square: 19th to 20th Cent. AD mining buildings; light green stars:
1192 Medieval site; 1: San Larenzu, 2: San Quilicu, 3: Teghja di Linu, 4: lower Argentella, 5: upper
1193 Argentella. B: Simplified geology and topography of the catchment basins ending in the Crovani
1194 Bay; Orange square: mining site Geographic coordinates are expressed in WGS 84 geodetic system.

1195
1196 Figure 2. View of the Crovani pond, borehole and Differential Global Positioning System- DGPS-
1197 profile (AA') locations. The light blue line (dash) indicates the present-day course of the rivers.
1198

1199 Figure 3. Age-Depth Model of the Crovani sequence, calculated through a Bayesian method using
1200 the computer program Bacon 2.5.5 ([Blaauw and Christen, 2011](#)). The Model is based on 14 AMS
1201 dates calibrated using the IntCal20 curve ([Reimer et al., 2020](#)).
1202

1203 Figure 4. Core lithology with ages expressed in cal. BC/AD and depths indicated in cm (left). For full
1204 details of the samples performed for ^{14}C AMS dating method (red squares), please check Table 1.
1205 Curves from left to right: Loss on ignition measurements with organic matter and carbonate contents,
1206 granulometric indexes (mean and mode), **mineralogical and geochemical proxies (halite, C/N ratio)**
1207 and Arboreal Pollen (AP) concentration (grains/gram).
1208

1209 Figure 5. A: Pb isotope results of the Crovani sedimentary core LCr18 reported in a binary diagram
1210 $^{207}\text{Pb}/^{206}\text{Pb}$ versus $^{208}\text{Pb}/^{206}\text{Pb}$. The dashed line indicates the linear regression trend between the
1211 Crovani samples. Circles: Crovani samples reported by different colors according to their
1212 stratigraphical position, i.e. pre-Roman samples, Roman and modern samples. The black circle
1213 indicates the average signature of the local geological background defined by the oldest measured
1214 **Chaleolithic Final Neolithic** samples. Black symbols: samples from different Pb-bearing mineral
1215 collected in West Corsica. The red triangle gives the averaged composition of modern **airborne**
1216 **[FN1]** particles collected above Roma in Italy (data from [Bollhöfer and Rosman, 2001](#)). Green squares:
1217 signature of Pb galene-rich ores from Sardinia. B: Close up emphasizing the representative signature
1218 of Pb ore mining districts surrounding the Mediterranean basin classed by country (green for Italy,
1219 blue for Greece, purple for Turkey and various colors from grey to orange for Spain ores). Data from
1220 literature reported in [Fagel et al., \(2017\)](#). The black arrow represents an extrapolation of the
1221 sedimentary mixing observed in core LCr18 in Figure 5A. It underlines the probable implication of
1222 the minerals of Tuscany in the Pb isotope signature of the Crovani sediments.
1223

1224 Figure 6. Pollen percentage diagram of Crovani, including the pollen zonation calculated with the
1225 CONISS method ([Grimm, 1987](#)).
1226

1227 Figure 7. Percentage diagram of Non-Pollen Palynomorphs from Crovani.
1228

1229 Figure 8. Summary pollen diagram including the cumulative percentages of gymnosperms, riparian
1230 trees, deciduous trees, evergreen trees and shrubs, OJCV curve, anthropogenic herbs, other herbs,
1231 coprophilous fungi, and saproxylic and phytopathogenic fungi), the Arboreal Pollen percentage
1232 record, the concentrations of Arboreal Pollen and Non-Arboreal Pollen, and the microcharcoal
1233 concentrations. The light green bars indicate phases of high storm activity in southern France

1234 (Sabatier et al., 2012). The blue bars indicate lake level highstands at Lake Accesa in central Italy
1235 (Magny et al., 2013). The orange bars indicate phases of dry climate conditions in south-central
1236 Mediterranean (Di Rita et al., 2018a). The NAO index is based on Franke et al. (2017).

1237

1238 Figure 9. REDFIT (A) analysis of the total Arboreal Pollen percentages (B) using the PAST 3.2
1239 software program (Hammer et al., 2001). In the REDFIT spectral analysis the time series is fitted to
1240 an AR1 red noise model (orange line). The 95% confidence levels of the χ^2 and Monte Carlo tests
1241 are reported on the graph with a green dashed line and a red dashed line, respectively.

1242

1243 Figure 10. Synoptic table with timing and nature of key environmental changes reconstructed from
1244 the Crovani record.

1245

1246

1247

1248

1249

Highlights

- A new palynological, sedimentological and geochemical study is presented from a coastal wetland of Corsica.
- The high-resolution 6000-year pollen record shows an unprecedented long persistence of *Erica* and *Quercus ilex* maquis.
- Human activities developed especially during the Late and Final Neolithic and the last 1000 years.
- Evidence of agriculture predates any Neolithic archaeological findings in this region.
- The 4.2 ka event, Homeric Minimum, and Little Ice Age are not associated with forest declines.

1 **Natural and anthropogenic dynamics of the coastal environment in**
2 **northwestern Corsica (Western Mediterranean) over the past six millennia**

3
4 **Federico Di Rita^{1*}, Matthieu Ghilardi², Nathalie Fagel³, Matteo Vacchi⁴, François Warichet³,**
5 **Doriane Delanghe², Jean Sicurani⁵, Lauriane Martinet⁶, Sébastien Robresco⁷**

6
7
8 ¹ Sapienza University of Rome, Department of Environmental Biology, Italy

9 ² CEREGE (CNRS UMR 7330-AMU-IRD-Collège de France-INRAE), Europôle de l'Arbois BP 80 13545 Aix-en-
10 Provence CEDEX 04 France

11 ³ AGES, Département de Géologie, Université de Liège, 4000 Liège, Belgium

12 ⁴ Dipartimento di Scienze della Terra, University of Pisa, Via Santa Maria 53, Pisa, Italy

13 ⁵ Association pour la Recherche Préhistorique et Protohistorique en Corse, Moncale, Corsica, France.

14 ⁶ CEPAM, CNRS UMR 7264-University of Nice Sophia Antipolis, Pôle Universitaire Saint Jean d'Angély, Nice,
15 France

16 ⁷ SIGOSPHERE, 69380 Chazay d'Azergues, France

17
18
19 * Corresponding author:

20 Federico Di Rita

21 +39 06 49912197

22 federico.dirita@uniroma1.it

23

24 Abstract

25

26 The present paper provides new insights into the climatic and anthropic factors that influenced a
27 6000-year coastal evolution in northwestern Corsica, the third largest island of the western
28 Mediterranean. Pollen, microcharcoal, sedimentary and geochemical analyses were carried out
29 on a core drilled in the Crovani coastal wetland to reconstruct the regional drivers of landscape
30 change. We show that anthropogenic and climate-induced fires favoured the development of
31 Mediterranean maquis, dominated by *Erica* and *Quercus ilex*, from ca. 6000 to 3350 cal. BP. A
32 change in arboreal vegetation triggered a short but intense sediment input in the Crovani pond
33 between ca. 3350 and 3200 cal. BP. This is consistent with a coeval process of runoff recorded in
34 several coastal sites of western Corsica and related to an arid climate change occurred in many
35 sites of the western Mediterranean around 3200 years ago. We provide evidence of agriculture
36 during the Late Neolithic from ca. 3900 BC, which is much earlier than any archaeological
37 evidence previously available in this area of Corsica, followed by a progressive decline of arable
38 farming practices. Human impact has been responsible for a degradation of the maquis only from
39 approximately 3000 cal. BP, and it intensified in Roman times, when the area experienced the
40 first phase of galena exploitation from the Argentella mines. Over the last 500 years, the present
41 work evidences a major development of *Castanea* related to cultivation during the Genoese
42 administration of Corsica. Our findings suggest that solar activity and the North Atlantic
43 Oscillation had an influence on centennial-scale forest cover variations during the last 6000 years.

44

45 **Keywords:** Corsica, pollen, palaeoenvironments, isotope geochemistry, geoarchaeology, western
46 Mediterranean, Holocene

47

48 1. Introduction

49 The island of Corsica hosts the largest number of coastal wetlands among the Mediterranean islands
50 ([Ghilardi, 2020 and 2021](#)). Most of them formed after the Mid-Holocene sea-level stabilization that
51 occurred in the Mediterranean Basin between 7000 and 6000 cal. BP ([Vacchi et al., 2016, 2018](#)).
52 Amongst the ~200 coastal wetlands of the island, brackish lagoons and coastal ponds are the most
53 common geomorphological features ([Ghilardi, 2020](#)).

54 The remarkable potential of pollen analysis to trace the main changes in the coastal landscape of the
55 island was first highlighted by the excellent palynological work of Maurice Reille ([Reille, 1984,](#)
56 [1991,1992a](#)). However, these pollen data were not provided with a robust chronology and did not
57 include the analysis of Non-Pollen Palynomorphs (NPPs) and other palaeoenvironmental proxies from
58 the same core.

59 In the last few years, several Corsican wetlands situated at a short distance of the sea were the subject
60 of multiproxy geoarchaeological research on the environmental impact of human activities, especially
61 in Prehistoric and Protohistoric times (Early Neolithic to Final Bronze Age, ca. 7500 BP to 2800 BP)
62 (Currás et al., 2017; Ghilardi et al., 2017a; Revelles et al., 2019; Vella et al., 2019; Figure 1). The
63 study of different palaeoecological proxies, such as ostracods, molluscs, and pollen, combined with
64 the chronostratigraphy of sediments, has shown the interest of reconstructing both the paleogeography
65 and the history of the vegetation of coastal Corsica starting from the ancient Neolithic (Cardial
66 culture, starting from 7500 ± 200 cal. BP; D'Anna et al., 2001; Lugliè, 2018).

67 The information of palaeoenvironmental records from Corsica is paramount for detailed
68 reconstructions of both land-use patterns and centennial-scale climate changes in the Mediterranean
69 Basin. Indeed, the island was a crossroad for many European and North African populations in the
70 conquest of the Mediterranean and occupies a strategic geographical location, potentially sensitive to
71 both North Atlantic climate patterns and north African atmospheric drivers (Sabatier et al., 2020).

72 The aim of this paper is to outline the landscape evolution in northwestern coastal Corsica over the
73 last six millennia, taking advantage of the recent progress in palaeoenvironmental reconstructions
74 (Henry et al., 2020), chronological models (Reimer et al., 2020), and new insights into the centennial-
75 scale patterns of atmospheric circulation during the Middle and Late Holocene (Franke et al., 2017;
76 Di Rita et al., 2018a; Sabatier et al., 2020).

77 Our new palynological and stratigraphical data are addressed to contribute to prominent unsolved
78 questions about times and drivers of vegetational change in Corsica, with a special focus on the
79 replacement of *Erica* shrublands with *Quercus ilex* woody formations during the Middle Holocene.
80 A second key topic is the origin and development of land use practices in northwestern Corsica. In
81 Neolithic times, there is sparse archaeological evidence for cereal cultivation and pastoral activities
82 along the coasts of Corsica. Cereal cultivation was revealed by pollen analyses only in the eastern
83 plain of Corsica and in the Saint Florent and Bonifacio-Piantarella areas (Currás et al., 2017; Revelles
84 et al., 2019), while the osteological identification of mammals buried in sheltered caves from southern
85 and northern Corsica provided evidence about the development of stockbreeding (Vigne, 1984, 1987).

86 A third unsolved question is related to the controversial role of climate changes in modifying the
87 vegetational landscape of Corsica. While at millennial time scale the influence of climate changes on
88 the vegetation and fires of the island has been clearly recognized (Reille 1992a; Leys et al., 2013;
89 Revelles et al., 2019; Lestienne et al., 2020a, b), the role of rapid climate changes (RCC) has been
90 seldom evoked in the regional palaeobotanical narrative. The apparent lack of vegetation responses
91 to centennial climate changes was attributed to either the overshadowing effect produced by local
92 resilient shrublands (Revelles et al., 2019) or the geographical position of Corsica, located in a

93 possible climate-unsensitive transitional area between the central and western Mediterranean (Di Rita
94 and Magri, 2019; Di Rita et al., 2022), two regions where RCC often produced contrasting moisture
95 changes (Di Rita et al., 2018a).

96 New detailed palaeoenvironmental data from Corsica are thus needed to disentangle these questions,
97 which are relevant for a better understanding of the natural and anthropogenic landscape changes in
98 the Mediterranean during the Holocene.

99

100 2. Study area

101 2.1. Present day landscape and vegetation

102 The Crovani pond is located in NW Corsica, in the westernmost part of a ~1 km² coastal plain (Fig.
103 1A). The plain collects the waters from two catchment basins with intermittent flow: the Argentella-
104 Cardiccia streams (catchment basin ~6 km²), incising metamorphic rocks (shales and micaschists)
105 and syenogranite, and the Marconcellu-Fiuminale streams (total catchment area: ca. 23 km²), draining
106 granodiorites, syenogranite, and Pliocene to Pleistocene scree in the lowermost river course (Fig.
107 1B).

108 Corsica has a typical Mediterranean climate highly influenced by its relief topography. The mean
109 annual temperature on the whole Island ranges between 14.5°C and 16.5°C and the mean annual
110 precipitation is 890 mm per year. On the coastal area, mean annual temperature is higher (17°C) and
111 freezing temperatures during the year are very seldom reported (Vella et al., 2019).

112 The Crovani wetland covers an area of ~0.3 km² behind a thick coastal barrier ≤5.30 m above the
113 mean sea level (amsl), made up of large well-rounded pebbles and cobbles (Fig. 2). The pond, which
114 is at 0.75 m amsl in the winter, is seasonal dry in the summer and has no direct link to the sea.

115 The surrounding wetland is a protected area, being included in the ZNIEFF (*Zone naturelle d'intérêt*
116 *écologique, faunistique et floristique*) n. 940004139 'Etang et zones humide de Crovani' with the aim
117 of preserving the following angiosperm species: *Euphorbia peplis* L., *Polygonum scoparium* Req. ex
118 Loisel., *Ranunculus ophioglossifolius* Vill., *Staphisagria picta* (Willd.) Jabbour, *Tamarix africana*
119 Poir., and *Vitex agnus-castus* L. The pond is surrounded by a belt of *T. africana* and is characterized
120 by a wet meadow covered by palustrine species dominated by *Bolboschoenus maritimus* (L.) Palla,
121 *Juncus acutus* L. and *Juncus maritimus* Lam. The coastal bar is occupied by a population of *Pistacia*
122 *lentiscus* L. and, on the top of the beach, by one of the most important Corsican populations of *Vitex*
123 *agnus-castus* (<https://inpn.mnhn.fr/zone/znief/940004139>). In spring, the very rare *S. picta* grows
124 among the pebbles (Jeanmonod and Schlüssel, 2006). The woody vegetation of the site consists of a
125 degraded *maquis* with *Erica arborea* L., *Arbutus unedo* L., *Pistacia lentiscus* L., *Phillyrea*
126 *angustifolia* L. and sparse *Quercus ilex* L. (Reille, 1992a).

127

128 2.2. Local archaeology and history of the human occupation

129 The first evidence of human settlement in Corsica dates back to the Mesolithic (Lugliè, 2018).
130 Abundant archaeological material allows to reconstruct the Neolithic settling history of the island
131 (Lugliè, 2018; Revelles et al., 2019). In northern Corsica a rich archaeological background is found
132 in a Mesolithic to Early Neolithic occupation in the Nebbiu area, at the Saint-Florent/Patrimonio sites
133 (Revelles et al., 2019). In the Balagne area, an important human occupation in a coastal context is
134 attested by the Early Neolithic site (Cardial culture) of La Petra, situated on a peninsula north of the
135 modern town of L'Île Rousse (Weiss, 2010).

136 In the Luzzipeu sector, situated in the southern part of the Balagne micro region, where the Crovani
137 pond is located (Fig. 1A), despite the paucity of recognized prehistoric settlements and uncovered
138 archaeological material, there is evidence of occupation during the Final Neolithic (starting from ca.
139 2800 cal. BC) at Teghja di Linu (Fig. 1A). The last site consists in a small village composed of huts,
140 located at an elevation of ~40 m amsl at ~1.5 km distance from the Crovani pond, where lithics were
141 discovered together with a menhir statue (Sicurani, 2008; Sicurani and Martinet, 2019; Ghilardi,
142 2020). Possible evidence of occupation during Late Neolithic times was hypothesized, but the lithics
143 uncovered are still under investigation (Sicurani and Martinet, 2019). Due to the presence of acidic
144 soils, derived from the erosion of the granitic bedrock, preservation of biological remains and
145 archaeological material in this stratigraphical context is difficult, so that there is no organic material
146 left in the archaeological layers that may help to evaluate the type of activities developed at the Teghja
147 di Linu site. Excavations conducted over the last two decades have revealed the existence of a habitat
148 composed of several circular large structures, delimited by tremendous rounded granitic boulders.
149 Protohistoric settlements are hardly documented in the Luzzipeu lowlands. Bronze Age sites are
150 situated more inland, generally on top of hills (Pecche-Quilichini, 2011). Iron Age and Roman times
151 are poorly documented, but archaeological surveys have revealed the presence of *tegulae* within the
152 mining complex of the Argentella, in use in the 19th to 20th century CE, indicating a first phase of
153 galena exploitation (Leleu, 2021). This sparse human occupation from Bronze Age to Roman times
154 radically contrasts with the Medieval archaeological remains attested at San Larenzu and San Quilicu
155 (Fig. 1A). Both are Romanic churches dated from the 11th Century CE and nowadays almost
156 disappeared due to their gradual destruction. From the Genovese administration to the French
157 administration, the region was attractive for the exploitation of natural resources, especially galena
158 minerals. Evidence for mining from the 16th to the early 20th centuries has been recorded (Leleu,
159 2021) but its impact in terms of landscape changes has never been investigated.

160

3. Materials and Methods

In this paragraph we present a synthetic version of materials analysed and techniques we used. For a more exhaustive explanation of the methodology applied in this research we refer to information reported in the Supplementary data.

The analyses presented in this study were carried out on a 6.25 m long sediment sequence, which was collected with a 50-mm vibracore (COBRA TT equipment – Atlas Copco) in the central part of the Crovani pond in August 2018 (Fig. 2).

The chronostratigraphy of the core was established using a series of 14 AMS radiocarbon determinations made in the Poznan and Gliwice (Poland) Radiocarbon Dating Laboratories. The Bayesian age-depth model (Fig. 3) was constructed using the software Bacon version 2.5.5 (Blaauw and Christen, 2011) with dates calibrated using the IntCal20 curve (Reimer et al., 2020).

Loss-on-ignition (LOI) measurements were performed on sediment samples of approximately 1 g taken at 10 cm intervals throughout the sequence, following the standard procedures published in Dean (1974) and Bengtsson and Enell (1986). (Fig. 4).

Samples used for LOI measurements were also analysed for granulometry. The grain-size distribution of the fine fraction (<2 mm) was measured by laser diffraction granulometry at CEREGE.

A C/N analysis was carried out on 28 samples from the core, selected according to their organic matter content: a minimum of 5% by weight of organic matter was required to continue. The method by Stax and Stein (1993) was used as a basis for the preparation of the samples. Results were obtained using an elementary analyser (Vario Microcube, Elementar) coupled to a mass spectrometer (Isoprime 1000) (Fig. 4).

The bulk mineralogy was measured on 28 samples in the upper 261 cm of the core. Most of the samples were retrieved from clayey sediments between 116 and 261 cm (20 samples), with a sampling resolution of 4 cm. In addition, 8 samples were retrieved between 11 and 106 cm. About 1 gram of dried bulk sediment sample was hand ground for mineralogical analyses. X ray diffraction (XRD) patterns of non-oriented powders (Moore and Reynolds 1997) were acquired between 2 and 30° 2 θ angle by using a Bruker D8-Advance Eco 1 Kw diffractometer equipped with a ceramic copper (K α radiance with $\lambda = 1.5418 \text{ \AA}$). The XRD data measured under a current intensity of 25 mA and a voltage of 40 KV were recorded with a Lynxeye Xe energy dispersive detector in the laboratory AGEs at the University of Liège. The minerals were identified by their peak positions and their abundance was calculated from the intensity on selected diffraction peaks (Cook et al. 1975).

The bulk samples for Pb isotopes analyses were digested using a tri-acid attack of HF/HNO₃/HCl in a laminar flow hood. The Pb purification was made according to the procedures published in Weis et

195 al. (2006). The Pb isotopes were measured by static multicollection in dry mode on a Nu Plasma I
196 MC-ICP-MS instrument at the University of Brussels. The values were normalized using the
197 recommended NBS981 values ($^{208}\text{Pb}/^{204}\text{Pb}$ 36.7219 ± 61 , $^{207}\text{Pb}/^{204}\text{Pb}$ 15.4963 ± 17 , $^{206}\text{Pb}/^{204}\text{Pb}$
198 16.9405 ± 24) from Galer and Abouchami (1998). The Pb isotopes ratios were measured on 24 clayey
199 samples retrieved in unit VI and VIII with a ~5 cm sampling resolution between 11 and 260 cm (Table
200 S1).

201 In addition, some Pb-bearing minerals were collected in different Corsican ores or mineralised veins
202 on the Paleozoic granites from west Corsica (Fig. 5). We have sampled the main Pb mineral galena
203 (PbS) and also some Pb-bearing minerals like arsenopyrite (FeAsS). Galena was sampled in the mine
204 of Argentella, 2.5 km from the Crovani pond but also in the mine of Lozari (along the northwestern
205 coast, east of Île Rousse) and in a mineralized vein in Prunelli (south of Porto - see locations in Fig.
206 1). In addition, an arsenopyrite mineral sample was collected in the Finosa Pb-Zn-Ag ore close to
207 Ghisoni (Fig. 1).

208 Pollen analysis was carried out on 62 samples. Pollen extraction followed the standard procedures
209 summarized by Magri and Di Rita (2015). Pollen grains and NPPs were identified by light microscope
210 at 400 and 640 magnifications, with the help of both pollen morphology atlases (e.g., Reille, 1992b;
211 Beug, 2004) and NPPs reference articles (e.g., Van Geel, 2001; Cugny et al., 2010; Gelorini et al.,
212 2011).

213 Microcharcoal analysis was carried out to reconstruct fire history, following the procedures described
214 by Clark (1982). A series of 150 microscope fields were checked for each sample. Microcharcoals
215 smaller than 5 μm were excluded from the sum. The computer program Psimpoll 4.27 (Bennett, 2009)
216 was used to plot the percentage and concentration diagrams, as well as to subdivide the pollen record
217 into 8 local assemblage zones, numbered from the base upwards and prefixed by the site abbreviation
218 CRO, by means of the CONISS method (Grimm, 1987).

219 A REDFIT spectral analysis (Schulz and Mudelsee, 2002) using the PAST 3.2 software (Hammer et
220 al., 2001) was applied to the unevenly spaced time series represented by the total Arboreal Pollen
221 (AP) percentages to detect the possible occurrence of a fundamental tempo in the forest cover
222 changes.

223

224 4. Results

225 4.1. Chronostratigraphy

226 Based on the laser grain size determination and on the organic matter/carbonate contents, eight
227 stratigraphic units were defined from the bottom to the top (Fig. 4).

228 Unit I is found between 6.25 and 5.95 m depth. It consists of a mixture of well-rounded pebbles
229 cemented within a sandy matrix and grey clays containing from 2 to 5% of organic matter. Due to the
230 paucity of organic material, radiocarbon dating of this sedimentary unit was impossible.

231 Unit II is found between 5.95 and 5.45 m depth. It comprises medium to coarse grey sands with local
232 intercalations of angular gravels (centimetric in size). Organic matter and carbonate content are very
233 low (1-2%), hindering any radiocarbon dating of Unit II. No biomarkers were identified.

234 Unit III is encountered between 5.45 and 3.73 m depth (~6300-5170 cal. BP; ~4350-3220 BC). It
235 consists of homogeneous grey clays. The organic matter content ranges between 10 and 15% while
236 carbonate content shows values comprised between 6 and 9%.

237 Unit IV occurs from 3.73 to 2.95 m depth (5170-4760 cal. BP; 3220-2810 BC). It shows features
238 similar to Unit II. It consists of coarse sands with intercalated layers of gravels with sharp edges,
239 witnessing variations in the energy of deposition, in particular at the point of changeover with Unit
240 III. In the lowermost part of Unit IV, a layer of 15 cm consists of angular gravels without sedimentary
241 matrix. Organic matter and carbonate contents (both < 2%) are low, like Unit II. Radiocarbon dating
242 of this lowermost portion is consistent with a time interval encompassing the Late to Final Neolithic.

243 Unit V, between 2.95 and 2.72 m depth (4760-4630 cal. BP; 2810-2680 BC), consists of organic
244 coarse sandy clays. Organic matter content increases upwards (1-7%). The carbonates content is
245 lower than 2%.

246 Unit VI is found from 2.72 and 1.42 m depth (4630-3320 cal. BP; 2680-1370 BC) and exhibits
247 sedimentological parameters similar to Unit V. It consists of organic clays with 10-20% of organic
248 matter and $\leq 8\%$ of carbonate. The XRD mineralogy (Fig. S1) reveals the dominance of detrital
249 minerals (~50% of quartz, K-feldspars and plagioclase with traces of amphibole and chlorite). They
250 are associated to clayey minerals (~30% of total undifferentiated clays), aragonite (3 to 8%) from
251 biogenic fragments and evaporites (8% < halite < 12% - Fig. 4). Radiocarbon dating of the unit is
252 consistent with a time interval ranging from Final Neolithic to Middle Bronze Age.

253 Unit VII is encountered from 1.42 to 1.32 m deep (3320-3190 BP; 1370-1240 BC). It consists in a
254 thin layer (10 cm) of homogeneous yellow fine sands showing a modal index of 90 μm with a mean
255 grain size of 20 μm (fine silts). The granulometric analyses exhibit a multimodal distribution of the
256 particles. Positive excursion in detrital minerals (cumulated abundance over 70 %) is observed for
257 Unit VII and corresponds to a significant increase in quartz (28%) and plagioclase (25 %) and a
258 relative drop in total clays minerals (13%) (Fig. S1).

259 Sedimentary Unit VIII is identified in the uppermost 1.32 m depth (3190-0 cal. BP; 1240 BC-1950
260 AD). Homogeneous grey clays record numerous traces of oxidation corresponding to rootlets. The
261 organic matter content is homogeneous (6 to 8%), while carbonate content is low (2-3%). The XRD

262 mineral association remains similar to unit VI, except the abundance of evaporites. A drop of halite
263 below 4% occurs between 166 and 150 cm, i.e. in the upper part of unit VII but close to the transition
264 with unit VI (Fig. 4). The rate of sediment accumulation for Unit VIII is very low, with values of ~4.3
265 mm per century.

266
267

268 4.2. C/N results

269 The uppermost 2 m sediment, spanning the last four millennia, were investigated for C/N ratio (Fig.
270 4). The averaged C/N ratio is high (> 10) and exceeds a value of 16 above 1.16 m suggesting a mainly
271 terrestrial origin of the organic matter. The values range between 11 to 14 from 1.16 to 2 m, indicating
272 a mixture of organic matter from vascular plants and algae. The highest value (~30) measured at 1.36
273 m indicates an episode of high input of sediments of continental origin, with a mix of vascular plants
274 and cellulosic plants, dated ca. 1430 to 1260 BC.

275

276 4.3. Lead isotopes analyses

277 The three Pb isotopic ratios evolve in parallel in the 260-upper cm, from Final Neolithic to present
278 (Fig. S2). The $^{208}\text{Pb}/^{204}\text{Pb}$ ranges between 38.60 and 39.01 (average 38.9353 ± 0.0019), the $^{207}\text{Pb}/^{204}\text{Pb}$
279 between 15.65 and 15.68 (average 15.6703 ± 0.0007), and the $^{206}\text{Pb}/^{204}\text{Pb}$ between 18.61 and 19.11
280 (average 19.02 ± 0.0008) (Table S1). Even if some scattering of the data is observed for the studied
281 pre-Roman period (i.e., 260-93 cm), the isotopic Pb ratios depict a marked decreasing trend upwards.
282 This major change starts at 73 cm (Fig. S2) during the Roman period and continues over the modern
283 period. The lowest isotopic ratios are measured in the shallowest samples at 11 and 17 cm.

284

285 4.4. Pollen analysis and statistical analysis on pollen time series

286 The results of pollen analysis are presented as: 1) a detailed percentage diagram, including most of
287 the pollen taxa and a summary Arboreal Pollen (AP)/Non Arboreal Pollen (NAP) percentage diagram,
288 plotted against age (Fig. 6); 2) a percentage diagram displaying the main NPPs (Fig. 7); 3) a synthetic
289 diagram including cumulative pollen percentages of ecological groups (conifers, riparian trees,
290 deciduous trees, evergreen trees and shrubs, OJCV (*Olea+Juglans+Castanea+Vitis*), anthropogenic
291 herbs, other herbs, coprophilous fungi, and saproxylic and phytopathogenic fungi), AP percentage,
292 the concentrations of AP and NAP, microcharcoals, and some climate proxies (Fig. 8).

293 The pollen preservation was good with percentages of undeterminable grains seldom exceeding 4%.

294 An average of 310 pollen grains of terrestrial taxa per sample were counted. The biodiversity was
295 represented by 92 different pollen taxa (terrestrial + aquatic plants) summed to 45 types of ferns,
296 algae, fungi, and other NPPs. The palynological richness, estimated by rarefaction analysis (Birks
297 and Line, 1992), is always over 15 terrestrial pollen types per sample. Total pollen concentrations
298 vary from 7000 to 321,000 terrestrial pollen grains/g sediment. The features of the local pollen
299 assemblage zones are summarized in the Supplementary Materials.

300 A REDFIT analysis was applied to the unevenly sampled time series represented by the total AP
301 percentages, which show a clear fluctuating trend consistent with changes in forest cover rather than
302 random fluctuations due to pollen representation and preservation (Fig. 9).

303 The results of the REDFIT exhibit a peak in power spectrum exceeding 95% of the false-alarm levels
304 of both χ^2 and Monte Carlo tests, corresponding to a statistically significant periodicity of ca. 228
305 years (time=1/frequency), and less significant frequencies centred at 996 and 430 years, which
306 however exceed 90% of the false-alarm levels of both χ^2 and Monte Carlo tests (Fig. 9).

307

308 5. Discussion

309

310 5.1. Evolution of the vegetational landscape

311 During the Middle and Late Holocene, from ca. 6100 to 1000 cal. BP (4150 BC-950 AD), the Crovani
312 pond was surrounded by a dense *Erica*-dominated tall *maquis*, accompanied by several evergreen
313 elements, such as *Q. ilex*, *Phillyrea*, *Pistacia*, and *Olea* (Figs 6, 8, and 10). This observation is
314 consistent with other palynological studies from southern Corsica (Reille, 1975, 1984; Revelles et al.,
315 2019, Vella et al., 2019) and on the Cavallo island, situated in the strait of Bonifacio (Poher et al.,
316 2017). An almost continuous record of *Arbutus* indicates that strawberry trees was a common
317 presence in the *Erica arborea* formations, as its pollen tetrads are poorly dispersed. The most
318 degraded sectors of this *maquis* vegetation were probably occupied by low shrublands of *Cistus*,
319 which played a prominent role in the dune and sandy soil vegetation together with *Olea*, *Pistacia* and
320 other thermophilous shrubs, as also reported from other coastal sites of western Corsica (Reille,
321 1992a).

322 The pollen record from Crovani provides new data to investigate the complex interplay between
323 *Erica*-dominated and *Q. ilex*-dominated vegetation and their turnover in Corsica. According to Reille
324 (1992a), *Erica* woodlands, representing the climax vegetation in lowland areas of western Corsica,
325 underwent a major degradation process since the neolithization of the island, as a result of increasing
326 human impact. It was largely replaced by *Quercus ilex* during the Mid- to Late Holocene (Reille,
327 1992a, Carcaillet et al., 1997). Recent palynological studies (Revelles et al., 2019) confirmed the

328 anthropic causation of this vegetation turnover and suggested that it started with the development of
329 agropastoral practices during the Early Neolithic, hence significantly earlier than the period
330 previously identified by Reille (1992a). Similar vegetation dynamics were reported also in Sardinia,
331 where a clear development of *Quercus ilex*, leading to a partial or complete replacement of the late
332 successional *Erica* shrublands, is recorded since the 6th millennium BP (Di Rita and Melis, 2013;
333 Beffa et al., 2016; Melis et al., 2017, 2018; Pedrotta et al., 2021). In contrast, the pollen record from
334 Crovani (Fig. 6) indicates that the frequencies of *Erica* were continuously high until ~2900 BP and
335 were not replaced by *Q. ilex*. Our pollen record even shows two temporary major increases in *Erica*
336 at the expense of holm oaks in the time-intervals 4700-4300 and 3350-2900 cal. BP. High frequencies
337 and concentrations of *Erica* and *Q. ilex* concur in depicting a *maquis* characterized by high biomass
338 and decomposed organic matter, as suggested by generally high values in the loss of ignition and a
339 significant presence of saproxylic and phytopathogenic fungi, such as *Kretzschmaria deusta*,
340 *Asterosporium* and Xylariaceae (Fig. 7)..

341 In Sardinia, Beffa et al. (2016) hypothesise that a protracted dominance of *Erica* and the absence of
342 evergreen oak forests in the first part of the Middle Holocene (until ca. 5300 cal. BP) were related to
343 warmer/drier summers and cooler/moister winters than today. They suggest that also in Corsica such
344 a climate regime, characterized by frequent and prolonged droughts during the spring and summer,
345 may have led to frequent seasonal wildfires advantaging communities dominated by *Erica scoparia*
346 and *Erica arborea*, which are two fire-adapted species able to quickly resprout and generate new
347 aboveground biomass after frequent and intense fires. In contrast, *Quercus ilex* is considered to have
348 been severely affected by natural and anthropogenic fires and favoured by a climate change leading
349 to increased summer rainfall and decreased fire occurred at the end of the Middle Holocene
350 (Colombaroli et al., 2009; Beffa et al., 2016; Pedrotta et al., 2021).

351 In contrast to this view, at Crovani, high concentrations of microcharcoal, reflecting fires, are
352 recorded in correspondence of high values of both *Erica* and *Q. ilex*. Contemporary high values of *Q.*
353 *ilex* and microcharcoal support the interpretation of Reille (1992a) and Carcaillet et al. (1997), which
354 suggest that the development of holm oak in Corsica was triggered by anthropogenic fires. At
355 Crovani, a substantial portion of the Mid-Holocene fires may be related to human activity, which is
356 witnessed by a significant presence of anthropogenic indicators (Figs 6-8). High frequencies of
357 microcharcoal in zones CRO-1 and CRO-2 are consistent with the coeval high incidence of fires
358 recorded in the region (Leys et al., 2014; Lestienne et al., 2020a, b), most of which are attributed to
359 human activity. According to Lestienne et al. (2020b), since 5000 cal. BP humans have taken control
360 of the fire regime through agro-pastoralism, favouring large and/or frequent fire events. For the same
361 reason, the marked decrease in microcharcoal recorded at Crovani during the Late Holocene after

362 ~3350 cal. BP, which matches a decrease in anthropogenic pollen indicators, may reflect decreased
363 human activity, at a time of an unsuitable climate for fires.

364 Starting from ~2900 cal. BP, there was a general decline in *Erica*, opposed to an increase in holm
365 oaks, which led to a turnover of the two woody taxa between 2300 and 1900 cal. BP. In this time-
366 interval, an increase in oaks may have been influenced by the forestry practices of Roman times. All
367 the same, in the last ~2500 years, a clear development of cork oak in Corsica (Reille, 1984, 1992a),
368 Sardinia (Di Rita and Melis, 2013), and the western Iberian Peninsula (Carrión et al., 2000) may be
369 related to silvicultural practices.

370 Between 1900 and 1000 cal. BP (pollen zone CRO-6), a new moderate increase in *Erica* at the
371 expense of *Q. ilex* suggests a new expansion of the native *Erica*-dominated shrublands.

372 Between 1000 and 500 cal. BP (pollen zone CRO-7), a major degradation of the forest cover is
373 recorded, with a massive decline of the tall *maquis* that was replaced by *Cistus*-dominated low
374 shrubland. After ~ 500 BP, *Erica* and *Q. ilex* recovered, as recorded also in other sites of Corsica (e.g.
375 Vella et al., 2019).

376 Modest oscillations of deciduous trees throughout the record (Fig. 6 and 8) suggest that they were
377 scarcely involved in the environmental processes influencing the evergreen vegetation, probably
378 because they were located at higher elevations in the island. Frequent finds of mesophilous trees such
379 as *Fagus* and *Betula*, which require temperate and humid conditions, confirm that part of the pollen
380 rain originated from the montane vegetation belt. The fingerprint of deciduous trees in the pollen
381 record of Crovani, as in other coastal pollen records of Corsica (Reille, 1992a; Currás et al., 2017;
382 Revelles et al., 2019), is clearly due the steep topography of the island, which determined a relatively
383 low distance of montane and sub-montane vegetation belts from the coast. However, it cannot be
384 excluded that sparse stands of mixed oak communities could also be preserved in humid areas at low
385 elevations, especially inside floodplain and riparian woodlands, dominated by *Alnus*, accompanied
386 by *Salix*, *Tamarix*, and possible wild *Vitis*, which are still documented in the area (Reille, 1992a).

387 Conifers are mostly represented by *Pinus*, substantially reflecting the persistence of *Pinus nigra*
388 subsp. *laricio* at montane and sub-montane elevations since the late glacial period (Leys et al. 2014).
389 The occurrence of *Pinus pinaster* since the Bronze Age is probably related to human activity (Reille,
390 1992a). In addition to pine, conifers include taxa distributed in both lowland/coastal areas, such as
391 *Juniperus*, and in montane sectors, such as *Abies* and *Taxus* (Fig. 7). Rare occurrences of *Picea*,
392 whose current natural range does not include Corsica, are of distant origin.

393

394

395

396 5.2. Environmental responses to hydrological and morphosedimentary processes

397 The local aquatic environment outlined by the pollen record ranged from brackish (6100-3400 cal.
398 BP) to freshwater conditions (~3400 cal. BP-present day) (Fig. 10). This range is documented by the
399 presence of freshwater taxa, such as *Spirogyra*, *Zygnema* and *Myriophyllum*, salt-tolerant species,
400 such as *Ruppia maritima*, and marine organisms, represented by foraminiferal linings, pointing to
401 inputs of salt-water into the pond (Bellotti et al., 2016). This was likely related to the morphological
402 response of the pond to the Mediterranean sea-level rise whose average rates decreased from ~2 mm
403 a⁻¹ at ~6100 BP to less than ~0.5 mm a⁻¹ in the last 3500 years (Vacchi et al., 2021). These major
404 changes in the rising rates probably have an influence on the connection of the pond with the open
405 sea as already observed in lagoonal setting both in Corsica (e.g. Vacchi et al., 2017; Revelles et al.,
406 2019) and in Sardinia (Melis et al., 2017, 2018). However, the absence of fossil faunal associations
407 hampered a detailed reconstruction of the nature of this backshore environment and its millennial
408 evolution.

409 The lower part of the record (~6100 to ~4800 cal. BP) is characterized by high frequencies of
410 *Spiniferites* sp. (Fig. 7), dinoflagellate cysts often difficult to identify at the species level by routine
411 observation in light microscopy (de Vernal et al 2018). The genus *Spiniferites* is characterized by
412 marine species, but it cannot be excluded that some Mediterranean species live in freshwater
413 environments (Kouli et al., 2001; Zonneveld et al., 2013). Based on pollen records obtained from
414 central Mediterranean regions, the presence of *Spiniferites* is often associated to brackish water (Di
415 Rita et al., 2018b). Irrespective of water salinity, high frequencies of *Spiniferites* in the lower part of
416 the Crovani sequence may reflect the pioneer stages of a hydrosere succession connected to the early
417 phases of development of the coastal pond.

418 From ~4800 to ~3350 cal. BP (zone CRO-2), a significant increase in *Ruppia maritima*, a submerged
419 angiosperm with large salinity tolerance (Kantrud, 1991), coupled with occurrences of foraminiferal
420 linings, highlights a brackish environment. It is consistent with the observed presence of halite in unit
421 VI (Fig. 4). Beds of submerged widgeongrass plants usually occur on muddy sand and mud in
422 brackish pools. They accumulate sediment and may be associated with terrestrial saltmarsh plants,
423 forming a hydrosere succession in coastal wetlands (Rodwell, 2000).

424 Starting from ~3350 cal. BP, the abrupt decrease in *Ruppia* and the disappearance of most spores of
425 fungi, coupled with a major increase in *Pseudoschizaea* (2%) and fern spores, are the results of
426 complex sedimentological and ecological changes leading to a lowering of the water level and to the
427 establishment of the present-day marshy environments. *Pseudoschizaea* suggests both desiccation
428 (Scott, 1992) and freshwater flows accompanied by erosive processes, sometimes associated with
429 runoff events (Pantaléon-Cano et al., 2003), while the disappearance of most fungal spores, the

430 decrease in pollen concentrations, and the high percentages of Cichorioideae (Figs 6-8) can be
431 interpreted as selective preservation of palynomorphs (Bottema, 1975; Havinga, 1984).

432 It is noteworthy that Reille (1992a) recorded a sharp drop in *Ruppia* at 150 cm depth and correlated
433 it with a local change in sediment accumulation. This was caused by an event of forest clearance,
434 followed by an increase in runoff, leading to the accumulation of a sandy layer and a significant
435 development of ferns. In our record, a phase of increased terrestrial runoff is revealed by an input of
436 organic matter of continental origin recorded by a positive excursion of C/N ratio at 1.36 m (ca. 3250
437 cal. BP - Fig. 4) and by a significant increase in detrital minerals (Fig. S1), but is not preceded by
438 clear changes in AP percentages that may testify to a deforestation process, although there is a drop
439 in AP concentrations around 3350 cal. BP. A clearance of local shrubs, represented by a sharp decline
440 in *Erica* frequencies, was recorded only after ~3100 cal. BP (Figs 6 and 8).

441 Summarizing, initially the opening of the vegetation did not change the composition of the shrubland,
442 which was later affected by the drop of *Erica*. Sedimentological analyses indicate an increase of the
443 granulometry within a broader context of swamp environment of deposition characterized by
444 homogeneous clays. At ~136 cm depth (ca. 3250 cal. BP), there is an event of higher energy of
445 deposition characterized by the punctual presence of coarse silts to fine sands. In the Canniccia pond,
446 located in SW Corsica, Ghilardi et al. (2017b) and Vella et al. (2019) identified a high detrital input
447 dated ca. 3350 cal. BP. At a regional scale, the southern France recorded an intense phase of
448 alluviation within the Rhone drainage basin (Berger et al., 2007) and the Pyrenean mountains (Galop
449 et al., 2007). This is possibly explained by the occurrence of a cooler and more arid period that resulted
450 in deforestation on a regional scale (Ghilardi et al., 2017a), recognized in western Mediterranean
451 pollen records (Carrión, 2002; Fletcher et al., 2013) and in speleothems from Tuscany located only
452 ca. 200 km from Crovani (Regattieri et al., 2014). However, the eastern coast of Corsica did not
453 record such event (Currás et al., 2017), which seems to have especially affected western Corsica.

454 Since ~2900 cal. BP, an expansion of ferns and other hydrophytes (Fig. 7) suggests stagnant water,
455 which may have been produced by a lowering of the lake enhanced by runoff, sediment infilling, and
456 a salinity change towards more freshwater conditions. This change is confirmed by the observed
457 decrease in the halite since the final part of units VI (Fig. 4). Such pattern is consistent with a
458 substantial sea-level stability, which occurred in the NW Mediterranean Sea in the last ~2000 years
459 (Vacchi et al., 2021). This stabilization process significantly decreased the salinity input within the
460 pond triggering the progressive transition in pure freshwater environment.

461 Overall, the sequence dinoflagellates (*Spiniferites*) → aquatic plants (*Ruppia maritima*) → ferns
462 profiled throughout the pollen record corresponds to a hydrosere succession, whose evolution is
463 strictly related to the sediment infilling of lakes (Fig. 6). This ecological succession typically involves

464 reed swamp vegetation at an intermediate stage, here represented by pollen of Cyperaceae and partly
465 of Poaceae, and *Alnus* at a mature stage. In several coastal sedimentary archives of the central
466 Mediterranean, temporary expansions of Cyperaceae and Poaceae are followed by an increase in
467 *Alnus* (Magri et al., 2019 and references therein). At Crovani this pattern is especially clear in the
468 interval between ~2600 and ~1700 cal. BP, when complete hydrosere succession with a climax
469 woodland stage occurred in marginal sectors of the basin, in relation to a lagoon reduction (Fig. 6).

470

471 5.3. Human impact on the landscape

472 Human activity is evident throughout the pollen record with different intensity and type of land use
473 (Fig. 10). During the Late Neolithic, from ~3900 to ~3250 BC, the continuous curve of cereal-type
474 pollen testifies to early cultivations (Fig. 6). Evidence for agriculture is also observed at the Saint
475 Florent site starting from ~4000 cal. BC (Revelles et al., 2019), but only the extreme south of the
476 island (Bonifacio-Piantarella area) exhibits continuous agricultural practices all along the Neolithic
477 period. At Crovani, the pollen record reveals human activity older than the archaeological finds,
478 indicating that farming was practiced ~1000 years before the earliest trace of human occupation at
479 the Teghja di Linu site (Sicurani and Martinet, 2019).

480 Cereal cultivation appears associated to livestock rearing activities, which contributed to the
481 development of disturbed meadows, as highlighted by a significant record of *Sporormiella*, *Sordaria*,
482 and *Podospora*, and by pollen indicators for Mediterranean pasturelands, such as *Carduus*-type,
483 *Plantago*, *Polygonum aviculare*-type, as well as some species of the subfamilies Asteroideae and
484 Cichorioideae (Desprat et al., 2013; Florenzano et al., 2015) (Figs 6 and 8). The high values of
485 microcharcoal may partly reflect the use of fire for farming purposes, such as slash-and-burn
486 practices, which however did not affect the fire-adapted local shrubland. In general, human activity
487 during the Late Neolithic certainly influenced the vegetation evolution of the area, but its impact did
488 not produce a marked local deforestation. While we cannot advance any precise explanation for this
489 pattern, we can speculate that local settlements were not populated enough to produce forest declines
490 detectable in the pollen diagram.

491 During the Final Neolithic and Bronze Age (from ~3000 to ~800 BC), both cereal cultivation and
492 livestock rearing appear less intense and discontinuous. The archaeological history of Corsica
493 indicates that Early to Middle Bronze Age are periods of human implantation in the upper part of the
494 hills (Casteddi) when lowlands and coastal areas were less occupied (Cesari and Pêche Quilichini,
495 2015). The pollen record from Crovani confirms this pattern, even if in some coastal areas the Mid-
496 to Late Bronze Age corresponds to a phase of renewed agriculture (Ghilardi et al., 2017a).

497 In the Iron Age, cereals disappeared and scattered occurrences of pasture weeds (e.g., *Carduus*,
498 *Plantago*, and *Rumex*) testify to poor farming practices addressed to livestock rearing, suggesting a
499 scarce human frequentation in the area (Fig. 6).

500 Human activity at Crovani is also revealed by the record of cultivated trees (OJCV curve, Fig. 8),
501 which also include pollen of wild individuals of *Olea* and *Vitis* that is difficult to differentiate from
502 pollen of cultivated plants (Reille, 1992a).

503 In the period encompassing the Neolithic to the Bronze Age the pollen record of Crovani shows some
504 early occurrences of *Juglans* (ca. 3700 BC) and *Castanea* (ca. 1200 BC) (Fig. 6). Similar early finds
505 are also recorded in pollen diagrams from recently published coastal sites (Poher et al., 2017; Currás
506 et al., 2017; Revelles et al., 2019). Although these occurrences are generally found during phases of
507 intense human activity, as confirmed by the presence of other anthropogenic pollen indicators, it is
508 difficult to hypothesize that cultivation of these trees was such early, without a clear archaeobotanical
509 evidence. Unfortunately, the palynological studies of Reille (1992a; 1999) and Lestienne (2020a) do
510 not contribute to solve this question, since their records do not show any *Castanea* and *Juglans* before
511 2500 cal. BP. They interpret these finds as a result of cultivation in the island in historical times. In
512 addition, the absence of palynological investigations from Pleistocene sediments prevents us to
513 speculate on a possible redeposition of pollen from older deposits. We would exclude a long-distance
514 origin, especially for *Juglans*, whose pollen dispersal occurs over short distance despite its renowned
515 anemophily (Carrión and Sánchez-Gómez, 1992).

516 Phylogeographical studies demonstrate that the post-glacial distribution of chestnut and walnut in
517 Europe and in the Mediterranean regions started from multiple glacial refugia (Mattioni et al., 2013;
518 Pollegioni et al., 2017). However, due to both the scarcity of palaeobotanical knowledge and
519 incomplete genetic sampling, as in the case of Corsica and Sardinia, there is still much uncertainty in
520 detecting glacial refugia and drawing up robust biogeographical histories of cultivated trees (Médail
521 et al., 2019).

522 In historical time, the OJCV record shows two major phases of tree cultivation. The first one, between
523 ~250 BC and ~150 AD, reflects a widespread exploitation of olive resources during the Roman
524 Period, also documented by archaeological evidence (Terral et al., 2004). The second increase, after
525 ~1450 AD, testifies to an intensification of *Olea* cultivation and a regional plantation of *Castanea* in
526 the uplands. From 1548 until the 17th century, the Genoese Authority introduced the compulsory
527 cultivation of chestnut, whose fingerprint in the Crovani record is represented by a peak of *Castanea*
528 (Fig. 6) (Michon, 2011). The consequence of this decree was a large reorganization of the food,
529 economy, and socio-cultural systems, as shepherds slowly became chestnut growers and settled more
530 permanently in mid-mountain villages. The chestnut culture fully developed during the 18th and 19th

531 centuries, providing flour for daily meals, fodder for animals, and fruits for trade. By the end of the
532 19th century, the development of local industries and the related outflow of rural population toward
533 urban centres determined the collapse of the chestnut culture (Michon, 2011).

534 Human impact on the forest cover is recorded since ~1000 BC (Final Bronze Age), mostly by
535 decreases in evergreen trees and shrubs staggered over time (Fig. 8), coupled with increases in both
536 herbaceous vegetation and *Cistus* dominated low shrublands (Figs 6 and 8). Considering the local
537 modest farming practices of the last three millennia, this pattern may mostly reflect clearance
538 practices of the *Erica* shrubland at a regional scale. This is consistent with the human-induced
539 opening of the forests recorded in several other pollen sites of Corsica (Reille, 1992a; Revelles et al.,
540 2019; Lestienne et al., 2020a), and in coastal sites of the central Mediterranean since ~1000 cal. BC
541 (Di Rita and Magri, 2012). According to Roberts et al. (2019), after ~1000 BC human activity became
542 the dominant causation in determining landscape openings in the Mediterranean regions

543 Despite clear land use changes are recorded, human activities at Crovani did not completely transform
544 the structure of the vegetation in terms of forest canopy, except for a temporary dramatic drop of the
545 *maquis* vegetation between 950 and 1450 AD (1000-500 cal. BP), for which a prominent
546 anthropogenic causation cannot be ruled out. Pollen indicators of human activity are scarce in this
547 period, but the reappearance of coprophilous fungi (*Sporormiella*) and the increase in *Castanea* and
548 *Olea*, together with a slight increase in fire frequency, may reflect silvicultural practices addressed to
549 the felling of shrublands to gain land available for both stock rearing and olive cultivation in the
550 lowlands, as well as for chestnut cultivation in the uplands. A similar observation was advanced in
551 the Saint-Florent area, where an important deforestation phase was coeval to the development of
552 pastoral activities (Revelles et al., 2019). Between ~1000 and ~500 cal. BP, also frequencies >2% of
553 *Pseudoschizaea* and *Glomus* support soil erosion and local deforestation (Figs 7 and 10). This was
554 also the time when several churches were locally built (Fig. 1A).

555 The human activities may also be tracked from the Pb isotope signature of the Crovani sediments.
556 The sedimentary Pb data are aligned along a linear trend in a binary $^{208}\text{Pb}/^{206}\text{Pb}$ - $^{206}\text{Pb}/^{207}\text{Pb}$ diagram
557 (Fig. 5A and B). Such distribution indicates a mixing between two end-members, a natural end-
558 member with higher isotope Pb ratios and a probable anthropogenic-derived end-member
559 characterised by lower isotope ratios.

560 (a) The first end-member has been defined by the average signature of 3 samples dated from the
561 Final Neolithic period (196 to 260 cm). They are used to define the local detrital source with low
562 isotopes ratios (i.e., $^{208}\text{Pb}/^{204}\text{Pb} = 38.9584 \pm 0.0020$, $^{207}\text{Pb}/^{204}\text{Pb} = ^{206}\text{Pb}/^{204}\text{Pb} 15,6719 \pm 0.0008$ and
563 $^{206}\text{Pb}/^{204}\text{Pb} = 19,0775 \pm 0.0008$) (Table S1). This end-member represents the natural background end-
564 member. The composition of the samples corresponding to the Iron Age, only defined by 2

565 measurements, is slightly different from the previous Bronze Age and Final Neolithic periods, with a
566 position closer to the sample from the Roman representative average. The Pb isotope ratios of the
567 sediments roughly decrease upwards from the natural background end-member. The oldest pre-
568 Roman samples (n= 19, 93-260 cm) are clustered with an average signature of 38.9667 ± 0.0235 ,
569 15.6716 ± 0.0007 and 19.0702 ± 0.0008 for $^{208}\text{Pb}/^{204}\text{Pb}$, $^{207}\text{Pb}/^{204}\text{Pb}$ and $^{206}\text{Pb}/^{204}\text{Pb}$, respectively.

570 (b) A shift towards lower Pb isotope ratios is marked for the Roman samples (53 and 73 cm) and
571 for the modern samples (11-23 cm). The first Roman shift may be related to some exploitation of Pb
572 ores. The isotope composition of both regional Pb-bearing ores and modern urban airborne particles
573 (Bollhöfer and Rosman, 2001) are reported in order to confirm any anthropogenic contribution in the
574 sediment Pb isotope composition. The isotope Pb ratios of the Roman and modern samples become
575 closer and closer to the Corsican Pb minerals (Fig. 5). The analysed Pb-bearing minerals display close
576 Pb isotope signatures, with an average composition of 1.1779 for $^{206}\text{Pb}/^{207}\text{Pb}$ and 2.0894 for
577 $^{208}\text{Pb}/^{206}\text{Pb}$. The first decrease of the Pb isotopic ratio observed in the Roman Crovani sediments is
578 in agreement with the historical exploitation of the Pb-Ag ores from the Argentella during the Roman
579 period (Gauthier, 2006). The linear trend defined by the modern samples does not point towards the
580 modern urban airborne particles but rather towards the Pb signature of the Sardinian ores (Stos-Gale
581 et al., 1995). In the Crovani sediments, Sardinia seems to be the most probable anthropogenic source
582 of Pb among the main Pb mines exploited in the Mediterranean area, i.e. in Greece, Turkey, Italy and
583 Spain since the Antiquity (see more details in Fagel et al., 2017). In the binary $^{206}\text{Pb}/^{207}\text{Pb}$ - $^{208}\text{Pb}/^{206}\text{Pb}$
584 diagram, the Crovani samples define a linear trend that, if extrapolated, points to the representative
585 average signature of Sardinian ores (Fig. 5 B).

586

587 *5.4. Effects of Rapid Climate Changes on the coastal tree-cover*

588 In the palaeobotanical narrative of Corsica, no clear tree-cover change has ever been attributed to a
589 “Bond event” (Bond et al., 2001) (Fig. 8) or other RCC of global interest, such as the 4.2 ka event
590 (Bini et al., 2019), the Homeric minimum (2.8 ka BP) (Martin-Puertas et al., 2012) and the Little Ice
591 Age (Trouet et al., 2009). These events have produced major changes in forest cover in many sites of
592 central and western Mediterranean regions, although with contrasting trends (Fletcher et al., 2013,
593 Magny et al., 2013; Di Rita et al., 2018a).

594 The 4.2 cal. BP event, perceived in south-central Italy as an aridity crisis producing a forest decline,
595 did not trigger a rapid response in the regional forest vegetation in Corsica and in the northern
596 Apennines (Di Rita and Magri, 2019; Revelles et al., 2019; Di Rita et al., 2022). However, previous
597 studies in Corsica have shown that the 4.2 event played an influence on geomorphological and
598 sedimentological processes, due to increased storm and fluvial activities as recorded in several lagoon

599 archives (Revelles et al., 2019 and references therein). In our record from Crovani, rapid fluctuations
600 of the forest cover are found, marked by maximum values of AP (92%) at ca. 4450 cal. BP (Figs 6
601 and 8). Between 4700 and 3500 cal. BP, a long-lasting increase in *Fagus* suggests permanent humid
602 conditions during the Mid- to Late Holocene transition (Fig. 6), which are recorded also in other
603 montane sites (Reille, 1975; Reille et al., 1999) and pollen sequences from coastal Corsica (Poher et
604 al., 2017; Revelles et al., 2019). The development of beech corresponds to relatively wet climatic
605 conditions in central Italy, as revealed by lake level highstands at Lake Accessa ca. 160 km far from
606 Crovani (Magny et al., 2013). Lake level highstands reflecting humid conditions are also recorded in
607 northern Italy (cf. Lake Ledro: Magny et al., 2012), and in west-central Europe (Magny et al., 2013
608 and references therein).

609 The development of beech corresponds also to periods of increased storm activity in southern France
610 (Sabatier et al., 2012) (Fig. 8). Although these periods were previously interpreted as a result of
611 southward westerly winds bringing moisture to mid-latitudes in Europe (Sabatier et al., 2012; Magny
612 et al., 2013), they may also reflect an increase in the frequency of marine storms that are not directly
613 interpretable as periods of regional increased precipitation (Azuara et al., 2020). An alkenone record
614 from the Gulf of Lion suggests moisture increase in southern France since ca. 4200 cal. BP (Jalali et
615 al., 2017; Azuara et al., 2020).

616 The general pattern of increased humidity in western Corsica contrasts with the drier conditions
617 indicated by precipitation proxies from the speleothems of the Corchia and Renella caves in Tuscany
618 (Zanchetta et al., 2016; Isola et al., 2019), and depicts a complex geographic expression of the 4.2 ka
619 event (Bini et al., 2019; Di Rita and Magri, 2019; Di Rita et al., 2022).

620 The Homeric Minimum (2750-2550 cal. BP, Martin-Puertas et al., 2012) was associated to forest
621 declines influenced by human impact and dryer climate conditions in many records of the south-
622 central Mediterranean (Di Rita et al., 2018c). At Crovani, it corresponds to a modest peak in AP,
623 possibly related to slightly wetter conditions. Relatively higher precipitations were recorded from
624 lake-level highstands since 2800 cal. BP at Lake Accessa (Fig 8), and from lake-level highstands and
625 pollen evidence at Lake Ledro (Magny et al., 2012; Peyron et al., 2017). More humid climate
626 conditions were also found in the western Mediterranean, possibly associated to the negative NAO
627 index that characterizes this interval (Fletcher et al., 2013). This phase corresponds also to increased
628 storm activity in the Gulf of Lion (Sabatier et al., 2012).

629 During the Little Ice Age, the record of Crovani shows a marked increase in *Erica* and *Q. ilex maquis*,
630 accompanied by significant frequencies of cultivated trees related to orchards and conifer plantations
631 (Figs 6 and 8). The development of natural and cultivated woody taxa was probably favoured by
632 relatively wet climate conditions, which were also recorded in both central and northern Italy from

633 lake-level highstands (Magny et al., 2013), as well as in southern France from records of major
634 flooding (Benito et al., 2015, Pichard et al., 2017), coinciding with a mostly negative NAO index
635 (Franke et al., 2017) (Figs 8 and 10). Climate reconstructions in Corsica are still fragmentary,
636 however the few published studies indicate the occurrence of periods characterized by wet and cool
637 conditions (Szymczak et al., 2012; Vella et al., 2014).

638 The archaeological and paleoenvironmental literature does not provide noticeable examples of rapid
639 and dry climate events in Corsica. As previously discussed, the complex sedimentological pattern at
640 ~3250. cal. BP (Fig. 4) might be related to an arid climate event observed around the same age in
641 other palaeoenvironmental records. Relatively dry and warm climate conditions may have also
642 contributed to produce the major forest decline recorded between 1000 and 500 cal. BP, limiting the
643 resprout of the natural forest vegetation affected by felling activities. In the western Mediterranean,
644 the dry and warm climate of the Medieval Climate Anomaly is usually associated to an overall
645 positive NAO index (Trouet et al., 2009; Franke et al., 2017) (Fig. 8).

646 Sabatier et al. (2020) have found a strong relationship between the transport of Saharan dust conveyed
647 to Corsica during the last ~3000 years and both total solar irradiance (TSI) and NAO activity. They
648 have shown that the NAO was the main climatic forcing for centennial to decadal variations since
649 ~1070 AD, with an increase in Saharan dust input during positive NAO phases. Before ~1070 AD,
650 TSI was the main forcing factor, with increases in African dust input during low TSI phases.

651 We applied a REDFIT analysis to the total AP percentages to investigate the effects of the
652 atmospheric circulation on the tree cover record from Crovani (Fig. 9). The prominent 230-year cycle
653 found in our statistical elaboration by and large corresponds to the Suess-de Vries cycle of solar
654 activity, which has been held responsible for environmental and atmospheric changes in several
655 records around the world, including the Mediterranean (Castagnoli et al., 1992; Galloway et al., 2013;
656 Di Rita, 2013; Degeai et al., 2014; Sabatier et al., 2020). The Suess-de Vries cycle is commonly
657 identified as a conventional 210-year periodicity; however, an increasing number of studies
658 demonstrates its non-stationary variability, which may have a range of ~200-300 years (Vecchio et
659 al., 2017). Similarly, its expression in palaeoenvironment proxies shows a non-stationary periodicity
660 (Galloway et al., 2013). A 230-year cycle was detected in direct proxies of solar magnetic activity,
661 such as ^{14}C time series and naked-eye observations of sunspots (Ma and Vaquero, 2020).

662 The REDFIT analysis from Crovani shows also two periodicities of ca. 430 and 1000 years,
663 respectively (Fig. 9). The first one corresponds to the ca. 430-years and 450-year cycles detected by
664 Sabatier et al. (2020) in the records of Saharan dust in Corsica, as shown by both TSI and ITCZ,
665 although the authors attribute a low significance to this cycle. A 440-year cycle (together with a 230-
666 year cycle) was found in $\delta^{13}\text{C}$ records of speleothems from northern Iberia and was interpreted as the

667 result of climate forcing mechanisms related to changes in solar irradiance and North Atlantic
668 circulation patterns (Mártin-Chivelet et al., 2011). Periodicities of ~400-years were recognized in
669 various palaeoclimate proxies from both marine (e.g., Bond et al., 2001) and lake records (e.g., Yu
670 and Ito, 2002; Wu et al., 2009) of the Middle-Late Holocene.

671 The last periodicity we found at Crovani matches a prominent ~1000-year cycle of moisture supply
672 reported in proxy records from the western Mediterranean, especially during the Early Holocene,
673 which have been associated to solar activity (Debret et al., 2009; Fletcher et al., 2013; Jiménez
674 Moreno et al., 2020 and references therein).

675 Overall, our results show that the forest oscillations at Crovani present a fundamental tempo of
676 variability consistent with the atmospheric forcing held responsible for the transport of Saharan dust
677 to Corsica. Although the relationship between solar activity and forest dynamics in Corsica is only
678 sketched, our findings encourage future research in the central Mediterranean, interpreted in the light
679 of the regional patterns of vegetation change.

680

681 5.5. Coastal landscape evolution of the Crovani area

682 Based on the cross combination of sedimentological, palynological and geochemical proxies, we
683 propose a synthetic palaeogeographical reconstruction of the investigated area, even if additional
684 cores would be necessary to evaluate in a comprehensive way both the morphological changes and
685 the spatial evolution of the Crovani wetland since the Mid-Holocene. The bottom of the core records
686 a detrital environment with a mixture of well-rounded pebbles and coarse material, ranging from
687 sands to gravels. Unfortunately, this section of the core did not contain enough organic material for
688 obtaining a radiocarbon age. Furthermore, facies identification was difficult due to the lack of fossil
689 fauna. However, on the basis of the sedimentological information, two types of energy of deposition
690 can be identified. The first is controlled by terrestrial dynamics being characterized by the finest
691 particles (grey clays). The second is conversely controlled by coastal dynamics as indicated by the
692 presence of well-rounded pebbles that are analogue in shape and petrography to the sediments which
693 compose the modern coastal barrier. These data suggest that the continental dynamics likely prevailed
694 during the first half of the Holocene. This was followed by a mid-Holocene marine transgression that
695 reached its maximum ~6500 cal. BP, when the sea-level in Corsica was ca. 3.5 to 4 m below the
696 present-day position (Vacchi et al., 2018). At that time, which broadly correspond to Middle to Late
697 Neolithic, a marine incursion occurred in the Crovani coastal pond following a pattern that was also
698 observed in other coastal lagoons in Corsica, such as Saint Florent (Revelles et al., 2019) and Del
699 Sale (Curras et al., 2017). As a result, the pond turned into brackish conditions after ~6100 cal. BP,
700 as confirmed by the presence of *Spiniferites*, which substantially indicates a connection with the sea

701 (Fig. 6 and 10). However, probably due to the presence of Late Pleistocene alluvial formations and
702 relict coastal deposits (former coastal barriers), the marine incursion inland was spatially limited. This
703 could explain the lack of faunal assemblages typical of coastal lagoon made by ostracods,
704 foraminifera and molluscs faunas. After ~5100 cal. BP, during the Late to Final Neolithic
705 characterized by the first occupation of the nearby site of Teghja di Linu, data show detrital input that
706 suddenly modified the brackish conditions of the pond. However, our data indicates that nor a climate
707 event neither human impact provoked deforestation associated to intense erosion on the foothills and
708 sedimentary accumulation of coarse material, even if there is a clear land-use at that time (Fig. 10).
709 A second phase of wetland development is well attested from the Final Neolithic to Middle/Recent
710 Bronze Age. Presence of salt intrusion is confirmed by both the vegetation composition and the
711 geochemical analyses (presence of halite) but there is no clear evidence for a direct of the coastal
712 pond connection to the sea (e.g., presence of faunal assemblages typical of coastal lagoons). A second
713 detrital input is observed during the Late Bronze Age (Unit VII). The C/N Ratio exhibits the highest
714 values for the entire sequence studied, thus indicating a terrestrial deposition of organic matter (see
715 section 4.2.) (Fig. 4). This is likely a rapid event (not more than a century in duration) that could have
716 caused the silting up of the wetland. Finally, the present-day landscape configuration is established
717 since Final Bronze Age (unit VIII) with very little morphological changes afterwards. Since ~3200
718 cal. BP, Crovani coastal pond has been a backshore freshwater body with probable aeolian input of
719 salt, no permanent connection to the sea, and low sediment accumulation rate (Fig. 10).

720

721

722 6. Conclusions

723 The new multidisciplinary dataset obtained from northwest Corsica helps to reconstruct the past
724 environmental dynamics (Fig. 10) within an archaeological context, and to frame it into the wider
725 scenario of the central Mediterranean landscape evolution. Our results contribute to the lively
726 discussion on the vegetation response to rapid climate changes, raising also new questions about
727 planetary drivers of past atmospheric circulation and their possible influence on the forested
728 ecosystems of this strategic region of the Mediterranean. In particular, the following conclusions can
729 be traced:

730 1) A dense *Erica*-dominated shrubland rich in many evergreen elements characterized the
731 landscape from ~6100 to ~1000 cal. BP, being temporarily replaced by mixed woodlands
732 dominated by *Q. ilex* between 2300 and 1900 cal. BP. A major opening of the landscape occurred
733 only between ~1000 and ~500 cal. BP, featured by a temporary decline in *Erica*-dominated tall

734 shrublands, paralleled by an expansion of *Cistus*-dominated low shrublands and followed by the
735 recovery of the tall *maquis* formations.

736 2) Fires played a prominent role in the development and maintenance of the *Erica*-dominated
737 shrublands, especially during the Middle Holocene (from ~5900 to ~5200 cal. BP), when frequent
738 and intense wild and anthropogenic fires boosted the sprout of *Erica* species. Differently from
739 other sites in Corsica and Sardinia, at Crovani fires did not affect *Q. ilex*, whose development
740 cannot be univocally explained in the region and may be influenced by a long-lasting ecological
741 legacy. The general decrease of fires after ~3300 cal. BP may reflect a combination of decreased
742 human activity and climate unsuitable for fires.

743 3) The Crovani wetland has been little influenced by marine incursions over the last six
744 millennia, as indicated by sedimentological data, pollen and NPPs. Moderate brackish conditions
745 occurred only from the Late Neolithic to part of the Bronze Age, while during the last three
746 millennia general freshwater conditions prevailed. The sequential development of dinoflagellates,
747 *Ruppia*, and ferns appears to reflect a hydrosere succession, whose evolution is strictly related to
748 the infilling of the lake. After ~3300 cal. BP, this ecological process was influenced by a sudden
749 deposition of continental organic-rich sediments, following rapid deforestation and runoff of
750 regional extension, coeval to an arid climate event occurred around ~3200 cal. BP.

751 4) Evidence for human activity is present throughout the pollen record, with important
752 differences through time. Between ~6000 and ~5200 cal. BP, a continuous curve of cereal-type
753 pollen testifies to the earliest cultivations in this area. Farming activities are also confirmed by the
754 presence of disturbed meadows for livestock rearing, indicated by coprophilous fungi and pollen
755 indicators of plants frequently living in Mediterranean pasturelands. Starting around 3300 cal. BP,
756 indicators of cereal cultivation and stock rearing practices became sparse, and evidence for human
757 activity comes from cultivated trees, especially after ca. 2000 cal. BP and even more after ~500
758 cal. BP. The former increase reflects olive exploitation during the Roman Period, the latter points
759 to both olive cultivation in lowland areas and chestnut culture in the uplands. A clear forest
760 degradation dates back to the last three millennia, with a dramatic opening of the landscape only
761 from ~1000 to ~500 cal. BP, related to human activity in the medieval times and Genovese
762 domination.

763 5) The spectral analysis applied to total AP revealed a ~230-year cycle, in the bandwidth of the
764 Suess-de Vries cycle, and other cyclicities attributed to the magnetic activity of the Sun,
765 recognized also in other climate proxies from the Mediterranean. This suggests that the
766 atmospheric modifications of solar activity and North Atlantic Oscillation had some influence on
767 the tree cover fluctuations in Corsica. However, known rapid climate changes, such as the 4.2 ka

768 BP event, the Homeric minimum, and the Little Ice Age, did not determine at Crovani extensive
769 forest declines as they did in sites of the south-central Mediterranean. In contrast, in northwestern
770 Corsica these phases correspond to a forest development consistent with the humid phases detected
771 in southern France and northern Italy. The high-resolution record from Crovani is an important
772 piece of information to define the spatial pattern of vegetation response to the atmospheric
773 arrangements produced by rapid climate changes over the Mediterranean Basin during the
774 Holocene.

775

776 Acknowledgements

777 This article is a contribution of the PCR “Approche géoarchéologique des paysages de Corse à
778 l’Holocène, entre mer et intérieur des terres « Tra Mare è Monti » programme, funded by the DRAC
779 Corsica and directed by Matthieu Ghilardi. It is also part of the MISTRALS-PALEOMEX
780 programme of CNRS (INEE-INSU scientific departments) and was funded by the ARCHEOMED
781 workshop (Dir. Laurent Lespez). This research was also supported by Sapienza University of Rome
782 (grant numbers RM11715C820D1E6F, RM1181641C0CB0C7, and RM120172AE4E11D6). The
783 authors are grateful to the Conservatoire du Littoral (branch of Corsica) and its Director, Michel
784 Muracciole, for delivering the work permits. We thank Donatella Magri for her precious suggestions
785 and two anonymous reviewers for helpful comments.

786

787

788

789 **Reference list**

790

- 791 Azuara, J., Sabatier, P., Lebreton, V., Jalali, B., Sicre, M.-A., Dezileau, L., Bassetti, M.-A., Frigola,
792 J., Combourieu-Nebout, N., 2020. Mid- to Late-Holocene Mediterranean climate variability:
793 contribution of multi-proxy and multi-sequence comparison using wavelet spectral analysis
794 in the northwestern Mediterranean basin. *Earth Sci. Rev.* 208, 103232.
795 <https://doi.org/10.1016/j.earscirev.2020.103232>.
- 796 Beffa, G., Pedrotta, T., Colombaroli, D., Henne, P.D., van Leeuwen, J.F.N., Süssstrunk, P.,
797 Kaltenrieder, P., Adolf, C., Vogel, H., Pasta, S., Anselmetti, F.S., Gobet, E., Tinner, W., 2016.
798 Vegetation and fire history of coastal north-eastern Sardinia (Italy) underchanging Holocene
799 climates and land use. *Veg. Hist. Archaeobotany* 25, 271-289
- 800 Bellotti, P., Calderoni, G., Di Rita, F., D'Orefice, M., D'Amico, C., Esu, D., Magri, D., Preite
801 Martinez, M., Tortora, P., Valeri, P., 2011. The Tiber river delta plain (central Italy): coastal
802 evolution and implications for the ancient Roman Ostia settlement. *Holocene* 21, 1105-1116.
- 803 Benito, G., Macklin, M. G., Zielhofer, C., Jones, A. F., Machado, M. J., 2015. Holocene flooding and
804 climate change in the Mediterranean. *Catena* 130, 13-33.
- 805 Bengtsson, L., Enell, M., 1986. Chemical analysis, in: Berglund, B. E. (ed.), *Handbook of Holocene*
806 *Palaeoecology and Palaeohydrology*. John Wiley & Sons Ltd., Chichester, 423–451.
- 807 Bennett, K., 2009. “psimpoll” and “pscomb”: CPrograms for Analysing Pollen Data and Plotting
808 Pollen Diagrams (Version 4.27). Available online from Queen's University Quaternary
809 Geology program at URL. <http://www.chrono.qub.ac.uk/psimpoll/psimpoll.html>.
- 810 Berger, J.F., Brochier, J.L., Vital, J., Delhon, C., Thiebault, S., 2007. Nouveau regard sur la
811 dynamique des paysages et l'occupation humaine à l'Âge du bronze en moyenne vallée du
812 Rhône, in: Mordant C., Richard H., Magny M. (Eds.), *Environnements et cultures à l'âge du*
813 *Bronze en Europe occidentale*. Actes du 129e colloque du CTHS, Besançon, avril 2004,
814 Editions du CTHS, Documents Préhistoriques 21, 260-283.
- 815 Beug, H., 2004. Leitfaden der Pollenbestimmung für Mitteleuropa und angrenzende Gebiete. Verlag
816 Dr. Friederich Pfeil, München.
- 817 Bini, M., Zanchetta, G., Perşoiu, A., Cartier, R., Català, A., Cacho, I., Dean, J.R., Di Rita, F.,
818 Drysdale, R.N., Finnè, M., Isola, I., Jalali, B., Lirer, F., Magri, D., Masi, A., Marks, L.,
819 Mercuri, A.M., Peyron, O., Sadori, L., Sicre, M.-A., Welc, F., Zielhofer, C., Brisset, E., 2019.
820 The 4.2 ka BP Event in the Mediterranean region: an overview. *Clim. Past* 15, 555-577.
- 821 Birks, H.J.B., Line, J.M., 1992. The use of rarefaction analysis for estimating palynological richness
822 from Quaternary pollen-analytical data. *The Holocene* 2, 1-10.
- 823 Blaauw, M., Christen, J. A., 2011. Flexible paleoclimate age-depth models using an autoregressive
824 gamma process. *Bayesian analysis* 6, 457-474.
- 825 Bollhöfer, A., Rosman, K.J.R., 2001. Isotopic source signature for atmospheric lead: the Northern
826 Hemisphere. *Geochim. Cosmochim. Acta* 65, 1727-1740.
- 827 Bond, G., Kromer, B., Beer, J., Muscheler, R., Evans, M.N., Showers, W., Hoffmann, S., Lotti-Bond,
828 R., Hajdas, I., Bonani, G., 2001. Persistent solar influence on North Atlantic climate during
829 the Holocene. *Science* 294, 2130-2136.
- 830 Bottema, S., 1975. The interpretation of pollen spectra from prehistoric settlements (with special
831 attention to Liguliflorae). *Palaeohistoria* 17, 17-35.
- 832 Carcaillet, C., Barakat, H. N., Panaïotis, C., Loisel, R., 1997. Fire and late- Holocene expansion of
833 *Quercus ilex* and *Pinus pinaster* on Corsica. *J. Veg. Sci.* 8, 85-94.
- 834 Carrión, J.S., 2002. Patterns and processes of Late Quaternary environmental change in a montane
835 region of southwestern Europe. *Quaternary Sci. Rev.* 21, 2047-2066.
- 836 Carrión, J.S., Sánchez-Gómez, P., 1992. Palynological data in support of the survival of walnut
837 (*Juglans regia* L.) in the western Mediterranean area during last glacial times. *J. Biogeogr.*
838 19, 623-630.

- 839 Carrión, J.S., Parra, I., Navarro, C., Munuera, M., 2000. Past distribution and ecology of the cork oak
840 (*Quercus suber*) in the Iberian Peninsula: a pollen-analytical approach. *Divers. Distrib.* 6, 29-
841 44.
- 842 Castagnoli, G.C., Bonino, G., Serio, M., Sonnett, C.P., 1992. Common spectral features in the 5500-
843 year record of total carbonate in sea sediments and radiocarbon in tree rings. *Radiocarbon* 34,
844 798–805.
- 845 Caudullo, G., Tinner, W., de Rigo, D., 2016. *Picea abies* in Europe: distribution, habitat, usage and
846 threats. In: San-Miguel-Ayán, J., de Rigo, D., Caudullo, G., Houston Durrant, T., Mauri, A.
847 (Eds.), *European Atlas of Forest Tree Species*. Publications Office of the European Union,
848 Luxembourg e012300b
- 849 Cesari, J., Pêche-Quilichini, K., 2015. L'âge du Bronze corse. L'émergence d'une élite guerrière, in
850 Leandri F., Istria D. (coord.), *Corse, richesses archéologiques de la Préhistoire à l'époque*
851 *moderne. Dossiers d'archéologie*, 370, 24-29
- 852 Clark, R.L., 1982. Point count estimation of charcoal in pollen preparations and thin sections of
853 sediments. *Pollen Spores* 24, 523–535.
- 854 Colombaroli, D., Tinner, W., Leeuwen, J. van, Noti, R., Vescovi, E., Vanniere, B., Magny, M.,
855 Schmidt, R., Bugmann, H., 2009. Response of broadleaved evergreen Mediterranean forest
856 vegetation to fire disturbance during the Holocene: in-sights from the peri-Adriatic region. *J.*
857 *Biogeogr.* 36, 314-326.
- 858 Cook, H.E., Johnson, P.D., Matti, J.C., Zemmels, I., 1975. Methods of sample preparation and X-ray
859 diffraction analysis in X-ray mineralogy laboratory, in: Kaneps, A.G., et al. (Eds.), *Init. Repts*
860 *DSDP XXVIII*. Print. Office, Washington DC, pp. 997-1007.
- 861 Cugny, C., Mazier, F., Galop, D., 2010. Modern and fossil non-pollen palynomorphs from the Basque
862 mountains (western Pyrenees, France): the use of coprophilous fungi to reconstruct pastoral
863 activity. *Veg. Hist. Archaeobot.* 19, 391–408.
- 864 Currás, A., Ghilardi, M., Pêche-Quilichini, K., Fagel, N., Vacchi, M., Delanghe, D., Contreras, D.,
865 Vella, C., Ottaviani, J.C., 2017. Reconstructing past landscapes of the eastern plain of Corsica
866 (NW Mediterranean) during the last 6000 years based on molluscan, sedimentological and
867 palynological analyses. *J. Archaeol. Sci.: Report* 12, 755-769.
- 868 D'Anna, A., Marchesi, H., Tramoni, P., Gilabert, C., Demouche, F., 2001. Renaghju (Sartène, Corse-
869 du-Sud), un habitat de plein-air néolithique ancien en Corse. *Bulletin de la Société*
870 *préhistorique française* 98, 431-444.
- 871 Dean, W.E. Jr., 1974. Determination of carbonate and organic matter in calcareous sediments and
872 sedimentary rocks by loss on ignition: Comparison with other methods. *J. Sed. Petrol.* 44:
873 242–248
- 874 Debret, M., Sebag, D., Crosta, X., Massei, N., Petit, J.R., Chapron, E., Bout-Roumazielles, V., 2009.
875 Evidence from wavelet analysis for a mid-Holocene transition in global climate forcing. *Quat.*
876 *Sci. Rev.* 28, 2675-2688.
- 877 Degeai, J.P., Devillers, B., Dezileau, L., Oueslati, H., Bony, G., 2015. Major storm periods and
878 climate forcing in the Western Mediterranean during the Late Holocene. *Quaternary Sci. Rev.*
879 129, 37-56.
- 880 Desprat, S., Combourieu-Nebout, N., Essallami, L., Sicre, M.A., Dormoy, I., Peyron, O., Siani, G.,
881 Bout Roumazielles, V., Turon, J.L., 2013. Deglacial and Holocene vegetation and climatic
882 changes in the southern Central Mediterranean from a direct land-sea correlation. *Clim. Past*
883 9, 767-787.
- 884 de Vernal, A., Eynaud, F., Henry, M., Limoges, A., Londeix, L., Matthiessen, J., Marret, F.,
885 Pospelova, V., Radi, T., Rochon, A., Van Nieuwenhove, N., Zaragosi, S., 2018. Distribution
886 and (palaeo)ecological affinities of the main *Spiniferites* taxa in the mid-high latitudes of the
887 Northern Hemisphere. *Palynology* 42, 182–202.
- 888 Di Rita, F., 2013. A possible solar pacemaker for Holocene fluctuations of a saltmarsh in southern
889 Italy. *Quatern. Int.* 288, 239-248.

- 890 Di Rita, F., Magri, D., 2012. An overview of the Holocene vegetation history from the central
891 Mediterranean coasts. *J. Mediterr. Earth Sci.* 4, 35-52.
- 892 Di Rita, F., Magri, D., 2019. The 4.2 ka event in the vegetation record of the central Mediterranean.
893 *Clim. Past* 15, 237-251.
- 894 Di Rita, F., Melis, R.T., 2013. The cultural landscape near the ancient city of Tharros (central West
895 Sardinia): vegetation changes and human impact. *J. Archaeol. Sci.* 40, 4271-4282.
- 896 Di Rita, F., Fletcher, W. J., Aranbarri, J., Margaritelli, G., Lirer, F., Magri, D., 2018a. Holocene forest
897 dynamics in central and western Mediterranean: periodicity, spatio-temporal patterns and
898 climate influence. *Scientific Reports* 8, 8929.
- 899 Di Rita, F., Molisso, F., Sacchi, M., 2018b. Late Holocene environmental dynamics, vegetation
900 history, human impact, and climate change in the ancient *Literna Palus* (Lago Patria;
901 Campania, Italy). *Rev. Palaeobot. Palyno.* 258, 48-61.
- 902 Di Rita, F., Lirer, F., Bonomo, S., Cascella, A., Ferraro, L., Florindo, F., Insinga, D.D., Lurcock, P.C.,
903 Margaritelli, G., Petrosino, P., Rettori, R., Vallefucio, M., Magri, D., 2018c. Late Holocene
904 forest dynamics in the Gulf of Gaeta (central Mediterranean) in relation to NAO variability
905 and human impact. *Quaternary Sci. Rev.* 179, 137–152.
- 906 Di Rita, F., Michelangeli, F., Celant, A., Magri, D., 2022. Sign-switching ecological changes in the
907 Mediterranean Basin at 4.2 ka BP. *Global Planet. Change* 208, 103713.
- 908 Fagel, N., Lechenault, M., Fontaine, N., Pleuger, E., Otten, J., Allan, M., Ghilardi, M., Mattielli, N.,
909 Goiran, J-P., 2017. Record of human activities in the Pb isotopes signatures of coastal
910 sediments from the Roman archaeological site of Cala Francese, Cape Corsica (France). *J.*
911 *Archaeol. Sci.: Reports* 12, 770-781.
- 912 Fletcher, W.J., Debret, M., Goñi, M.F.S., 2013. Mid-Holocene emergence of a low-frequency
913 millennial oscillation in western Mediterranean climate: Implications for past dynamics of the
914 North Atlantic atmospheric westerlies. *The Holocene*, 23, 153-166.
- 915 Florenzano, A., Marignani, M., Rosati, L., Fascetti, S., Mercuri, A.M., 2015. Are Cichorieae an
916 indicator of open habitats and pastoralism in current and past vegetation studies? *Plant*
917 *Biosyst.* 149, 154-165.
- 918 Franke, J.G., Werner, J.P., Donner, R.V., 2017. Reconstructing Late Holocene North Atlantic
919 atmospheric circulation changes using functional paleoclimate networks. *Clim. Past* 13, 1593-
920 1608.
- 921 Galloway, J.M., Wigston, A., Patterson, R.T., Swindles, G.T., Reinhardt, E., Roe, H.M., 2013.
922 Climate change and decadal to centennial-scale periodicities recorded in a late Holocene NE
923 Pacific marine record: Examining the role of solar forcing. *Palaeogeography,*
924 *Palaeoclimatology, Palaeoecology* 386, 669-689.
- 925 Galop, D., Carozza, L., Marembert, F., Bal, M.C., 2007. Activités agropastorales et climat durant
926 l'Âge du Bronze dans les Pyrénées : l'état de la question à la lumière des données
927 environnementales et archéologiques, in: Mordant C., Richard H., Magny M. (Eds.),
928 Environnements et cultures à l'âge du Bronze en Europe occidentale. Actes du 129e colloque
929 du CTHS, Besançon, avril 2004, Editions du CTHS, Documents Préhistoriques, 21, 107-119.
- 930 Gauthier, A., 2006. Des roches, des paysages et des hommes. *Géologie de la Corse*, Ajaccio, Edition
931 Albiana, France, 276 p.
- 932 Gelorini, V., Verbeken, A., van Geel, B., Cocquyt, C., Verschuren, D., 2011. Modern non-pollen
933 palynomorphs from East African lake sediments. *Rev. Palaeobot. Palyno.* 164, 143-173.
- 934 Ghilardi, M., 2020. Lagunes et marais littoraux de Corse. *De la Préhistoire à nos jours. Collec. Orma:*
935 *la Corse archéologie*, Editions ARAC, 5, 105 p.
- 936 Ghilardi, M., 2021. Geoarchaeology: Where Geosciences Meet the Humanities to Reconstruct Past
937 Human–Environment Interactions. An Application to the Coastal Areas of the Largest
938 Mediterranean Islands. *Appl. Sci.* 11, 4480. <https://doi.org/10.3390/app11104480>
- 939 Ghilardi, M., Istria, D., Currás, A., Vacchi, M., Contreras, D., Vella, C., Dussouillez, P., Crest, Y.,
940 Colleu, M., Guiter, F., Delanghe, D., 2017a. Reconstructing the landscape evolution and the

941 human occupation of the Lower Sagone River (Western Corsica, France) from the Bronze
942 Age to the Medieval period, in: Ghilardi M. and Lespez L. (Eds.), *Geoarchaeology of the*
943 *Mediterranean islands*. *J. Archaeol. Sci.: Reports*, 12, 741-754.

944 Ghilardi, M., Delanghe, D., Demory, F., Leandri, F., Pêche-Quilichini, K., Vacchi, M., Vella, M.A.,
945 Rossi, V., Robresco, S., 2017b. Enregistrements d'événements extrêmes et évolution des
946 paysages dans les basses vallées fluviales du Taravo et du Sagone (Corse occidentale, France)
947 au cours de l'âge du Bronze moyen à final: une perspective géoarchéologique.
948 *Géomorphologie, Relief, Processus et Environnement* 23, 15-35.

949 Grimm, E.C., 1987. CONISS: a FORTRAN 77 program for stratigraphically constrained cluster
950 analysis by the method of incremental sum of squares. *Computers & Geosciences* 13, 13-35.

951 Hammer, Ø., Harper, D.A.T., Ryan, P.D., 2001. PAST: paleontological Statistics software package
952 for education and data analysis. *Palaeontol. Electron.* 4, 9.

953 Havinga, A.J., 1984. A 20-year experimental investigation into the differential corrosion
954 susceptibility of pollen and spores in various soil types. *Pollen Spores* 26, 541-58.

955 Henry, A.G. (Ed.), 2020. *Handbook for the Analysis of Micro-particles in Archaeological Samples*.
956 Springer International Publishing.

957 Isola, I., Zanchetta, G., Drysdale, R.N., Regattieri, E., Bini, M., Bajo, P., Hellstrom, J.C., Baneschi,
958 I., Lionello, P., Woodhead, J., 2019. The 4.2 ka event in the Central Mediterranean: new data
959 from a Corchia speleothem (Apuan Alps, Central Italy). *Clim. Past* 15, 135-151.

960 Jalali, B., Sicre, M.-A., Kallel, N., Azuara, J., Combourieu-Nebout, N., Bassetti, M.-A., Klein, V.,
961 2017. High-resolution Holocene climate and hydrological variability from two major
962 Mediterranean deltas (Nile and Rhone). *The Holocene* 27 (8), 1158-1168.

963 Jeanmonod, D., Schlüssel, A., 2006. Notes and contributions on Corsican flora, XXI. *Candollea*, 61,
964 93-134.

965 Jiménez-Moreno, G., Anderson, R.S., Ramos-Román, M.J., Camuera, J., Mesa-Fernández, J.M.,
966 García-Alix, A., Jiménez-Espejo, F.J., Carrión, J.S., López-Avilés, A., 2020. The Holocene
967 *Cedrus* pollen record from Sierra Nevada (S Spain), a proxy for climate change in N Africa.
968 *Quaternary Sci. Rev.* 242, 106468.

969 Kantrud, H.A., 1991. Wigeongrass (*Ruppia maritima* L.): A Literature Review, vol. 10. U.S. Fish and
970 Wildlife Service, Fish and Wildlife Research, 58 pp.

971 Kouli, K., Brinkhuis, H., Dale, B., 2001. *Spiniferites cruciformis*: a fresh water dinoflagellate cyst?.
972 *Rev. Palaeobot. Palynolo* 113, 273-286.

973 Lestienne, M., Jouffroy-Bapicot, I., Leysse, D., Sabatier, P., Debret, M., Albertini, P. J.,
974 Colombaroli, D., Didier, J., Hély, C., Vannièrè, B., 2020a. Fires and human activities as key
975 factors in the high diversity of Corsican vegetation. *The Holocene* 30, 244-257.

976 Lestienne, M., Hely, C., Curt, T., Jouffroy-Bapicot, I., Vannièrè, B., 2020b. Combining the Monthly
977 Drought Code and Paleoecological Data to Assess Holocene Climate Impact on
978 Mediterranean Fire Regime. *Fire* 3(2), 8.

979 Leleu, F., 2021. Calenzana-Les mines de l'Argentella. Prospection thématique (2018). ADLFI.
980 Archéologie de la France - Informations [Online], Corse, Online since 08 January 2021,
981 connection on 14 December 2021. URL: <http://journals.openedition.org/adlfi/50226>

982 Leys, B., Carcaillet, C., Dezileau, L., Ali, A.A., Bradshaw, R.H., 2013. A comparison of charcoal
983 measurements for reconstruction of Mediterranean paleo-fire frequency in the mountains of
984 Corsica. *Quaternary Res.* 79, 337-349.

985 Leys, B., Finsinger, W., Carcaillet, C., 2014. Historical range of fire frequency is not the Achilles'
986 heel of the Corsican black pine ecosystem. *J. Ecol.* 102, 381-395.

987 Lugliè, C., 2018. *Your path led trough the sea...* the emergence of Neolithic in Sardinia and Corsica.
988 *Quatern. Int.* 470, 285-300.

989 Ma, L., Vaquero, J.M., 2020. New evidence of the Suess/de Vries cycle existing in historical naked-
990 eye observations of sunspots. *Open Astronomy* 29, 28-31.

- 991 Magny, M., Joannin, S., Galop, D., Vanni re, B., Haas, J. N., Bassetti, M., Bellintani, P., Scandolari,
992 R., Desmet, M., 2012. Holocene palaeohydrological changes in the northern Mediterranean
993 borderlands as reflected by the lake-level record of Lake Ledro, northeastern Italy. *Quaternary*
994 *Res.*, 77, 382–396.
- 995 Magny, M., Combourieu-Nebout, N., de Beaulieu, J.L., Bout-Roumazeilles, V., Colombaroli, D.,
996 Desprat, S., Francke, A., Joannin, S., Ortu, E., Peyron, O., Revel, M., Sadori, L., Siani, G.,
997 Sicre, M.A., Samartin, S., Simonneau, A., Tinner, W., Vanni re, B., Wagner, B., Zanchetta,
998 G., Anselmetti, F., Brugiapaglia, E., Chapron, E., Debret, M., Desmet, M., Didier, J.,
999 Essallami, L., Galop, D., Gilli, A., Haas, J.N., Kallel, N., Millet, L., Stock, A., Turon, J.L.,
1000 Wirth, S., 2013. North-south palaeohydrological contrasts in the central Mediterranean during
1001 the Holocene: tentative synthesis and working hypotheses. *Clim. Past* 9, 2043-2071.
- 1002 Magri, D., Di Rita, F., 2015. Archaeopalynological preparation techniques, in: Yeung, E.C.T.,
1003 Stasolla, C., Sumner, M.J., Huang, B.Q. (Eds.), *Plant Microtechniques and Protocols*. Springer
1004 International Publishing, Cham, pp. 495–506.
- 1005 Magri, D., Celant, A., Di Rita, F., 2019. The vanished *Alnus*-dominated forests along the Tyrrhenian
1006 coast. *Catena* 182, 104136.
- 1007 Mart n-Chivelet, J., Mu oz-Garc a, M.B., Edwards, R.L., Turrero, M.J., Ortega, A.I., 2011. Land
1008 surface temperature changes in Northern Iberia since 4000 yr BP, based on $\delta^{13}\text{C}$ of
1009 speleothems. *Global Planet. Change* 77, 1-12.
- 1010 Mart n-Puertas, C., Matthes, K., Brauer, A., Muscheler, R., Hansen, F., Petrick, C., Aldahan, A.,
1011 Possnert, G., van Geel, B., 2012. Regional atmospheric circulation shifts induced by a grand
1012 solar minimum. *Nat. Geosci.* 5, 397-401.
- 1013 Mattioni, C., Martin, M. A., Pollegioni, P., Cherubini, M., Villani, F., 2013. Microsatellite markers
1014 reveal a strong geographical structure in European populations of *Castanea sativa* (Fagaceae):
1015 evidence for multiple glacial refugia. *Am. J. Bot.* 100, 951-961.
- 1016 M dail, F., Monnet, A.-C., Pavon, D., Nikoli c, T., Dimopoulos, P., Bacchetta, G., Arroyo, J., Barina,
1017 Z., Albassatneh, M.C., Domina, G., Fady, B., Matevski, V., Mifsud, S., Leriche, A., 2019.
1018 What is a tree in the Mediterranean Basin hotspot? A critical analysis. *Forest Ecosyst.* 6, 17.
- 1019 Melis, R.T., Depalmas, A., Di Rita, F., Montis, F., Vacchi, M., 2017. Mid to late Holocene
1020 environmental changes along the coast of western Sardinia (Mediterranean Sea *Global Planet.*
1021 *Change* 155, 29-41.
- 1022 Melis, R.T., Di Rita, F., French, C., Marriner, N., Montis, F., Serreli, G., Sulas, F., Vacchi, M., 2018.
1023 8000 years of coastal changes on a western Mediterranean island: a multiproxy approach from
1024 the Posada plain of Sardinia. *Mar. Geol.* 403, 93-108.
- 1025 Michon, G., 2011. Revisiting the resilience of chestnut forests in Corsica: from social-ecological
1026 systems theory to political ecolog. *Ecol. Soc.* 16, 5.
- 1027 Moore, D.M., Reynolds, R.C. Jr., 1997. X-Ray diffraction and the identification and analysis of clay
1028 minerals. Oxford New York, Oxford Univ. Press, 378 pp.
- 1029 Pantale n-Cano, J., Yll, E.I., P rez-Obiol, R. Roure, J.M., 2003. Palynological evidence for
1030 vegetational history in semi-arid areas of the western Mediterranean (Almer a, Spain). *The*
1031 *Holocene* 13, 109–19.
- 1032 Peche-Quilichini, K., 2011. Les monuments turriformes de l'Age du bronze en Corse: tentative de
1033 caract risation spatiale et chronologique sur fond d'historiographie. In: Dominique Garcia
1034 (ed.) *L'Age du bronze en M diterran e. Recherches r centes*, Errance, Paris, 155-170.
- 1035 Pedrotta, T., Gobet, E., Schw rer, C., Beffa, G., Butz, C., Henne, P.D., Morales-Molino, C., Pasta,
1036 S., van Leeuwen, J.F.N., Vogel, H., Zwimpfer, E., Anselmetti, F.S., Grosjean, M., Tinner, W.,
1037 2021. 8,000 years of climate, vegetation, fire and land-use dynamics in the thermo-
1038 mediterranean vegetation belt of northern Sardinia (Italy). *Veget Hist Archaeobot.* 30, 789-
1039 813.
- 1040 Peyron, O., Combourieu-Nebout, N., Brayshaw, D., Goring, S., Andrieu-Ponel, V., Desprat, S.,
1041 Fletcher, W., Gambin, B., Ioakim, C., Joannin, S., Kotthoff, U., Kouli, K., Montade, V., Pross,

- 1042 J., Sadori, L., Magny, M., 2017. Precipitation changes in the Mediterranean basin during the
1043 Holocene from terrestrial and marine pollen records: a model-data comparison. *Clim. Past* 13,
1044 249-265.
- 1045 Pichard, G., Arnaud-Fassetta, G., Moron, V., Roucaute, E., 2017. Hydro-climatology of the Lower
1046 Rhône Valley: historical flood reconstruction (AD 1300–2000) based on documentary and
1047 instrumental sources. *Hydrolog. Sci. J.* 62, 1772-1795.
- 1048 Poher, Y., Ponel, P., Médail, F., Andrieu-Ponel, V., Guiter, F., 2017. Holocene environmental history
1049 of a small Mediterranean island in response to sea-level changes, climate and human impact.
1050 *Palaeogeogr. Palaeoecol.* 465, 247-263.
- 1051 Pollegioni, P., Woeste, K., Chiocchini, F., Del Lungo, S., Ciolfi, M., Olimpieri, I., Tortolano, V.,
1052 Clark, J., Hemery, G.E., Mapelli, S., Malvolti, M.E., 2017. Rethinking the history of common
1053 walnut (*Juglans regia* L.) in Europe: its origins and human interactions. *PLoS One* 12,
1054 e0172541.
- 1055 Regattieri, E., Zanchetta, G., Drysdale, R.N., Isola, I., Hellstrom, J.C., Dallai, L., 2014. Lateglacial
1056 to holocene trace element record (Ba, Mg, Sr) from corchia cave (Apuan Alps, central Italy):
1057 paleoenvironmental implications. *J. Quaternary Sci.* 29, 381-392.
- 1058 Reille, M., 1975. Contribution pollen analytique à l'histoire tardiglaciaire et holocène de la végétation
1059 de la montagne corse. Thèse des sciences Aix-Marseille III.
- 1060 Reille, M., 1984. Origine de la végétation actuelle de la Corse sud-orientale; analyse pollinique de
1061 cinq marais côtiers. *Pollen Spores* 1 XXVI, 43-60.
- 1062 Reille, M., 1991. Les données de l'analyse pollinique. Rapport fouille programme Grotte du Norte di
1063 Tuda. *Olmata di Tuda*, pp. 149-160.
- 1064 Reille, M., 1992a. New pollen-analytical researches in Corsica: the problem of *Quercus ilex* L. and
1065 *Erica arborea* L., the origin of *Pinus halepensis* Miller forests. *New Phytol.* 122, 359-378.
- 1066 Reille, M., 1992b. Pollen et spores d'Afrique du nord. *Laboratoire de Bot. Hist. et Palynologie*,
1067 Marseille
- 1068 Reille, M.J., Gamisans, V., Andrieu-Ponel, V., De Balieu, J.-L., 1999. The Holocene at Lac de Creno,
1069 Corsica, France: a key site for the whole island. *New Phytol.* 141, 291-307.
- 1070 Reimer, P.J., Austin, W.E., Bard, E., Bayliss, A., Blackwell, P.G., Ramsey, C.B., Butzin, M., Cheng,
1071 H., Edwards, R.L., Friedrich, M., Grootes, P.M., et al., 2020. The IntCal20 Northern
1072 Hemisphere Radiocarbon Age Calibration Curve (0-55 cal kBP). *Radiocarbon* 62, 725-757.
- 1073 Revelles J., Ghilardi, M., Vacchi, M., Rossi, V., Currás, A., López-Bultò, O., Brkojewitsch, G., 2019.
1074 Coastal landscape evolution of Corsica: palaeoenvironments, vegetation history and human
1075 impacts since the Early Neolithic period. *Quaternary Sci. Rev.* 225, 105993.
- 1076 Revelles, J., Ghilardi, M., 2021. 49. Saint Florent (north Corsica, France). *Grana* 60, 158-160.
- 1077 Roberts, C. N., Woodbridge, J., Palmisano, A., Bevan, A., Fyfe, R., Shennan, S., 2019. Mediterranean
1078 landscape change during the Holocene: Synthesis, comparison and regional trends in
1079 population, land cover and climate. *The Holocene*, 29(5), 923-937.
- 1080 Rodwell, J.S. (ed.), 2000. *British plant communities*, vol. 5, Maritime communities and vegetation of
1081 open habitats. Cambridge: Cambridge University Press.
- 1082 Sabatier, P., Dezileau, L., Colin, C., Briquieu, L., Bouchette, F., Martinez, P., Siani, G., Raynal, O.,
1083 Von Grafenstein, U., 2012. 7000 years of paleostorm activity in the NW Mediterranean Sea
1084 in response to Holocene climate events. *Quat. Res.* 77, 1–11.
- 1085 Sabatier, P., Nicolle, M., Piot, C., Colin, C., Debret, M., Swingedouw, D., Perrette, Y., Bellingery,
1086 M.-C., Chazeau, B., Develle, A.-L., Leblanc, M., Skonieczny, C., Copard, Y., Reyss, J.-L.,
1087 Malet, E., Jouffroy-Bapicot, I., Kelner, M., Poulénard, J., Didier, J., Arnaud, F., Vannièrè, B.,
1088 2020. Past African dust inputs in the western Mediterranean area controlled by the complex
1089 interaction between the Intertropical Convergence Zone, the North Atlantic Oscillation, and
1090 total solar irradiance. *Clim. Past* 16, 283–298
- 1091 Schulz, M., Mudelsee, M., 2002. REDFIT: estimating red-noise spectra directly from unevenly
1092 spaced paleoclimatic time series. *Computers & Geosciences* 28, 421-426.

- 1093 Scott, L., 1992. Environmental implications and origin of microscopic *Pseudoschizaea* Thiergart and
1094 Frantz ex R Potonié emend. in sediments. *J. Biogeogr.* 19, 349-354.
- 1095 Szymczak, S., Joachimski, M. M., Bräuning, A., Hetzer, T., Kuhlemann, J., 2012. A 560 yr summer
1096 temperature reconstruction for the Western Mediterranean basin based on stable carbon
1097 isotopes from *Pinus nigra* ssp. *laricio* (Corsica/France). *Clim. Past* 8, 1737-1749.
- 1098 Sicurani, J., 2008. Étude technologique et typologique du matériel lithique taillé néolithique trouvé
1099 en place sur quelques sites majeurs du Nord-Ouest (Balagne) de la Corse. Thèse de Doctorat,
1100 Université de Corse, 714 p.
- 1101 Sicurani, J., Martinet, L., 2019. Teghja di Linu: un site de plein air du début du iiiie millénaire av. J.-
1102 C. (Luzipeu, Haute-Corse). In Sicurani J. (dir.), *L'habitat pré- et protohistorique/L'alloghju*
1103 *prestoricu è protostoricu*, acte du Ier colloque de Calvi (Calvi, 28-30 avril 2017), ARPPC, 45-
1104 70.
- 1105 Stax, R., Stein, R., 1993. Long-term changes in the accumulation of organic carbon in Neogene
1106 sediments, Ontong Java Plateau, Proc. Ocean Drill. Program Sci. Results 130, 573-584.
- 1107 Stos-Gale, Z., Gale, N.H., Houghton, J., Speakman, R., 1995. Lead isotope data from the Isotracer
1108 Laboratory, Oxford: Archaeometry data base 1, ores from the Western Mediterranean.
1109 *Archaeometry* 37, 407-415.
- 1110 Terral, J.-F., Alonso, N., Buxó i Capdevila, R., Chatti, N., Fabre, L., Fiorentino, G., Marinval, P.,
1111 Pérez Jordá, G., Pradat, B., Rovira, N., Alibert, P., 2004: Historical biogeography of olive
1112 domestication (*Olea europaea* L.) as revealed by geometrical morphometry applied to
1113 biological and archaeological material. *J. Biogeogr.* 31, 63-77.
- 1114 Trouet, V., Esper, J., Graham, N.E., Baker, A., Scourse, J. D., Frank, D.C., 2009. Persistent positive
1115 North Atlantic Oscillation mode dominated the medieval climate anomaly. *Science*
1116 324(5923), 78-80.
- 1117 Vacchi, M., Ghilardi, M., Spada, G., Currás, A., Robresco, S., 2017. New insights into the sea-level
1118 evolution in Corsica (NW Mediterranean) since the late Neolithic. *J. Archaeol. Sci.: Reports*,
1119 12, 782-793.
- 1120 Vacchi, M., Joyse, K. M., Kopp, R. E., Marriner, N., Kaniewski, D., Rovere, A., 2021. Climate pacing
1121 of millennial sea-level change variability in the central and western Mediterranean. *Nature*
1122 *communications* 12(1), 1-9.
- 1123 Vacchi, M., Marriner, N., Morhange, C., Spada, G., Fontana, A., Rovere, A., 2016. Multiproxy
1124 assessment of Holocene relative sea-level changes in the western Mediterranean: sea-level
1125 variability and improvements in the definition of the isostatic signal. *Earth Sci. Rev.* 155, 172-
1126 197.
- 1127 Vacchi, M., Ghilardi, M., Melis, R.T., Spada, G., Giaime, M., Marriner, N., Lorscheid, T., Morhange,
1128 C., Burjachs, F., Rovere, A., 2018. New relative sea-level insights into the isostatic history of
1129 the Western Mediterranean. *Quat. Sci. Rev.* 201, 396-408.
- 1130 van Geel, B., 2001. Non-pollen palynomorphs. In: Smol, J.P., Birks, H.J.B., Last, W.M. (Eds.),
1131 *Tracking Environmental Change Using Lake Sediments. Terrestrial, Algal and Silicaceous*
1132 *Indicators, Volume 3.* Kluwer, Dordrecht, pp. 99-119.
- 1133 Vecchio, A., Lepreti, F., Laurenza, M., Alberti, T., Carbone, V., 2017. Connection between solar
1134 activity cycles and grand minima generation. *Astronomy & Astrophysics* 599, A58.
- 1135 Vella, M. A., Tomas, É., Thury-Bouvet, G., Muller, S., 2014. Nouvelles données sur le petit âge de
1136 glace en Corse: apports de l'analyse croisée des informations géomorphologique,
1137 palynologique et archéologique de la piève de Santo Pietro (désert de l'Agriate, Corse).
1138 Méditerranée. *Revue géographique des pays méditerranéens/Journal of Mediterranean*
1139 *geography*, (122), 99-111.
- 1140 Vella, M.A., Andrieu-Ponel, V., Cesari, J., Leandri, F., Pêche-Quilichini, K., Reille, M., Poher, Y.,
1141 Demory, F., Delanghe, D., Ghilardi, M., Ottaviani-Spella, M.D., 2019. Early impact of
1142 agropastoral activities and climate on the littoral landscape of Corsica since mid-Holocene.
1143 *PloS One*, 14(12), e0226358.

- 1144 Vigne, J.D., 1984. Premières données sur les débuts de l'élevage du Mouton, de la Chèvre et du Porc
1145 dans le sud de la Corse (France), in: Clutton-Brock J. et Grigson C. (Eds.), *Animals and*
1146 *Archaeology*, 3 - Early Herders and their Flocks. Proceedings 4th Int. Council for
1147 *Archaeozoology*, Londres, 1982, Oxford, Archaeopress, BAR International Series, 202, 47-
1148 65.
- 1149 Vigne, J.D., 1987. L'exploitation des ressources alimentaires en Corse du VIIe au IVe millénaire. In
1150 : Guilaine, J., Courtin, J., Roudil, J.L. et al. (Eds.), *Premières communautés paysannes en*
1151 *Méditerranée occidentale*. CNRS éditions, 193-199.
- 1152 Weis, D., Kieffer, B., Maerschalk, C., Barling, J., de Jong, J., Williams, G.A., Hanano, D., Pretorius,
1153 W., Mattielli, N., Scoates, J.S., Goolaerts, A., Friedman, R.M., Mahoney, J.B., 2006. High-
1154 precision isotopic characterization of USGS reference materials by TIMS and MC-ICP-MS.
1155 *Geochem. Geophys. Geosyst.* 7, Q08006.
- 1156 Weiss, M.-C., 2010. Au VIe millénaire avant notre ère. A Petra à L'île Rousse : campagnes de fouilles
1157 (2003-2006), Ajaccio, Albiana, 247 p.
- 1158 Wu, J., Yu, Z., Zeng, Z., Wang, N., 2009. Possible solar forcing of 400-year wet-dry climate cycles
1159 in northwestern China. *Climatic Change* 96, 473-482.
- 1160 Yu, Z.C., Ito, E., 2002. The 400-year wet-dry climate cycle in Interior North America and its solar
1161 connection. In: West, G.J., Blomquist, N.L. (Eds.), *Proceedings of the nineteenth annual*
1162 *pacific climate workshop*. Technical Report 71, 159-163.
- 1163 Zanchetta, G., Regattieri, E., Isola, I., Drysdale, R., Bini, M., Baneschi, I., Hellstrom, J., 2016. The
1164 so-called "4.2 event" in the central Mediterranean and its climatic teleconnections. *Alp.*
1165 *Mediterr. Quat.* 29, 5-17.
- 1166 Zonneveld, K.A.F., Marret, F., Versteegh, G.J.M., Bonnet, S., Bouimetarhan, I., Crouch, E., de
1167 Vernal, A., Elshanawany, R., Edwards, L., Esper, O., Forke, S., Grøsfjeld, K., Henry, M.,
1168 Holzwarth, U., Kieft, J.-F., Kim, S.-Y., Ladouceur, S., Ledu, D., Chen, L., Limoges, A.,
1169 Londeix, L., Lu, S.-H., Mahmoud, M.S., Marino, G., Matsouka, K., Matthiessen, J.,
1170 Mildenhall, D.C., Mudie, P., Neil, H.L., Pospelova, V., Qi, Y., Radi, T., Richerol, T., Rochon,
1171 A., Sangiorgi, F., Solignac, S., Turon, J.-L., Verleye, T., Wang, Y., Wang, Z., Young, M.,
1172 2013. Atlas of modern dinoflagellate cyst distribution based on 2405 datapoints. *Rev.*
1173 *Palaeobot. Palynol.* 191, 1-197.
- 1174
1175

LabID	Material	Depth (cm)	¹⁴ C Age±error BP	Cal. yr BP (2σ)	Cal. yr AD/BC (2σ)
GdA-5806	Organic sediment	49	1585±25	1527-1404	423-546 AD
Poz-115796	Organic sediment	50	3090±40	3389-3179	1440-1230 BC
GdA-5807	Organic sediment	77	2215±30	2330-2146	381-197 BC
GdA-5808	Organic sediment	93	2280±25	2349-2177	400-209 BC
Poz-110261	Charcoal	125	3260±90	3699-3252	1750-1301 BC
GdA-5809	Organic sediment	138	3090±35	3382-3210	1433-1261 BC
GdA-5810	Organic sediment	154	3215±30	3480-3373	1531-1424 BC
Poz-110260	Plant + Peat	185	3420±35	3823-3569	1874-1620 BC
GdA-5811	Organic sediment	229	4170±40	4834-4577	2885-2628 BC
Poz-110258	Peat	270	4175±35	4835-4580	2886-2631 BC
Poz-109794	Charcoal	340	4470±40	5297-4967	3348-3018 BC
Poz-110198	Peat	397	4530±30	5312-5051	3363-3102 BC
Poz-109887	Charcoal	450	4730±40	5581-5325	3632-3376 BC
Poz-105992	Bulk Sediment	487	5080±40	5917-5730	3968-3781 BC

1176

1177 Table 1. AMS Radiocarbon ages obtained from the materials of Crovani core. The calibrated ages
1178 are based on Intcal20 dataset ([Reimer et al., 2020](#)).

1179

1180 Figure Captions

1181 Figure 1. Location map of the study area and coastal sites of previous palynological research (white
1182 circle) conducted over the last decade for Corsica island (Del Sale: [Currás et al., 2017](#); Sagone:
1183 [Ghilardi et al., 2017a](#); Palo, Piantarella and Saint-Florent: [Revelles et al., 2019](#), [Revelles and](#)
1184 [Ghilardi, 2021](#); Canniccia: [Vella et al., 2019](#)). The purple squares indicate the position of known
1185 mining sites of galena/lead in Corsica. A: Hydrography and archaeology of the catchment basins
1186 ending in the Crovani Bay, green circle: Final Neolithic to Bronze Age site; Red circle: possible
1187 roman site of occupation; Orange square: 19th to 20th Cent. AD mining buildings; light green stars:
1188 Medieval site; 1: San Larenzu, 2: San Quilicu, 3: Teghja di Linu, 4: lower Argentella, 5: upper
1189 Argentella. B: Simplified geology and topography of the catchment basins ending in the Crovani
1190 Bay; Orange square: mining site Geographic coordinates are expressed in WGS 84 geodetic system.

1191
1192 Figure 2. View of the Crovani pond, borehole and Differential Global Positioning System- DGPS-
1193 profile (AA') locations. The light blue line (dash) indicates the present-day course of the rivers.

1194
1195 Figure 3. Age-Depth Model of the Crovani sequence, calculated through a Bayesian method using
1196 the computer program Bacon 2.5.5 ([Blaauw and Christen, 2011](#)). The Model is based on 14 AMS
1197 dates calibrated using the IntCal20 curve ([Reimer et al., 2020](#)).

1198
1199 Figure 4. Core lithology with ages expressed in cal. BC/AD and depths indicated in cm (left). For full
1200 details of the samples performed for ¹⁴C AMS dating method (red squares), please check Table 1.
1201 Curves from left to right: Loss on ignition measurements with organic matter and carbonate contents,
1202 granulometric indexes (mean and mode), mineralogical and geochemical proxies (halite, C/N ratio)
1203 and Arboreal Pollen (AP) concentration (grains/gram).

1204
1205 Figure 5. A: Pb isotope results of the Crovani sedimentary core LCr18 reported in a binary diagram
1206 ²⁰⁷Pb/²⁰⁶Pb versus ²⁰⁸Pb/²⁰⁶Pb. The dashed line indicates the linear regression trend between the
1207 Crovani samples. Circles: Crovani samples reported by different colors according to their
1208 stratigraphical position, i.e. pre-Roman samples, Roman and modern samples. The black circle
1209 indicates the average signature of the local geological background defined by the oldest measured
1210 Final Neolithic samples. Black symbols: samples from different Pb-bearing mineral collected in West
1211 Corsica. The red triangle gives the averaged composition of modern airborne particles collected above
1212 Roma in Italy (data from [Bollhöfer and Rosman, 2001](#)). Green squares: signature of Pb galene-rich
1213 ores from Sardinia. B: Close up emphasizing the representative signature of Pb ore mining districts
1214 surrounding the Mediterranean basin classed by country (green for Italy, blue for Greece, purple for
1215 Turkey and various colors from grey to orange for Spain ores). Data from literature reported in [Fagel](#)
1216 [et al., \(2017\)](#). The black arrow represents an extrapolation of the sedimentary mixing observed in core
1217 LCr18 in Figure 5A. It underlines the probable implication of the minerals of Tuscany in the Pb
1218 isotope signature of the Crovani sediments.

1219
1220 Figure 6. Pollen percentage diagram of Crovani, including the pollen zonation calculated with the
1221 CONISS method ([Grimm, 1987](#)).

1222
1223 Figure 7. Percentage diagram of Non-Pollen Palynomorphs from Crovani.

1224
1225 Figure 8. Summary pollen diagram including the cumulative percentages of gymnosperms, riparian
1226 trees, deciduous trees, evergreen trees and shrubs, OJCV curve, anthropogenic herbs, other herbs,
1227 coprophilous fungi, and saproxylic and phytopathogenic fungi, the Arboreal Pollen percentage
1228 record, the concentrations of Arboreal Pollen and Non-Arboreal Pollen, and the microcharcoal
1229 concentrations. The light green bars indicate phases of high storm activity in southern France

1230 (Sabatier et al., 2012). The blue bars indicate lake level highstands at Lake Accesa in central Italy
1231 (Magny et al., 2013). The orange bars indicate phases of dry climate conditions in south-central
1232 Mediterranean (Di Rita et al., 2018a). The NAO index is based on Franke et al. (2017).

1233

1234 Figure 9. REDFIT (A) analysis of the total Arboreal Pollen percentages (B) using the PAST 3.2
1235 software program (Hammer et al., 2001). In the REDFIT spectral analysis the time series is fitted to
1236 an AR1 red noise model (orange line). The 95% confidence levels of the χ^2 and Monte Carlo tests
1237 are reported on the graph with a green dashed line and a red dashed line, respectively.

1238

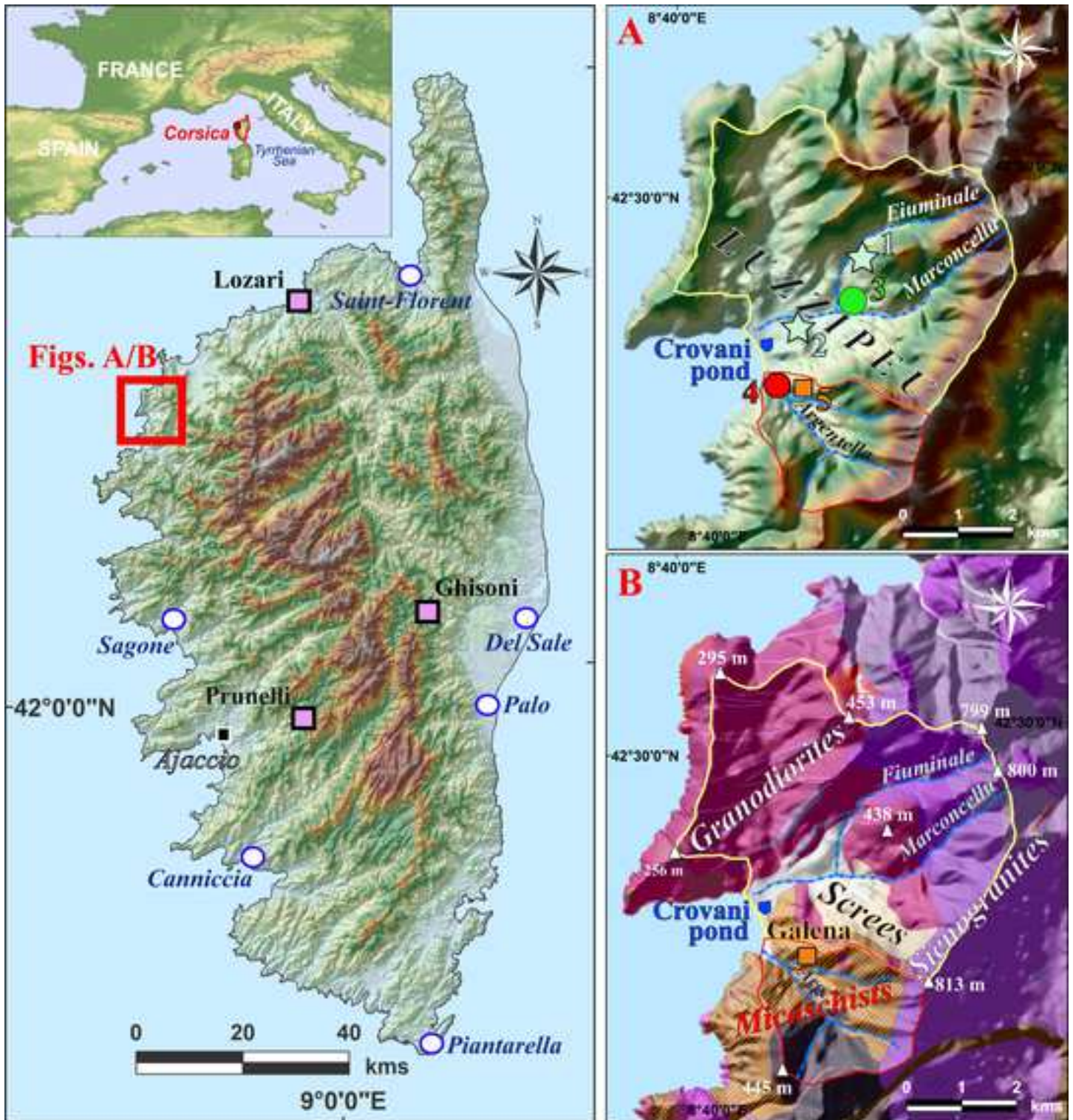
1239 Figure 10. Synoptic table with timing and nature of key environmental changes reconstructed from
1240 the Crovani record.

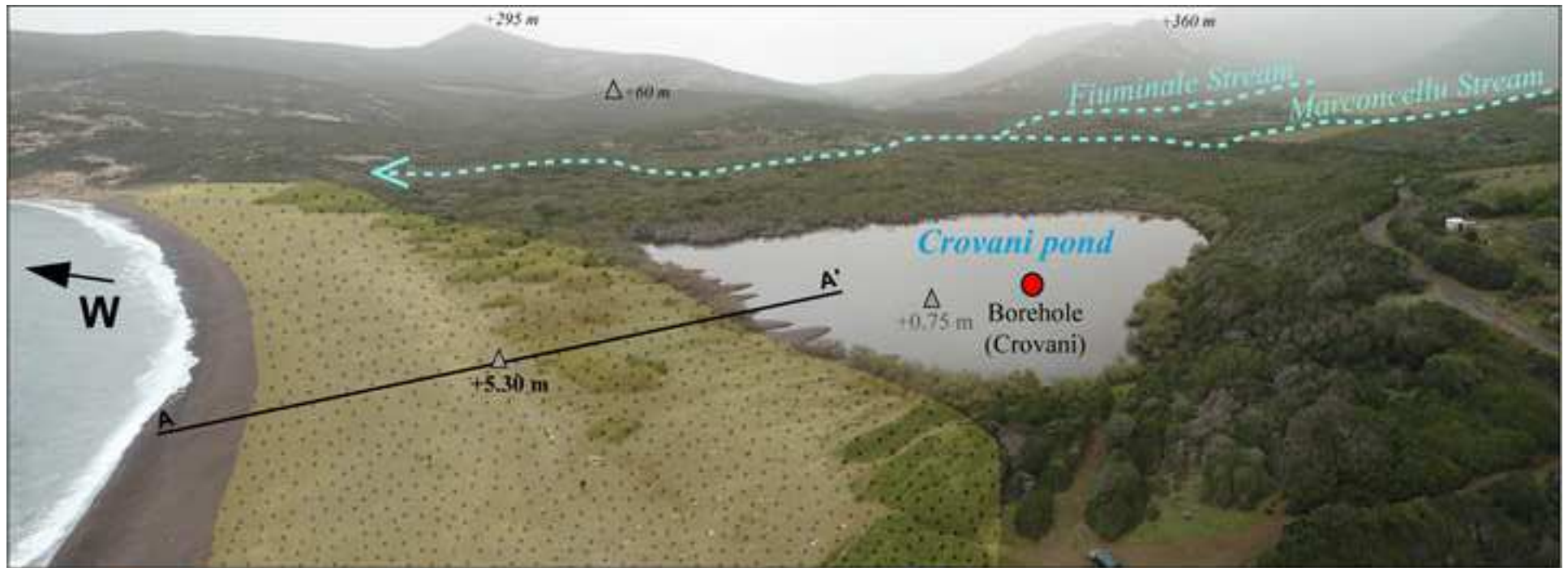
1241

1242


1243

1244





Elevation in m (AMSL)

 Coastal barrier (well rounded pebbles)

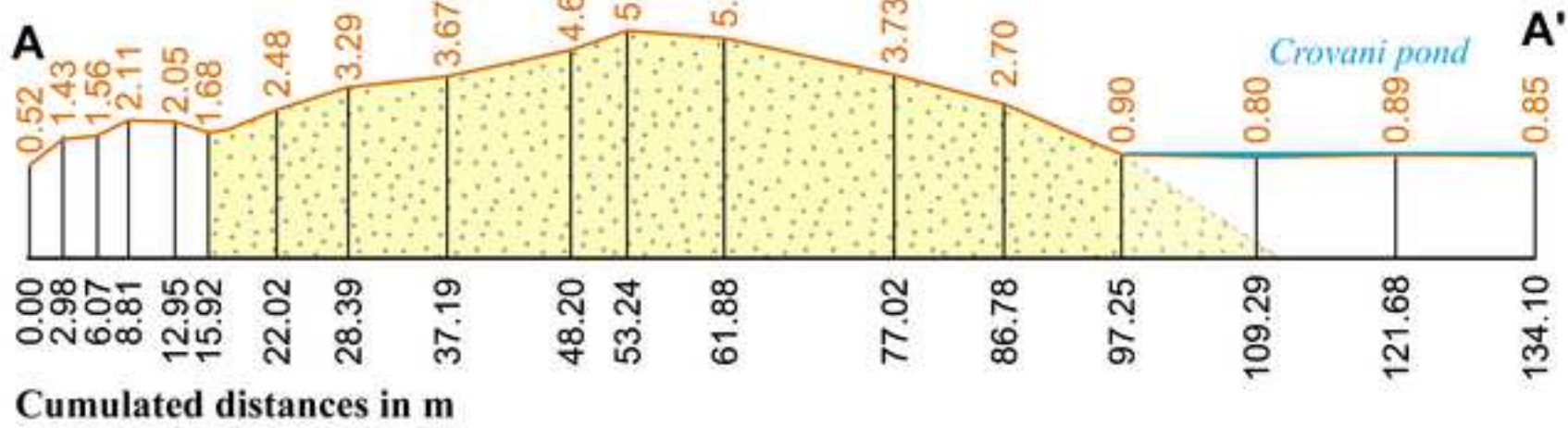
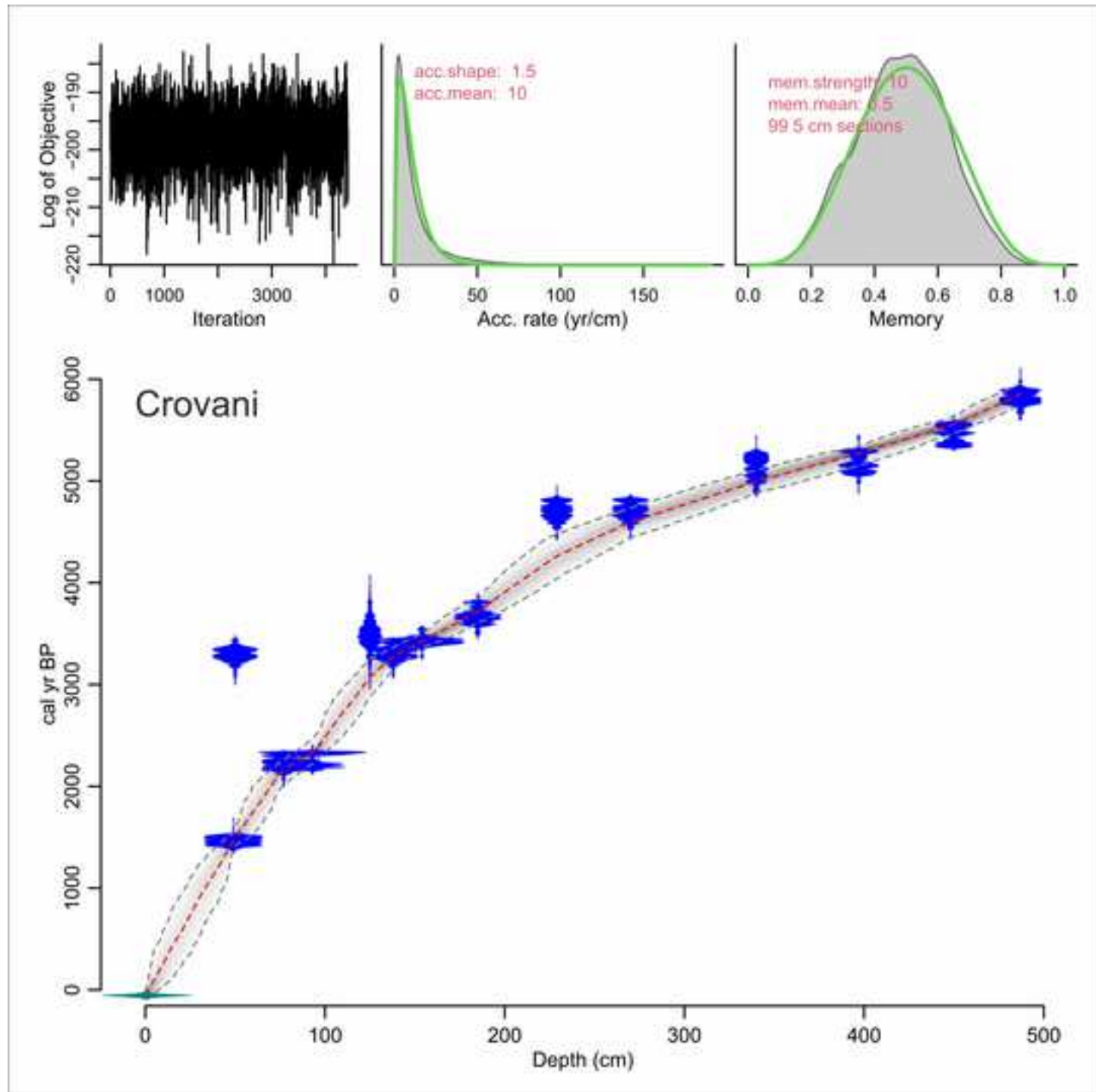
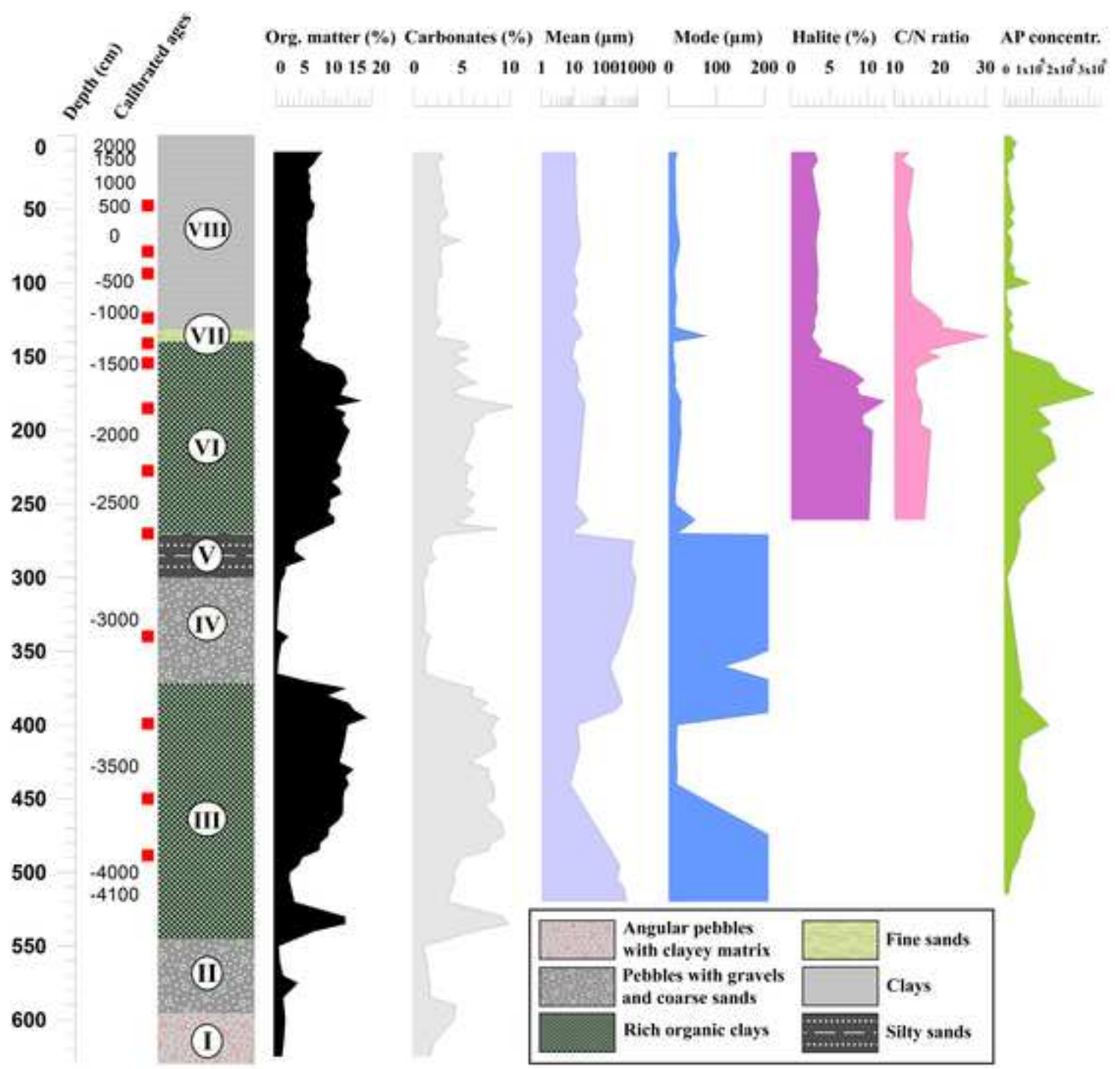
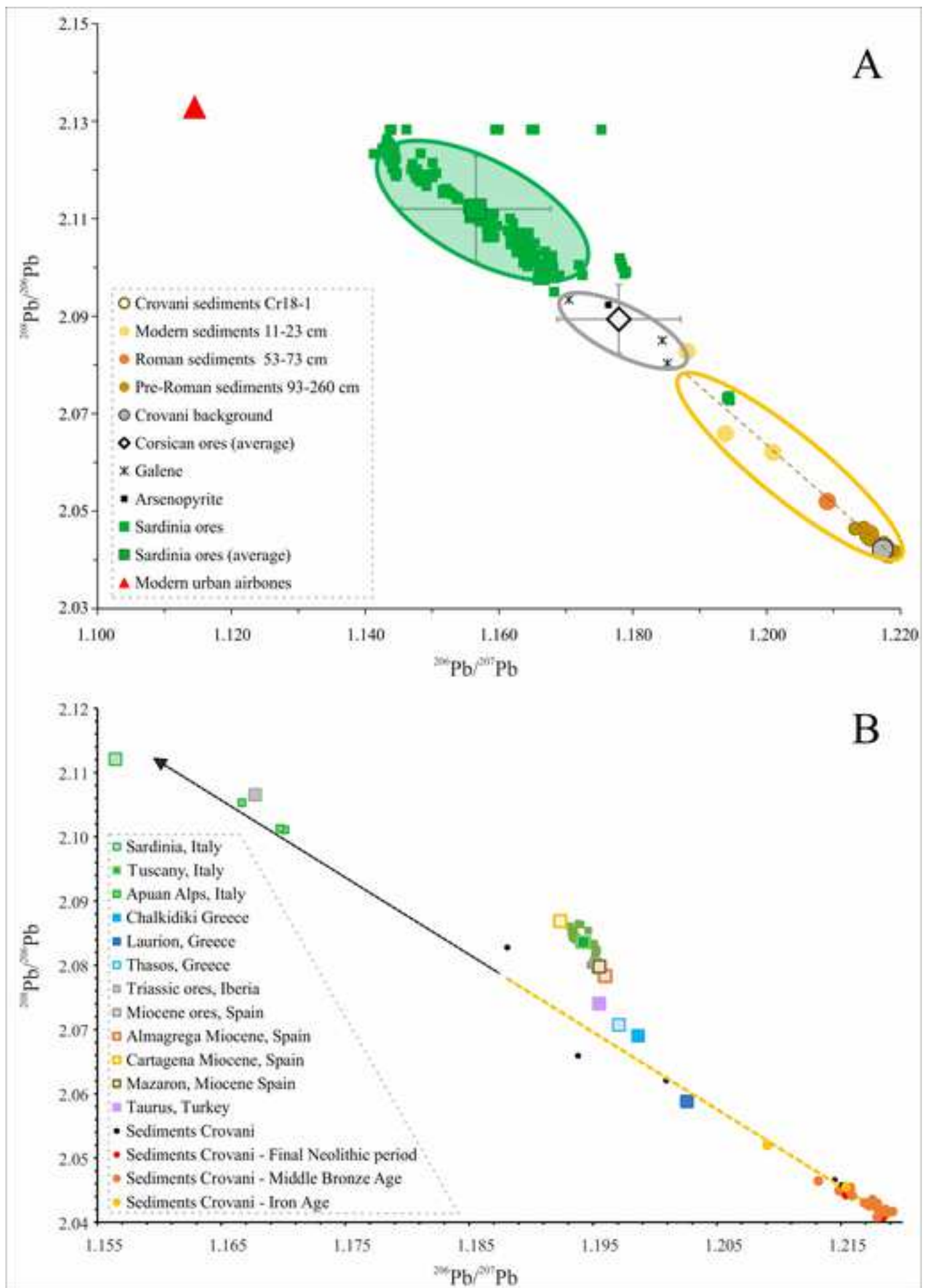
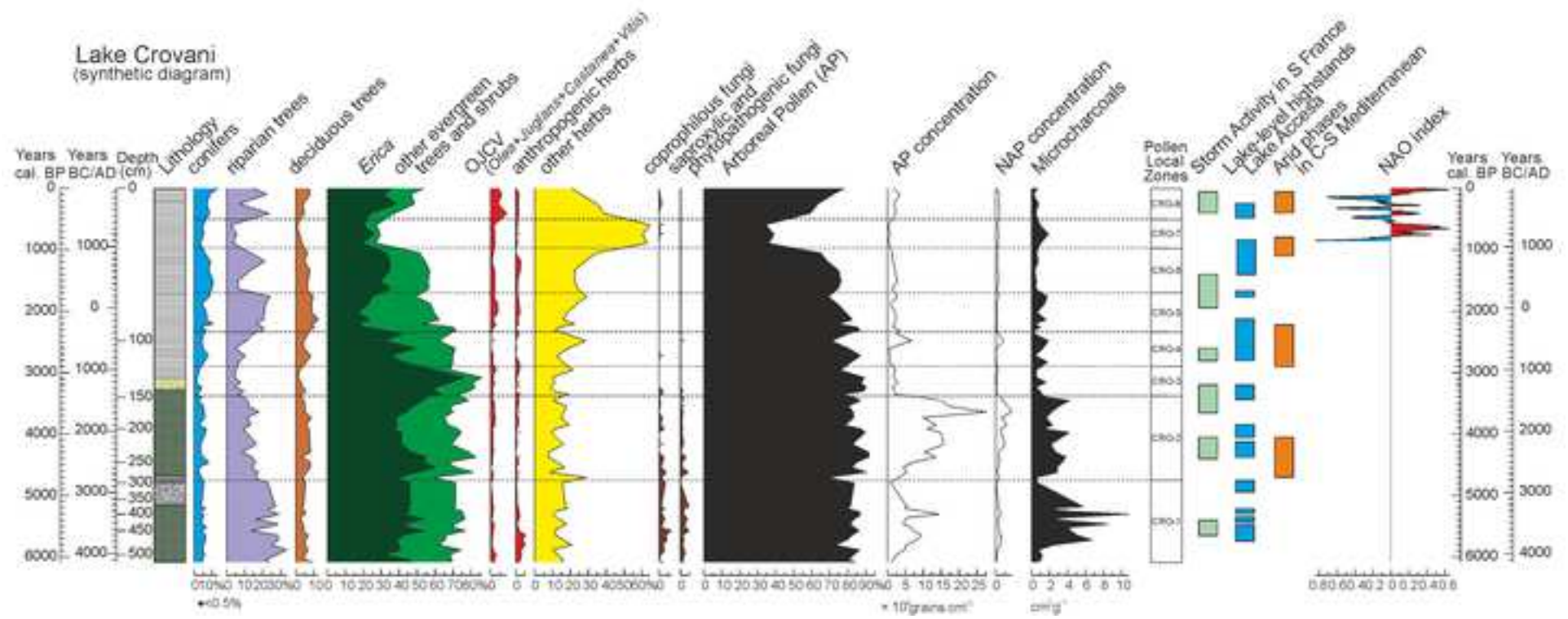


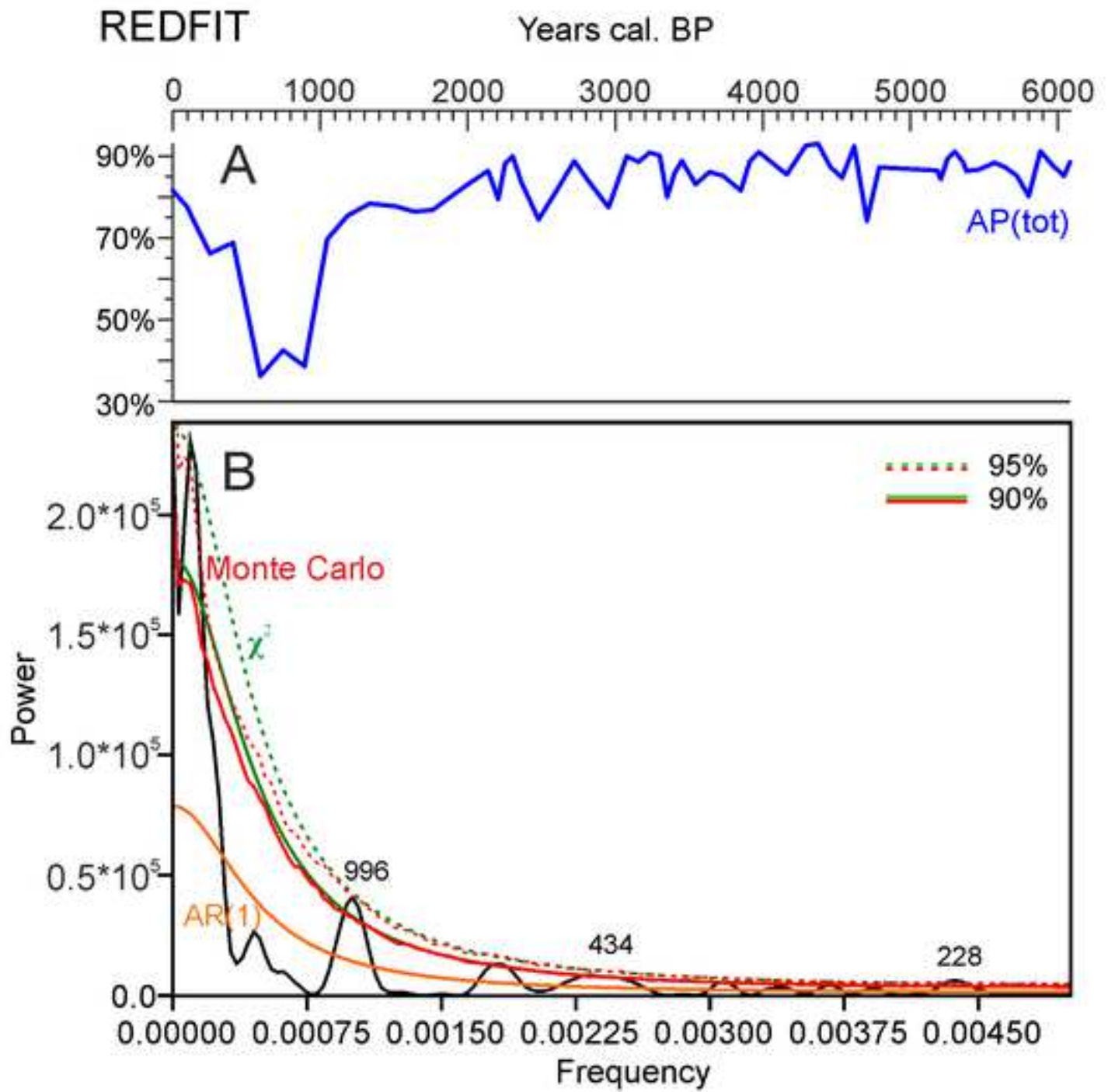
Figure 3











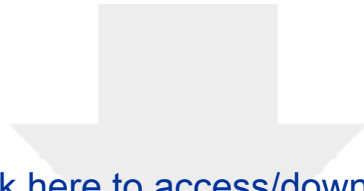
Declaration of interests

The authors declare that they have no known competing financial interests or personal relationships that could have appeared to influence the work reported in this paper.

The authors declare the following financial interests/personal relationships which may be considered as potential competing interests:

Authors' Contributions

All authors have materially participated in the research project and article preparation, as follows. Conceptualization: FDR, MG, NF, and MV. Sediment collection: MG, JS and LM. Methodology: FDR, MG, NF, and MV. Formal analyses: FDR, MG, NF, MV, FW, DD, and SR. Data collection: FDR, MG, NF, MV, FW, DD, JS, LM, and SR. Results interpretation: FDR, MG, NF, and MV. Writing original draft: FDR, MG, NF, and MV. Contribution in interpreting results and writing the paper: FW, DD, JS, LM, and SR. Funding acquisition: MG.



[Click here to access/download](#)

[e-Component/Supplementary data](#)

[Di Rita et al_Supplementary material_rev_2.docx](#)

